

Observatoire de la CÔTE d'AZUR

How can Corsica be visible from Nice ?

author: F. Mignard

affiliation : Univ. Nice Sophia-Antipolis, CNRS, OCA

reference: OCA-TN-FM-Corsica

status: Version 1.3, August 2010

date: 2013-01-11

Abstract

This document deals with various issues related to the visibility of Corsica from the city of Nice and its surrounding hills. The presentation develops gradually from simple geometric considerations to help grasp the problem, followed by a more detailed modelling allowing for the curvature of the light rays caused by atmospheric refraction. Finally the problem is solved with an exact integration of the differential equation for the light ray propagation in an heterogeneous medium with spherical symmetry. Tables are added providing the lowest elevations that can be sighted from the hills around Nice as a function of their altitude. These tables help precise the exact role of the refraction to answer the question of how much of Corsica can be actually seen from Nice. Then others related topics are considered like the mirage formation near the sea level, the flattening of the sun when it sets or rises, the conditions of observations of the sunrise behind the Cap Corse. Several pictures of Corsica taken around sunrise provide vivid illustrations of the properties described in mathematical form in the body of the document. A table with more than 100 entries is supplied, covering all the landscape features visible in Corsica from areas around Nice for observers up to an altitude of 600 m, with azimuths and altitude of each recognisable feature from the Cap Corse to the Bay of Porto.

Document History

Issue	Revision	Date	Author	Comment
1	3	2010-08-30	FM	Comments of A. Young incorporated and few more typos
1	2	2010-05-28	FM	First set of typos fixed
1	1	2010-05-24	FM	First version released
1	0	2009-12-22	FM	Start of the initial document

Contents

1 Introduction **6**

2 Presention and main issues **10**

3 Geometric propagation of light **15**

3.1 Grazing rays 15

3.2 The flying rays 18

4 Curved light rays: constant curvature **28**

4.1 Empirical approach 28

4.2 Refraction and curvature of light rays 29

5 Curved light rays: full derivation **46**

5.1 General equation 46

5.2 Spherical symmetry 46

5.3 Differential equation for the light ray 50

5.4 Accuracy of the constant curvature path 53

6 Mirages **55**

6.1 True position and refracted position 55

6.2 Is the vision of Corsica a mirage? 55

6.3 True mirages with Corsica 56

6.4 Ray tracing in the atmosphere 58

7 Contrast and visibility **70**

7.1 Qualitative description 70

7.2 Visibility during daylight 70

7.3 Visibility before sunrise 73
7.4 Visibility after sunset 75

8 Rising sun above the Cap Corse **77**

9 Application to the Pic of Canigou **81**

10 The apparent shape of the sun **86**
10.1 Astronomical refraction 88
10.2 Physical approach 102

11 Atmospheric parameters **110**
11.1 Tropospheric model 110
11.2 Full atmospheric model 113

12 Radius of Curvature of the earth **116**

13 Identification of the summits of Corsica **121**
13.1 Methodology 121
13.2 Angular height 122
13.3 List and coordinates of landscape features 123
13.4 Results in tabular form 123
13.5 Marked-up panoramas 129

14 Final gallery **134**

15 References **140**
15.1 Books 140
15.2 Websites 140

1 Introduction

The present document is the result of a personal quest after I started, few years ago, taking pictures of Corsica at dawn, in the glowing morning sky illuminated by the twilight rays of the still hidden sun, typically thirty to forty minutes before sunrise. Observing from different altitudes on the eastern hills of Nice in late fall or early winter, donned in winter gear with a thick coat, gloves, scarf and a woolly hat, I noticed that beyond the general outline of the highest peaks, lesser summits became visible or vanished according to the altitude of my observing place, discovered by accident that one could see the Cap Corse and the rising sun just behind the Monte Stello or the Folicce. I also witnessed strange optical effects with just the emerging tops of the main peaks floating like islands on a glowing sea. All that aroused my interest and I went repeatedly into Internet searches expecting to find answers to all of my interrogations, eventually to be left unsatisfied. Despite several beautifully and very informative Websites (listed in the references) with high quality pictures, none goes into a scholarly physical and mathematical investigation of the visibility conditions, and several even remaining very vague about the exact role of the refraction of the light rays. I started doing my own evaluations, drawing a couple of plots to improve my insight and storing few handwritten notes in a *Corsica folder*. This gradually grew into a much larger document than I initially thought, mixing the mathematical derivations, explanatory diagrams with relevant digital pictures taken during my early morning hunts to shoot **The Picture** that would strikingly reveal a particular pattern.

Quick evaluation with pure geometry and straight light-rays proved rapidly insufficient to explain what I saw, at what altitude a particular feature would become visible or would just float above the horizon. While the general picture was easily understood, the details required a deeper investigation taking into consideration the propagation of light rays curved by the varying refractive index with altitude. Therefore what was initially planned as a compilation of few formulas, a couple of figures and tables, developed over the weeks into a much larger piece of work involving atmospheric optics, the physical properties of the lower atmosphere, the non spherical shape of the earth, very accurate sunrise computation with horizon depression and refractions for zenithal distances larger than 90 degrees, the subtle difference between earth and astronomical refraction, numerical integration with boundary conditions for the propagation of light rays between two points, optical mirages altogether coupled with numerous numerical applications and digital picture enhancing for the illustrations. The identification of all the landscape features proved also particularly tedious and comprises now more than 110 entries, located in

distance, azimuth and altitude.

The document has been designed to be explored electronically rather than with a printed version. Sections, equations, tables, figures, URLs are all linked throughout the pdf file for an easy navigation with a pdf reader. All the diagrams can be looked at with high resolution and several pictures at the end of the document are expressly designed for that purpose, using a zoom between 200 or 300 % to see the details comfortably and read the small toponymic labels. The information content or the quality of some of the pictures will be degraded with ordinary printing, while a good computer screen has a much better resolution allowing to tell between two neighbouring light paths and also a better colour rendering for the pleasure of the eyes.

What audience is this document meant at? As I mentioned already, I was initially the only targeted reader, plus few close colleagues who got involved with me in discussions about the visibility of Corsica, but as the work progressed I got convinced that a wider group would be interested and decided for a more comprehensive coverage including related subjects, like the solar flattening near the horizon and a detailed investigation of the inferior mirages, both connected to the observations of Corsica at dawn.

As it stands now, this work is hard to categorise among the usual publications types:

- it is not strictly a research work, nothing is really original, although several results regarding the astronomical refraction or the mirages may be hard to find elsewhere. It lacks the numerous references which are also a trademark for research papers. I actually used very few existing works, and the few books I consulted are listed at the end of the document, together with the most relevant websites.
- it may look like lecture notes on atmospheric optics, but the scope is too restricted and specialised to be lectured, and in any case I have never lectured on theses topics myself. Although I had some general ideas of the subject before I start putting them in a more structured form, I clearly learnt the matter as the sections gradually unfolded in the TEX file. I had no prior expertise, as expected from a lecturer, but just a keen interest in the subject.
- clearly it cannot be qualified as a popularisation work, given the underlying physical arguments, let alone the mathematical developments involved and the numerical techniques used to carry out the computations. These are not complementary sections that could be skipped: they contain the essential of the arguments and carry the deductive machinery.

- Let call it a small monograph on a topic of local interest (who cares about Corsica visibility from Nice ?), whose treatment pertains to subjects of more general interest with applications overflowing its initial narrow scope. In that sense I think that it will be of interest to a wider range of readers than its parochial title suggests. At least it was enjoyable for the author who naively hopes that his enthusiasm will be shared by few readers.

Acknowledgements

I thank Andrew T. Young, from the Department of Astronomy of the San Diego State University, for his careful reading of an earlier version of this document and his thoughtful comments that have been incorporated at their relevant locations without further credit. I particularly appreciated his warning against the overly trust I placed in the Standard Atmosphere model, specifically for nearly horizontal rays.

TABLE 1.1: *Notations used throughout this document*

Symbol	Meaning	Units
h, z	altitude above the ground	m, km
h_0	altitude of the observer	m
h_1	altitude of a landscape feature	m
θ	angular arclength between two points on the earth	rad, deg
$x = R\theta$	spherical distance on the earth between two points	km
d, D	Euclidean distance between two points	km
d_{h}	distance to optical horizon	km
R_{c}	local radius of curvature of the earth	km
T	absolute temperature	K
P	atmospheric pressure	Pa
γ	temperature lapse rate $(-dT/dz)$	K km^{-1}
n	refractive index of the air	-
α	gradient of refractive index $(-dn/dz)$	km^{-1}
σ	extinction coefficient in the atmosphere	km^{-1}
C	brightness contrast	-
ϵ	direction of a light ray (> 0 below the horizontal plane)	rad, deg, arcmin
ϵ_{h}	depression of the optical horizon	rad, deg, arcmin
h	direction of a light ray (> 0 above the horizontal plane)	rad, deg, arcmin
ρ	radius of curvature of a light ray	km
ϕ	geodetic latitude on the earth	rad, deg
λ	longitude on the earth	rad, deg
A_z	azimuth on the earth, counted from the north	rad, deg
a	equatorial radius of the earth ellipsoid	km
b	polar radius of the earth ellipsoid	km
$M(\phi), N(\phi)$	radii of curvature of the spheroid at latitude ϕ	km
$\mathcal{F}, \mathcal{S}$	solar flattening and skewness	-



FIGURE 2.1: Central view of Corsica above the Cap Ferrat taken at an altitude of 250 m in the east of Nice, 20 mn before sunrise in late November. The altitudes at the centre are above 2500 m and the lowest visible slopes on the left or right are at about 1400 m. Without refraction, and in the same conditions, this lowest altitude would be 1750 m instead. The horizon line stretches out about 60 km away from the observer and $\sim 27'$ below his/her horizontal plane, whereas the ridge line is ~ 200 km off from Nice. The highest peak, the Monte Cinto near the centre, rises at a mere $25'$ above the horizon line, and yet, it is still below the horizontal plane (by $2'$) of the observer. Identification of all the prominent peaks is given in Sect. 13.

2 Presention and main issues

In this document I discuss various questions of atmospheric optics with the primarily motivation of accounting for the sighting of Corsica top mountains for observers located around Nice. The altitude of the observers may range from the sea level, along the Promenade des Anglais, to the much higher viewpoints in the Mercantour at altitude above 2500 m. However most of the numerical examples and images refer to observers between 100 and 550 m which are easy to reach from Nice to observe Corsica before the sunrise. I have no access to the top of the Mont Agel, at the border between France and Monaco which culminates at 1150 m within 2 km inland from the Mediterranean sea, and must be a remarkable site to observe Corsica. In the caption of Fig 2.1, I give purposely an assorted set of numerical quantities related to the features seen in the picture: they are

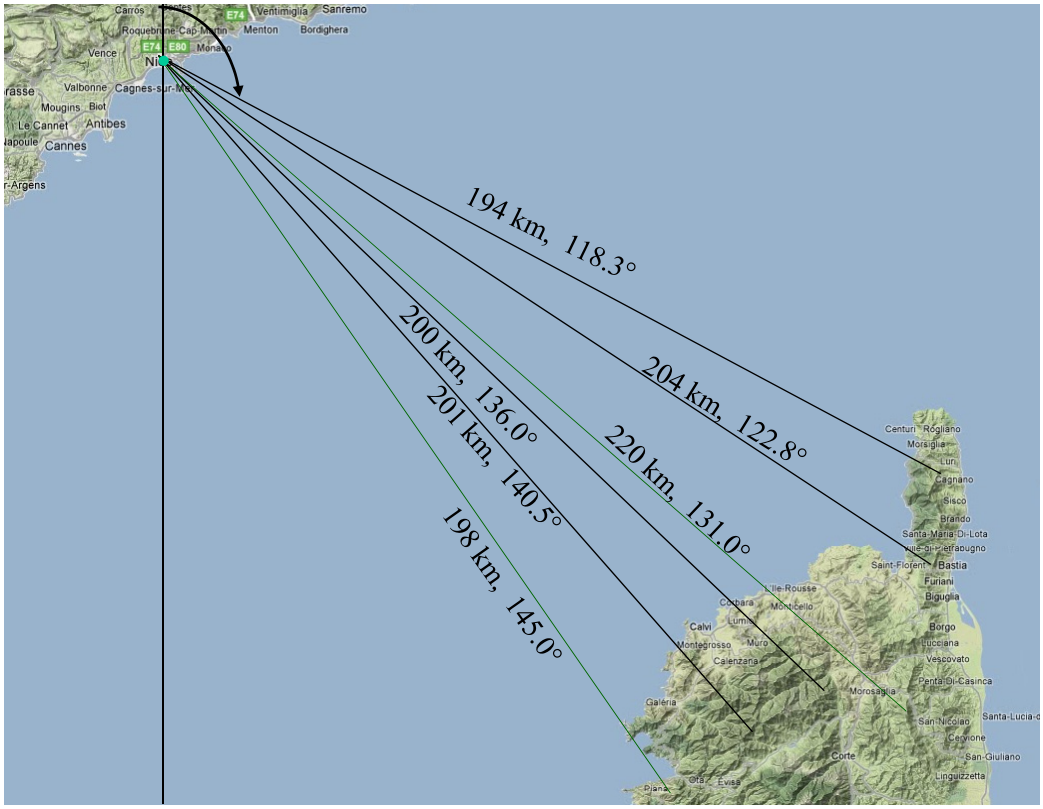


FIGURE 2.2: Geographic setting of the Nice area relative to Corsica. The areas of interest in Corsica, at far as the visibility from Nice is concerned, are located in the Cap Corse, in the north of the island with azimuths around 120 deg and altitudes below 1300 m, and in the regions with the highest peaks in the azimuth range $136 - 140$ deg and altitude higher than 2500 m. The typical distances are about 200 km, although there is an isolated peak at 1700 m (Monte San Petrone) as far as 220 km well visible from the hills surrounding Nice. The smallest distance between Nice and Corsica is 170 km, at the Revellata lighthouse in the north of Calvi.

all derived from simple formulas and tables given in the text and illustrate what one can expect out of its reading.

The geographical setting is shown in Fig. 2.2, with the distances of the order of 200 km and the main directions where the peaks are high enough to be seen from Nice area.

The main areas visible from a moderate altitude are indicated in the following map (Fig. 2.3) of the northern part of Corsica. Within the two green rectangles, one has the main landscape feature visible. The major peaks are in the centre and include the Monte Cinto, the highest in Corsica with an altitude of 2710 m. This central part is well visible

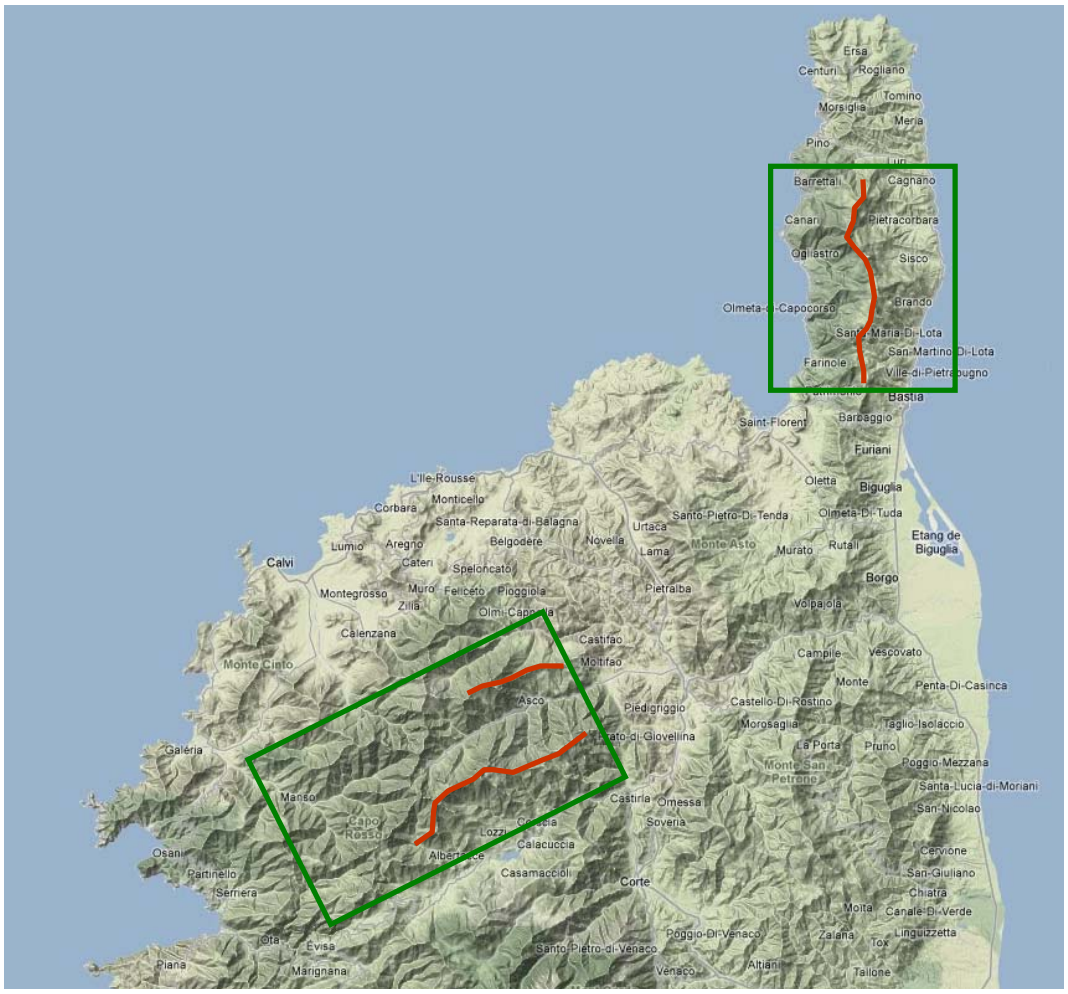


FIGURE 2.3: The two main areas in Corsica where the most visible peaks can be seen from moderate altitude around Nice. For the Cap Corse, on the top right, the observer must be located at an altitude higher than 300 m. The highest peaks of the central and most mountainous region of Corsica, can even be glimpsed from the beach front at sea level in exceptionally clear conditions. Scattered and less prominent peaks are also visible between these two areas and in the direction of the Bay of Porto on the west coast, at the lower left of the picture. A complete marked-up panorama is shown in Sect. 13.

as soon as the observer's altitude is above 50 m, and for higher observing positions, lower features become visible. The altitude of the mountains in the Cap Corse are all lower than 1310 m, and one needs to be above 300 m to see the crest line in the morning. A clean horizon is mandatory, since the peaks are only few arcmin above that horizon for these moderate observing altitudes. These two groups are completed by more scattered features, more difficult to identify, but all well visible from 500 m and above. The main

direction of Corsica from Nice is south-east, and the best observing conditions are in winter and before sunrise, when the sky is already illuminated by the sun still below the observer horizon. The direction of the sun at sunrise is strongly variable during the year as illustrated in Fig. 2.4. This diagram explains why winter time is more favorable, when the sunrise is no too far from the direction of Corsica and then one can benefit from the beautiful colours surrounding the rising sun, but extending not too far from the sunrise directions. Also we see that near the winter solstice the sun rises behind the Cap Corse, a optimal condition to produce the best contrast minutes before sunrise. Afterwards, few minutes later, the sun emerges above the sinuous ridge line of the Cap Corse.

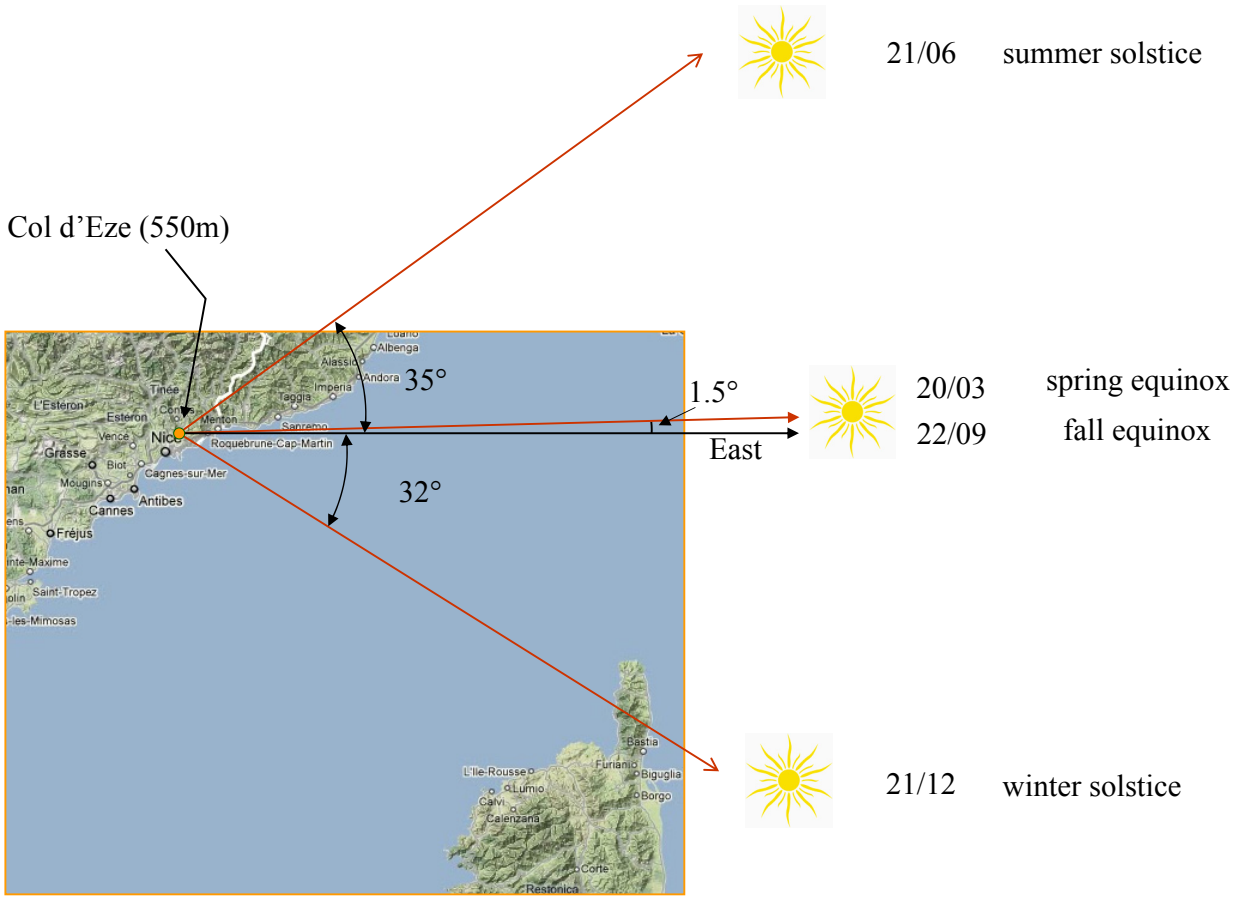


FIGURE 2.4: Directions of the sunrise in Nice Col d'Eze at different periods of the year. In late fall and early winter the orientation of the rising glow is the most favorable to see the outline of a dark Corsica against the iridescent sky illuminated by the twilight glow. The difference between the northward and southward elongations from the east comes from the horizontal refraction ($\sim 33'$) and the effect of the horizon depression at 550 m altitude ($45'$). Both shift the rising sun northward by respectively 0.65 and 0.85 deg. At the sea level and without refraction the maximum elongations from the east would be both equal to 33.5 deg. At the equinoxes, the azimuth of the rising sun is also shifted from the east by 1.5 deg to the north, hence restoring the axis of symmetry between the two solstices. The azimuth change with the refraction may puzzle many an astronomer, since astronomical refraction raises the apparent direction of a source toward the zenith without changing its azimuth. This is here an indirect effect specific to the rising or setting: the azimuth of the refracted direction is the same as the azimuth of the geometric direction taken at the **same time**, but the rising or setting times of a refracted celestial body are not the same as those without refraction.

3 Geometric propagation of light

In this section one neglects the effect of the refractive index of the atmosphere in the propagation of the light rays between a landscape feature (typically a peak) in Corsica to an observer located around Nice. Therefore the light propagates in straight line and the visibility conditions, the angular heights of the features seen in Corsica can be deduced from elementary considerations involving only plane trigonometry in a triangle and simple geometry of the circle to take into account the spherical shape of the earth.

It is important throughout this paper, to bear in mind the difference between the *horizontal plane*, (*i.e.* the astronomical horizon), defined as the reference **plane** normal to the local vertical, and the *optical horizon*, (often abbreviated as the horizon), a **line** where the sea and the sky merge. The latter is basically an optical concept and not a geometrical one, and only in the very simple case of straight ray propagation and an observer at sea level are the two ideas identical. For a given place, the astronomical horizon is fixed (neglecting the small tidal variations of the vertical) and unaffected by the light propagation, while the optical horizon depends on the behaviour of the refractive index, which is linked to the temperature gradient and is highly variable. The direction of the grazing ray which materialises that of the optical horizon, depends also on the height of the observer above the sea level. Finally, anomalous temperature gradients above the sea, or temperature inversions modify both the altitude of the horizon line with respect the horizontal plane and its distance from the observer.

3.1 Grazing rays

I consider here only the grazing rays, that is to say the case when during the propagation between the two end points, the rays become tangent to the surface of the earth, or in the case of Corsica and Nice, when the rays touch the surface of the sea. This gives the relationship between the maximum distance to see a particular altitude,or the minimum altitude visible for a given separation.

Let's call h_1 the altitude of the observer somewhere around Nice and h_2 that of a landscape feature (typically the top of a mountain) in Corsica. Given the altitude of the observer, the limiting situation when the light ray just connects the two end points by touching the surface of the sea at some intermediate point is illustrated in Fig. 3.1.

The distance of the observer horizon d_1 and is given by,

$$d_1 = \sqrt{2Rh_1(1 - \frac{h_1}{2R})} \tag{3.1}$$

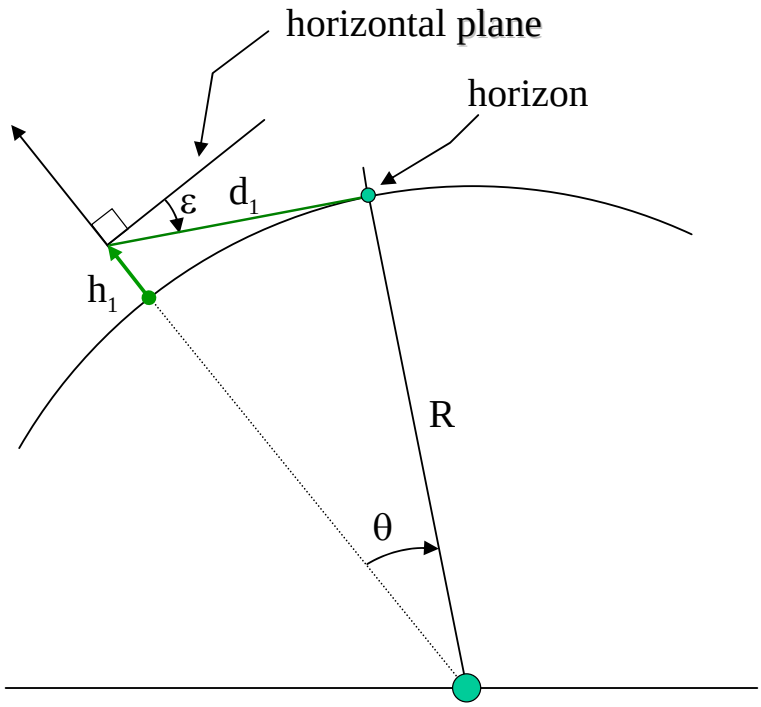


FIGURE 3.1: Visibility and optical horizon from an altitude h_1 above the sea level, when light propagates in straight line. The horizontal plane is perpendicular to the local vertical at the observer place and the angle ϵ is the horizon depression, or horizon dip. At the optical horizon, the sky and the sea meet for this observer.

However we will have always $h_1 < 3\,\mathrm{km}$ and then $h_1/R \ll 1$ and correcting terms in h/R will be neglected. This is equivalent in Fig. 3.1 to taking $\sin\theta \sim \tan\theta \sim \theta$ and identifying the distances d_1 along the light path to the arc on the surface of the earth. This gives,

$$d_1 = \sqrt{2Rh_1} \tag{3.2}$$

Using the altitude in m and the distance in km, this gives the practical expression for a quick numerical evaluation,

$$d_1 \approx 3.57\sqrt{h_1} \tag{3.3}$$

The direction of the horizon defined as above, is no longer perpendicular to the local vertical and the excess is known as the *depression of the horizon* and denoted ϵ. We have

also $\theta = \epsilon$ and with $d_1 = R\theta$ this gives with (3.2),

$$\epsilon = \sqrt{\frac{2h_1}{R}} \tag{3.4}$$

which can be expressed numerically in degrees by,

$$\epsilon \approx 0.0321\,\sqrt{h_1} \tag{3.5}$$

Now the distance at which a peak of altitude h_2 is (geometrically) visible by an observer at h_1 in Nice is shown in Fig. 3.2.

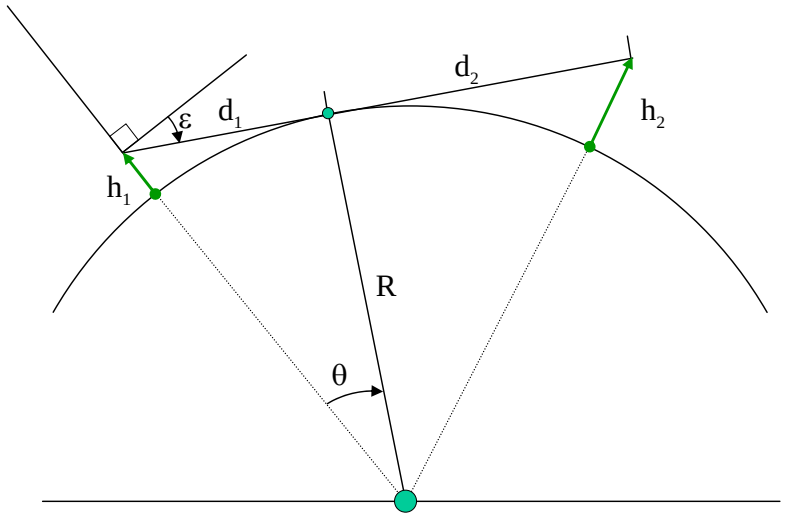


FIGURE 3.2: Distance of visibility between two points at respective altitudes h_1 and h_2 when light propagates in straight line. The maximum distance is determined by the grazing ray, tangent to the sea at the optical horizon.

It is is given by adding the two horizon distances $d = d_1 + d_2$, which leads for the mutual visibility condition,

$$d < \sqrt{2Rh_1} + \sqrt{2Rh_2} \tag{3.6}$$

When the distance d is given, as between Nice and Corsica, one can use (3.6) to find the smallest altitude h_2 visible from Nice at an altitude h_1. One has

$$h_2 > (\frac{d}{\sqrt{2R}} - \sqrt{h_1})^2 \tag{3.7}$$

Numerically with d in km, and the altitudes in metres,

$$h_2 > (0.28\,d - \sqrt{h_1})^2 \tag{3.8}$$

and even more specialised for Corsica with $d = 200\,\text{km}$,

$$h_2 > 3136(1 - 0.0178\sqrt{h_1})^2 \tag{3.9}$$

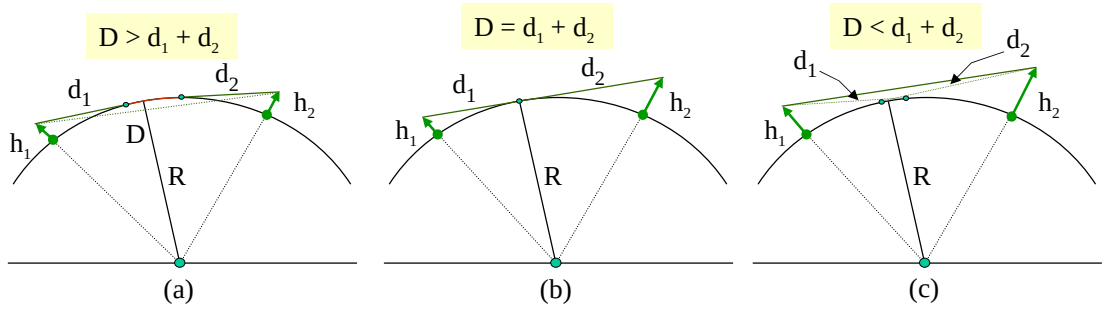


FIGURE 3.3: Condition of mutual visibility between two points at respective altitudes h_1 and h_2 and separated by a distance D. The distances to the respective horizons are d_1 and d_2. There is no inter-visibility in (a), horizon limited visibility in (b) and full inter-visibility above horizon in (c).

3.2 The flying rays

Still within the geometrical approximation of straight line propagation, I consider now a more general initial values problem with a light ray starting at an altitude h_1 in the direction $\epsilon \ll 1$ as illustrated in Fig. 3.4. This angle is counted positive below the horizontal plane and negative above. I will need also to consider the boundary values problem defined by the distance and altitudes of the end points, which for straight line propagation is just a particular case since the geometry is very simple. Although all the results can be obtained by elementary geometrical considerations, I use a less elegant, but more powerful, analytical approach, since it will be the natural way to handle the bent light-rays in the next section. Thus, both models develop along the same lines and it is very easy to see in the formulas where the refraction appears.

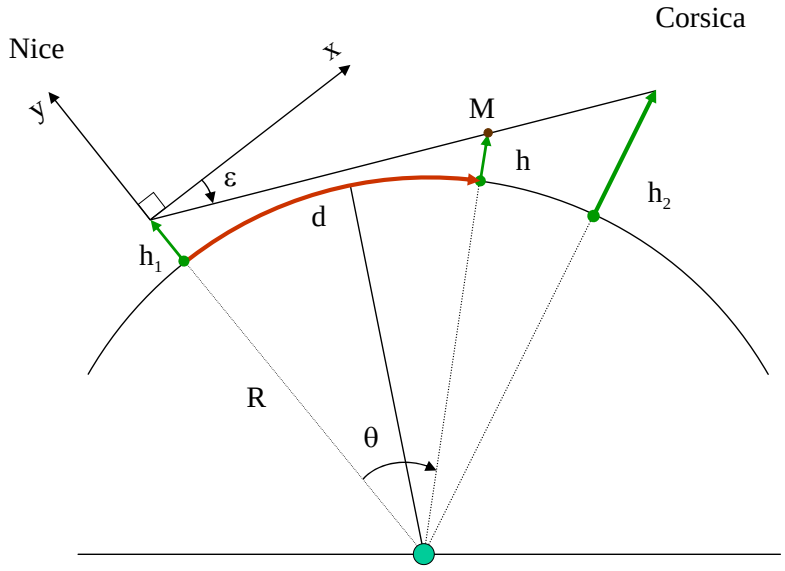


FIGURE 3.4: Light ray propagation in straight line from a point at an altitude h_1 and a direction ϵ below the horizontal plane. With the sign convention adopted in this note $\epsilon > 0$ in this configuration, when the ray starts below the horizontal plane.

3.2.1 Initial values problem

The equation of the straight line in the X, Y axes is given by,

$$y = h_1 - \epsilon x \tag{3.10}$$

The altitude h of a point $M(x, y)$ on the light ray is,

$$h = \left[x^2 + (y + R)^2\right]^{1/2} - R \tag{3.11}$$

or equivalently by expanding to first order in y/R,

$$h(x, y) = \frac{x^2 + 2Ry}{2R} \tag{3.12}$$

and by inserting (3.10),

$$h(x) = \frac{x^2 - 2R\epsilon x + 2Rh_1}{2R} \tag{3.13}$$

or equivalently,

$$\frac{h(x)}{R} = \frac{1}{2}\left(\frac{x}{R}\right)^2 - \epsilon\frac{x}{R} + \frac{h_1}{R} \tag{3.14}$$

where the quadratic term results from the reference to the curved earth surface.

Within the approximations of this work, one has $x \sim d$ and the above equation can be rewritten with the distance as independent parameter,

$$\boxed{\frac{h(d)}{R} = \frac{1}{2}\left(\frac{d}{R}\right)^2 - \epsilon\frac{d}{R} + \frac{h_1}{R}} \tag{3.15}$$

and using $r = R + h$ and $d = R\theta$, this gives the equation of the light ray in polar coordinates referred to the centre of the earth,

$$\frac{r(\theta)}{R} = \frac{1}{2}\theta^2 - \epsilon\theta + \frac{r_1}{R} \tag{3.16}$$

with $r_1 = R + h_1$.

Based on the expression (3.15) for the light ray, it is easy now to derive all the additional properties related to the visibility problem, when the influence of the refraction is neglected. However, it must be borne in mind that the analytical approach encompasses a large variety of cases illustrated in Fig. 3.5, most of them are not relevant for the Nice-Corsica visibility. The nominal case appears in Fig. 3.5-a, with the minimum altitude of the ray lying somewhere between the two end-points.

3.2.2 Boundary conditions problem

The light ray in (3.15) is determined by the starting point and the initial direction of the ray. It is also convenient to have the ray defined by the two end points altitudes h_1 and h_2 and their distance D, like a boundary values problem. By solving (3.15) for ϵ when $d = D$ and $h = h_2$ this yields,

$$\epsilon = \frac{1}{2}\frac{D}{R} - \frac{h_2 - h_1}{D} \tag{3.17}$$

and by inserting back into (3.15) one gets,

$$\boxed{\frac{h(d)}{R} = \frac{1}{2}\left(\frac{d}{R}\right)^2 - \left[\frac{1}{2}\frac{D}{R} - \frac{h_2 - h_1}{D}\right]\frac{d}{R} + \frac{h_1}{R}} \tag{3.18}$$

giving the altitude (positive or negative) of the light ray at a distance d from the start at altitude h_1. One can verify that $h(0) = h_1$ and $h(D) = h_2$. Stated differently, when the two end-points are given, the geometric direction of the ray from the starting point is given (3.17).

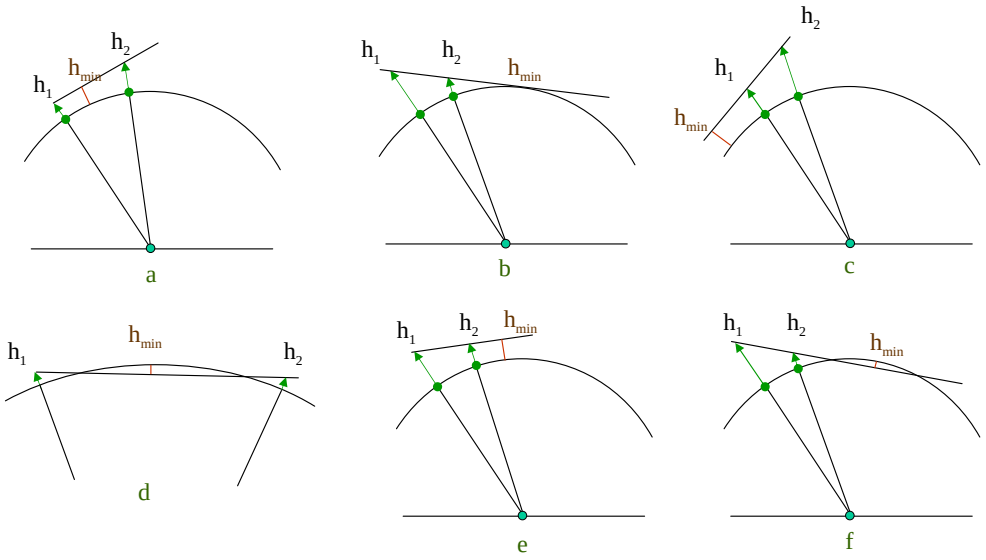


FIGURE 3.5: Possible configurations for light ray propagating in straight line between two points at altitude h_1 and h_2. The nominal situation for the visibility of Corsica from Nice is in the top left panel with the minimum altitude reached somewhere between the two ends points.

3.2.3 Lowest altitude

One considers two points of altitudes h_1 and h_2 separated by a distance D and joined by a light ray without refraction. The minimum altitude is obtained from the derivative with respect to d of (3.15) or (3.18).

The minimum altitude is reached for $d/R = \epsilon$, which is geometrically obvious since at this point the ray is perpendicular to the earth radius and $\theta = \epsilon$. With (3.17), this is equivalent to,

$$\frac{d_{\text{min}}}{R} = \frac{1}{2}\frac{D}{R} - \frac{h_2 - h_1}{D} \tag{3.19}$$

for the distance of the point with minimum altitude and then

$$\frac{h_{\text{min}}}{R} = \frac{h_1}{R} - \frac{1}{2}\left[\frac{1}{2}\frac{D}{R} - \frac{h_2 - h_1}{D}\right]^2 \tag{3.20}$$

or equivalently for the initial condition form,

$$\frac{h_{\text{min}}}{R} = \frac{h_1}{R} - \frac{\epsilon^2}{2} \tag{3.21}$$

For the two end-points to be in direct visibility, one needs that the light ray remains above the sea level all the way through its journey between the two points. Therefore, when the minimum altitude is reached between the two points, its must be positive. In Fig. 3.5, this corresponds to the case (a) and the condition is violated in case (d). There are no visibility problems (at least from the geometrical standpoint) in cases (b), (c), (e) and (f). let's focus on the canonical case for Nice-Corsica with the minimum altitude reached somewhere over the sea. This happens when,

$$0 < d_{\text{min}} < D \tag{3.22}$$

or with (3.19),

$$\frac{1}{2}\frac{D}{R} - \frac{h_2 - h_1}{D} > 0 \tag{3.23a}$$

$$\frac{1}{2}\frac{D}{R} + \frac{h_2 - h_1}{D} > 0 \tag{3.23b}$$

The first expresses the fact that ϵ is positive (the ray goes below the horizontal plane) and the second is always true when $h_2 > h_1$ and otherwise this is similar to (3.2) for the maximum distance. When these conditions are satisfied, the minimum altitude occurs between the two end-points, and the visibility condition reduces to

$$h_{\text{min}} > 0 \tag{3.24}$$

for the ray to be always above the sea level, or

$$\frac{h_1}{R} - \frac{1}{2}\left[\frac{1}{2}\frac{D}{R} - \frac{h_2 - h_1}{D}\right]^2 > 0 \tag{3.25}$$

and with (3.23a), this is equivalent to,

$$\sqrt{\frac{2h_1}{R}} > \frac{1}{2}\frac{D}{R} - \frac{h_2 - h_1}{D} \tag{3.26}$$

This is conveniently rewritten as,

$$D^2 - 2\sqrt{2Rh_1}D + 2Rh_1 < 2Rh_2 \tag{3.27}$$

or

$$(D - \sqrt{2Rh_1})^2 < 2Rh_2 \tag{3.28}$$

or equivalently,

$$-\sqrt{2Rh_2} < D - \sqrt{2Rh_1} < \sqrt{2Rh_2} \tag{3.29}$$

The left inequality is always true if $h_2 > h_1$, and in the opposite case one has the condition 3.23b $D > \sqrt{2R(h_1 - h_2)}$ which implies the left inequality in (3.29) since

$$\sqrt{2R(h_1 - h_2)} > \sqrt{2Rh_1} - \sqrt{2Rh_2} \tag{3.30}$$

when $h_1 > h_2$.

Finally this yields the more symmetrical expression for the constraint between D, h_1 and h_2 for the inter-visibility as,

$$\boxed{D < \sqrt{2Rh_1} + \sqrt{2Rh_2}} \tag{3.31}$$

fully identical to the initial geometric derivation of in (3.6). The analytical method is obviously more complex, but will readily extend to the case with refraction in the forthcoming section.

One must notice that with $h_1 = h_2 = 0$ a direct light ray between Corsica and Nice would go to $D^2/8R$ below the sea level, or for Nice-Corsica with $D \sim 200$ km a depth of 780 m.

TABLE 3.1: *Visibility of Corsica from Nice at the altitude h with light rays propagation in* **straight lines** *(no refraction). The distance between the two end points range from 190 to 205 km to cover all the situations for Corsica from Nice. The columns give the altitude of the observer, the distance to its optical horizon, the depression of the horizon below the horizontal plane and the lowest altitude visible for each distance. The figures tell that no part of Corsica would be visible from the sea level with straight line propagation. A similar table (table 4.1) is given in the next section with refracted rays*

h observer	horizon	depression	h visibility			
m	km	arcmin	m	m	m	m
			190 km	195 km	200 km	205 km
0	0.0	0.0	2830	2981	3135	3294
5	8.0	4.3	2597	2742	2890	3043
10	11.3	6.1	2503	2645	2791	2941
25	17.9	9.6	2323	2460	2601	2745
50	25.3	13.6	2127	2259	2394	2533
100	35.7	19.2	1866	1989	2116	2246
200	50.5	27.2	1525	1636	1752	1871
300	61.9	33.3	1287	1389	1496	1606
400	71.4	38.5	1102	1197	1296	1398
550	83.8	45.1	885	970	1059	1152
750	97.8	52.7	666	740	818	901
1000	112.9	60.9	465	528	594	664
1250	126.3	68.1	318	370	426	486
1500	138.3	74.6	209	252	298	348
2000	159.7	86.1	72	97	127	161
2500	178.6	96.2	10	21	36	55

TABLE 3.2: *Lowest altitude in m of a* **straight line light ray** *between a point in Corsica at altitude h_2 in m (columns) and an observer in Nice at altitude h_1 in m (line) and separated by a distance of 200 km. Values < 0 indicates the ray goes under the sea and that there is no mutual visibility. The light ray from the top of the Monte Cinto ($\sim$ 2700 m) observed at an altitude of 200 m near Nice would go as low as 168 m above the surface of the sea.*

h_1 \ h_2	0	500	1000	1250	1500	1750	2000	2250	2500	2700
0	-784	-554	-364	-283	-213	-153	-103	-63	-32	-15
5	-781	-551	-360	-280	-210	-149	-99	-58	-28	-10
10	-779	-548	-357	-276	-206	-145	-95	-54	-23	-6
25	-771	-539	-347	-266	-195	-134	-82	-41	-10	8
50	-759	-525	-331	-249	-177	-114	-62	-20	13	31
100	-735	-497	-298	-214	-140	-76	-22	23	57	77
200	-687	-441	-235	-147	-69	0	58	106	144	168
300	-641	-387	-173	-81	1	73	136	188	230	257
400	-597	-335	-113	-16	70	146	212	268	315	344
550	-533	-259	-25	77	169	251	323	386	438	473
750	-454	-164	86	196	296	386	467	537	597	638
1000	-364	-54	216	336	446	546	636	717	787	836
1250	-283	46	336	466	586	696	796	886	967	1023
1500	-213	136	446	586	716	836	946	1046	1136	1201
2000	-103	287	636	796	946	1086	1216	1336	1446	1527
2500	-32	397	787	967	1136	1296	1446	1586	1716	1813

TABLE 3.3: *Dip below the horizon in arcmin of the initial direction of* **straight line light ray** *between a point in Corsica at altitude h_2 in m (columns) and an observer in Nice at altitude h_1 in m (line) and separated by a distance of 200 km. Value larger than the horizon depression of table 3.1, means that the ray goes under the sea level. Negative values means the direction is above the horizontal plane. The straight line from a point near Nice at an altitude of $\sim$ 200 m to the top of the Monte Cinto ($\sim$ 2700 m) starts $11'$ below the horizontal plane and the top of the Monte Cinto lies below this plane (within this geometric approximation of the light propagation).*

h_1 \ h_2	0	500	1000	1250	1500	1750	2000	2250	2500	2700
0	54	45	37	32	28	24	20	15	11	7
5	54	45	37	32	28	24	20	15	11	8
10	54	45	37	33	28	24	20	15	11	8
25	54	46	37	33	29	24	20	16	11	8
50	55	46	38	33	29	25	20	16	12	8
100	56	47	38	34	30	26	21	17	13	9
200	57	49	40	36	32	27	23	19	14	11
300	59	50	42	38	33	29	25	20	16	13
400	61	52	44	39	35	31	26	22	18	14
550	63	55	46	42	38	33	29	25	20	17
750	67	58	50	45	41	37	32	28	24	20
1000	71	62	54	50	45	41	37	32	28	25
1250	75	67	58	54	50	45	41	37	32	29
1500	80	71	62	58	54	50	45	41	37	33
2000	88	80	71	67	62	58	54	50	45	42
2500	97	88	80	75	71	67	62	58	54	50

TABLE 3.4: *Angular height (in arcmin) above the optical horizon of a* **straight line light ray** *between a point in Corsica at altitude h_2 in m (columns) and an observer in Nice at altitude h_1 in m (line), situated 200 km apart. Values < 0 indicates the ray goes under the sea and that there is no mutual visibility. The top of the Monte Cinto ($\sim$ 2700 m) observed at an altitude of 200 m near Nice would be seen $16'$ above the optical horizon, but below the horizontal plane (within this geometric approximation of the light propagation).*

h_1 \ h_2	0	500	1000	1250	1500	1750	2000	2250	2500	2700
0	-54	-45	-37	-32	-28	-24	-20	-15	-11	-7
5	-50	-41	-32	-28	-24	-20	-15	-11	-7	-3
10	-48	-39	-31	-26	-22	-18	-14	-9	-5	-2
25	-45	-36	-28	-23	-19	-15	-10	-6	-2	2
50	-41	-33	-24	-20	-15	-11	-7	-2	2	5
100	-36	-28	-19	-15	-11	-6	-2	2	7	10
200	-30	-22	-13	-9	-4	0	4	9	13	16
300	-26	-17	-9	-4	0	4	9	13	17	21
400	-22	-14	-5	-1	4	8	12	16	21	24
550	-18	-10	-1	3	8	12	16	20	25	28
750	-14	-5	3	7	12	16	20	25	29	32
1000	-10	-2	7	11	16	20	24	28	33	36
1250	-7	1	10	14	18	23	27	31	36	39
1500	-5	3	12	16	21	25	29	34	38	41
2000	-2	6	15	19	24	28	32	36	41	44
2500	-1	8	17	21	25	29	34	38	42	46

4 Curved light rays: constant curvature

I include now the influence of the variable refractive index of the air on the light propagation between the two end-points. The light path is no longer a straight line, but is bent with a curvature determined by the gradient of the refractive index.

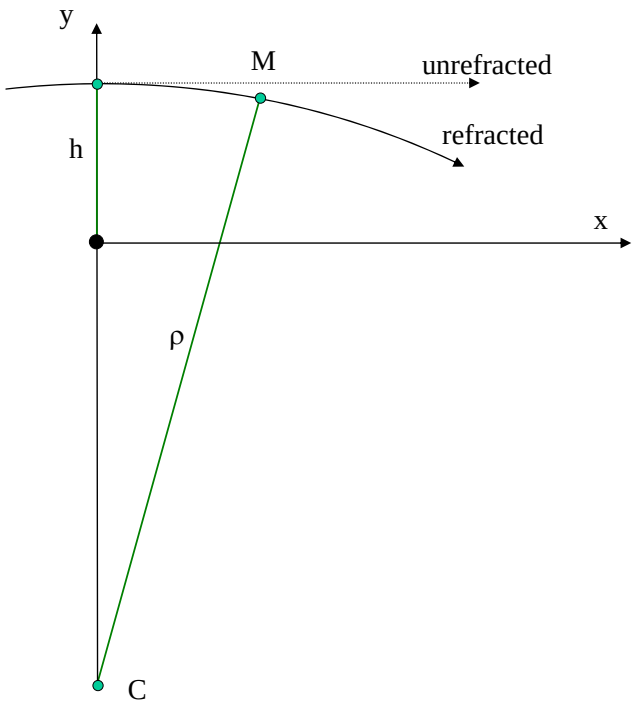


FIGURE 4.1: Refraction of a light ray starting horizontally from an altitude h and modelled with a circle path of radius ρ. In the earth atmosphere the curvature of the ray is about 0.14 that of the earth.

4.1 Empirical approach

For a homogeneous atmosphere with constant refractive index, the light propagates on a straight line. Due to the change of density of the air with altitude, resulting itself from a combination of the change in pressure and temperature, the refractive index of the air n is no longer constant and decreases slowly with altitude[1]. The main effect on the ray is to

[1] I am not considering here the extreme situations few metres above the surface of sea, when the water is warmer or colder than the air, leading to large positive or negative gradient of the refractive index and producing the inferior or superior mirages

curve the light path. The simplest departure from the straight line would be a circle, the curve with a constant curvature, as illustrated in Fig. 4.1, where in practice $\rho \gg h$, with $\rho \sim 5 \times 10^4$ km and $h \sim 1$ km.

In the coordinate system x, y the cartesian equation of the ray would be,

$$x^2 + (y - h + \rho)^2 = \rho^2 \tag{4.1}$$

and with $y \gg x$ and $\rho \gg h$, this reduces to,

$$y = h - \frac{x^2}{2\rho} \tag{4.2}$$

that is to say a parabola with curvature $1/\rho$ at the origin. If we take $\rho = 5 \times 10^4$ km and $x = 200$ km, the departure of the ray from the straight propagation is just 400 m. This would be the order of magnitude of the effect of refraction in increasing the range of altitudes of Corsica mountains visible from Nice. Allowing now for the curvature, Equation (3.10) for light ray starting with an inclination ϵ becomes,

$$\boxed{y = h_1 - \epsilon x - \frac{x^2}{2\rho}} \tag{4.3}$$

from which one could compute the altitude at any time and the visibility condition as in Sect. 3.2. What is needed now is the relationship between the curvature and the refractive index, which is the subject of the next sections, with an intuitive derivation first, followed by a full mathematical solution of the rigourous propagation equation.

4.2 Refraction and curvature of light rays

As said earlier, the refractive index in the atmosphere depends primarily on the altitude. While the curvature of the earth is important for the geometry as shown in Sect. 3.2, the refraction is a smaller effect superimposed to the effect of the earth overall shape. For propagation over few 100s km, a simple model with a plane-parallel atmosphere is sufficient to obtain a good approximation of the light path. Imagine the atmosphere as consisting of horizontal strata with refractive index $n_0, n_1, \ldots, n_k$ as shown in Fig. 4.2. The refractive index decreases with height, with n_0 being its value at the top. Applying the Snell's law at each interface between two layers yields,

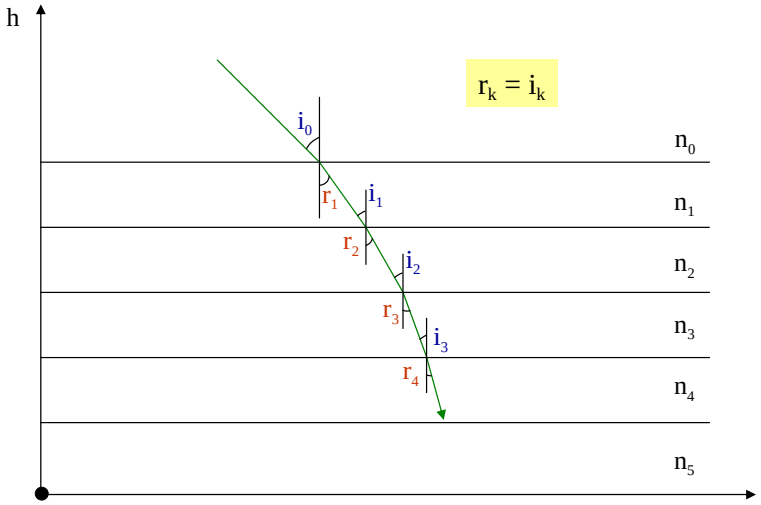


FIGURE 4.2: Refraction of a light ray in a atmosphere stratified in horizontal planes. The quantity $n\,sini$ remains constant during the propagation.

$$n_0 \sin i_0 = n_1 \sin r_1 \tag{4.4a}$$

$$n_1 \sin i_1 = n_2 \sin r_2 \tag{4.4b}$$

$$\vdots \quad = \quad \vdots \tag{4.4c}$$

$$n_{k-1} \sin i_{k-1} = n_k \sin r_k \tag{4.4d}$$

and with the plane-parallel assumption,

$$r_k = i_k \tag{4.5}$$

leading to the conservation equation along the path,

$$n(h) \sin i = cte \tag{4.6}$$

While this may lead to the first order differential equation of the trajectory, it is more interesting to use this equation to derive directly the expression of the curvature of the ray as a function of the rate of change of the refractive index. Just apply this equation to the nearly horizontal ray shown in Fig. 4.3. The radius of curvature is ρ and between two

nearby points one has to first order,

$$\delta s = \rho \, \delta i \tag{4.7}$$

where δs is the curvilinear distance between the two points on the light ray. By differentiating now (4.6) one finds,

$$\frac{dn}{dh} \sin i \, \delta h + n(h) \, \cos i \, \delta i = 0 \tag{4.8}$$

or with $i \sim \pi/2$, $n(h) \sim 1$ in the earth atmosphere and,

$$\delta h \sim \delta s \, \cos i \sim \rho \cos i \, \delta i \tag{4.9}$$

this yields,

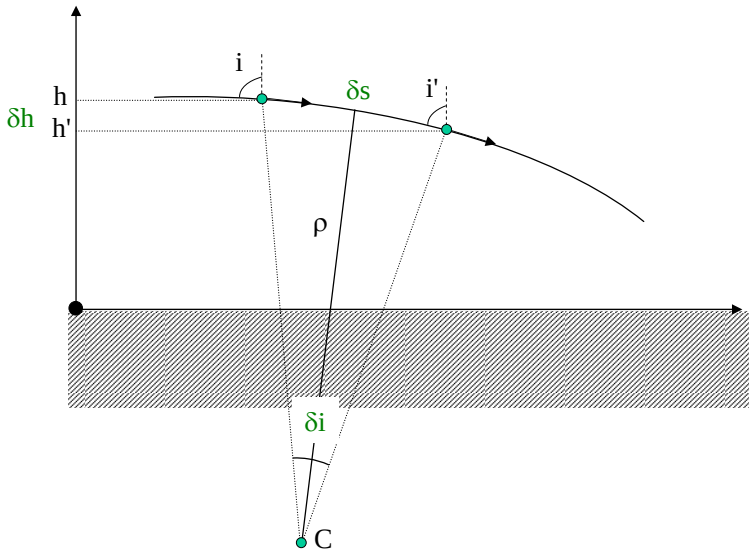


FIGURE 4.3: Refraction of nearly horizontal light ray in a stratified atmosphere with the refractive index changing with altitude. The radius of curvature ρ is such that $\rho \, di = ds$, the arc between the two points.

$$\boxed{\frac{dn}{dh} = -\frac{1}{\rho}} \tag{4.10}$$

relating the curvature of the light-ray to the vertical gradient of the refractive index. By denoting $\alpha = -dn/dh$, so that $\alpha > 0$, we have for the earth atmosphere in normal condition, $\alpha = 2.5 \times 10^{-5}$ km^{-1}. One can now rewrite (4.3),

$$\boxed{y = h_1 - \epsilon x - \frac{\alpha}{2} x^2} \tag{4.11}$$

and with (3.15) on has the equivalent expression for the altitude along the refracted light path as,

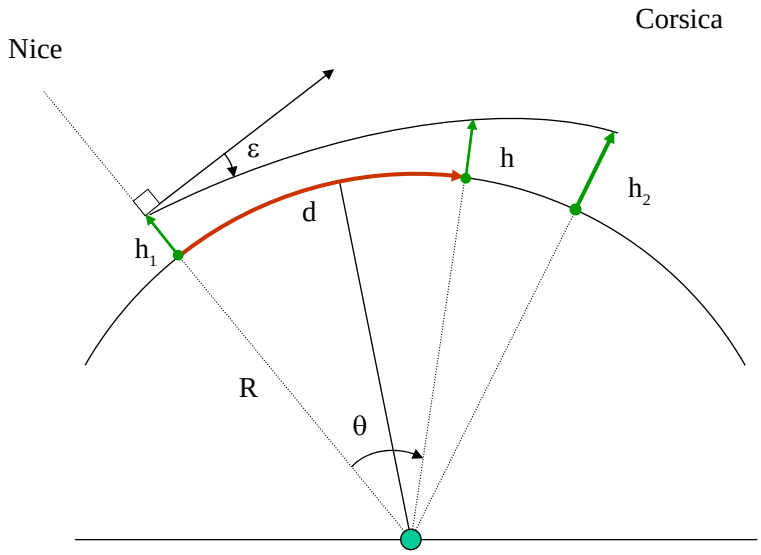


FIGURE 4.4: Light propagation of a refracted ray from a point of altitude h_1, staring in the direction ϵ, counted positive below the horizontal plane. Equation (4.12) gives the expression of $h(d)$ as a function of the initial conditions.

$$\boxed{\frac{h(d)}{R} = \frac{1 - \alpha\, R}{2} \left(\frac{d}{R}\right)^2 - \epsilon \frac{d}{R} + \frac{h_1}{R}} \tag{4.12}$$

with the correcting term $1 - \alpha\, R \sim 0.84$ in comparison with the propagation without refraction. Since α is the curvature of the light-ray, then the dimensionless quantity $\alpha\, R$ is the ratio between the radius of the earth and the radius of curvature of the ray, or the inverse of the radius of curvature of the light ray measured with the earth radius. In all the subsequent formulas, the $\alpha\, R$ term will account for the atmospheric refraction (more accurately: for the change of the refractive index with altitude).

The light-ray in (4.12) is defined by the initial conditions at the starting point h_1, ϵ, and as for the geometric approximation, it is easy to handle the more important case with boundary conditions, when the ray goes through two end points at altitudes h_1, h_2 separated by the distance D. Solving (4.12) for ϵ we have,

$$\epsilon = \frac{(1-\alpha\,R)}{2}\,\frac{D}{R} - \frac{h_2-h_1}{D} \tag{4.13}$$

giving the direction of the lightray at the starting point and finally the equation of the light path determined by the boundary conditions,

$$\boxed{\frac{h(d)}{R} = \frac{1-\alpha\,R}{2}\left(\frac{d}{R}\right)^2 - \left[\frac{1-\alpha\,R}{2}\frac{D}{R} - \frac{h_2-h_1}{D}\right]\frac{d}{R} + \frac{h_1}{R}} \tag{4.14}$$

This gives the altitude (positive or negative) of the light ray at a distance d from the start at altitude h_1 for a ray going through a point of altitude h_2 at a distance D. One can verify that $h(0) = h_1$ and $h(D) = h_2$.

Now for the lowest altitude, the derivation is identical as in the case of the geometric ray. The distance at which the minimum altitude is reached is,

$$\frac{d_{\text{min}}}{R} = \frac{1}{1-\alpha\,R}\left[\frac{(1-\alpha\,R)}{2}\,\frac{D}{R} - \frac{h_2-h_1}{D}\right] \tag{4.15}$$

or in terms of the initial direction,

$$\frac{d_{\text{min}}}{R} = \frac{\epsilon}{1-\alpha\,R} \tag{4.16}$$

Then by inserting (4.15) in (4.14) we have for the minimum altitude along the a refracted ray linking to points with distance D and at respective altitudes h_1 and h_2 ,

$$\frac{h_{\text{min}}}{R} = \frac{h_1}{R} - \frac{1}{2(1-\alpha\,R)}\left[\frac{1-\alpha\,R}{2}\frac{D}{R} - \frac{h_2-h_1}{D}\right]^2 \tag{4.17}$$

or equivalently for the initial condition form,

$$\frac{h_{\text{min}}}{R} = \frac{h_1}{R} - \frac{\epsilon^2}{2(1-\alpha\,R)} \tag{4.18}$$

While these equations have been obtained using very intuitive arguments, in particular by handling independently the curvature from the refraction and the effect of the curvature

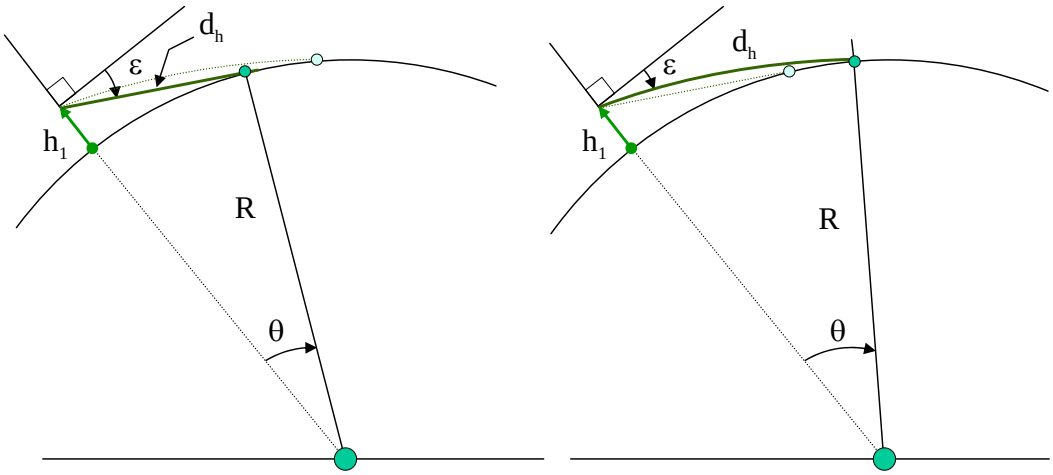


FIGURE 4.5: Comparison of the light ray propagation between the geometric model (left) and the optical (right). For a given altitude h_1 of the observer the diagram shows the distance to the horizon d_h, the place where a light ray starting from the observer at h_1 grazes the earth. The distance is increased by refraction while the depression to the horizontal plan is smaller. Also while we have $\theta = \epsilon$ in the straight line propagation this is no longer true with refraction, where $\theta > \epsilon$.

of the earth, it is shown in the next section that this is in fact the solution of the light propagation in a radially symmetric atmosphere when n depends only on the distance to the centre of the earth.

As a straightforward application one can recompute the distance of the horizon and its depression for an observer located at altitude h_1, as done in Sect. 3.1 for the propagation in straight lines. Using (4.12) with $h_1 = 0$ and $\epsilon = 0$ we have the altitude of the ray after it has propagated over a distance d,

$$\frac{h(d)}{R} = \frac{1 - \alpha\, R}{2} \left(\frac{d}{R}\right)^2 \tag{4.19}$$

or equivalently the horizon distance d_h for an observer at altitude h_1,

$$d_h = \sqrt{\frac{2Rh_1}{1 - \alpha\, R}} \tag{4.20}$$

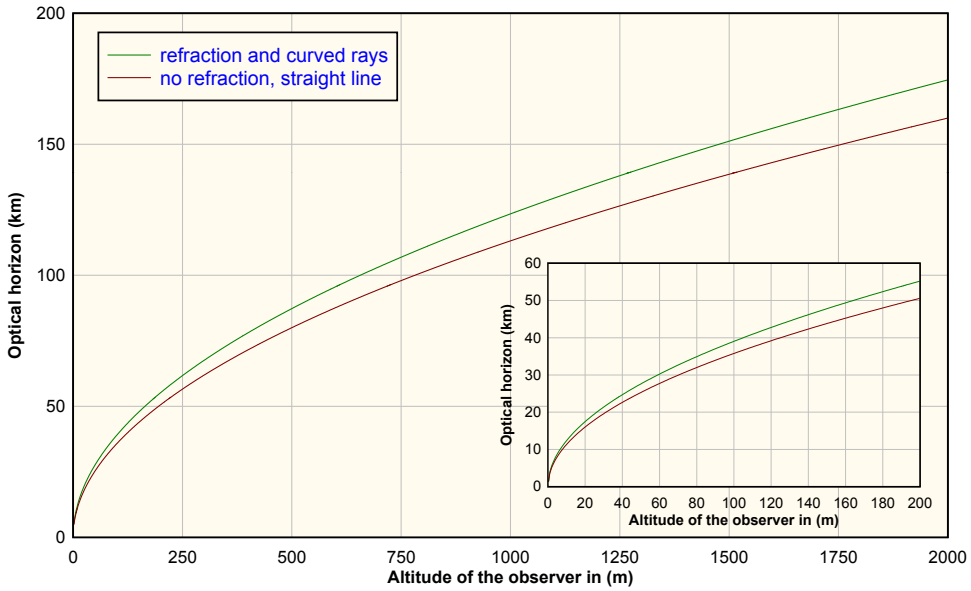


FIGURE 4.6: Comparison of the distances to the optical horizon for an observer at the height h according to the light propagation model. The distance of visibility is larger with refraction than without. Inset: magnification around $h = 0$. The horizon distance increases quickly, as $\sqrt{h}$, near the sea level.

which is larger by a factor $1/\sqrt{1-\alpha\,R}$ from that derived in (3.2) without refraction. This expression for the horizon with refraction appears already in the theorem XXXI in the treatise of J.H. Lambert [2] on the *Les propriétés remarquables de la route de la lumière par les airs* printed in 1758 and whose title page is shown in Fig. 4.7. The result became classic in surveying with $\alpha\,R \sim 1/7$ and can also be found in `http://williams.best.vwh.net/avform.htm#Altimetry` with reference to the *American Practical Navigator* of Bowditch, whose first edition can be traced to 1802 and is still updated and regularly reissued by the Hydrographic Office of the US Navy. Note that Lambert derivation is essentially of mathematical nature with the introduction of a curvature whose radius, or equivalently $\alpha\,R$ is determined with observations.

Using the altitude in m and the distance in km, this gives the practical expression for a quick numerical evaluation,

$$d_h \approx 3.90\sqrt{h_1} \tag{4.21}$$

[2] European mathematician born in Mulhouse in 1728 and died in Berlin in 1777. He introduced hyperbolic functions in trigonometry, investigated the parallel axiom and proved that π is an irrational number. He worked on perspective and geometrical optics, on the motion of comets and the general structure of the Universe and introduced several map projections that still are named after him.

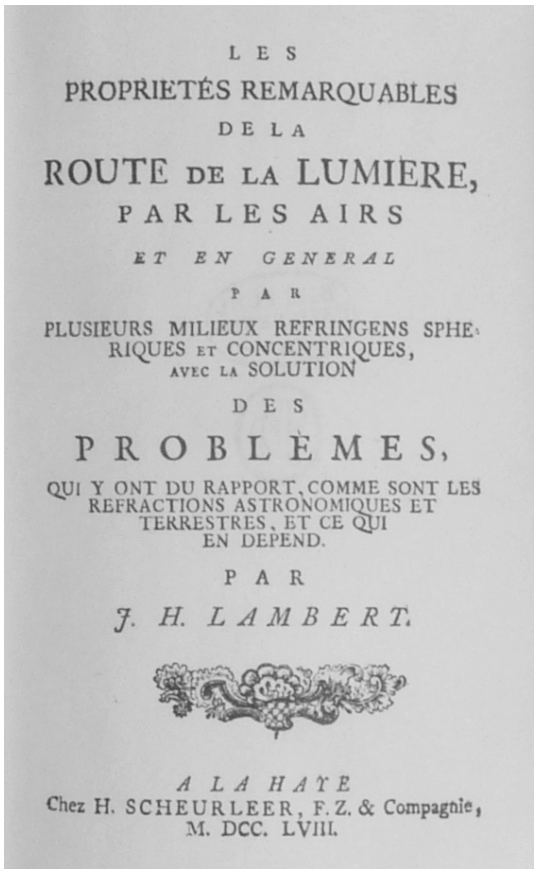

LES
PROPRIETÉS REMARQUABLES
DE LA
ROUTE DE LA LUMIÈRE,
PAR LES AIRS
ET EN GENERAL
PAR
PLUSIEURS MILIEUX REFRINGENS SPHERIQUES ET CONCENTRIQUES,
AVEC LA SOLUTION
DES
PROBLÈMES,
QUI Y ONT DU RAPPORT, COMME SONT LES REFRACTIONS ASTRONOMIQUES ET TERRESTRES, ET CE QUI EN DEPEND.
PAR
J. H. LAMBERT.
A LA HAYE
Chez H. SCHEURLEER, F. Z. & Compagnie,
M. DCC. LVIII.

FIGURE 4.7: Title page of J.H. Lambert monograph on the path of the light rays in the air, published in 1758.

The direction to horizon is derived similarly by solving for ϵ_{H} when $h = 0$ at the distance d_h. This gives,

$$\epsilon_{\mathrm{H}} = \sqrt{\frac{2h_1}{R}\,(1 - \alpha\,R)} \tag{4.22}$$

which can be expressed numerically in degrees by,

$$\epsilon_{\mathrm{H}} \approx 0.0294\,\sqrt{h_1} \tag{4.23}$$

with h_1 in m. As expected, this is smaller than (3.5) for straight line propagation.

The angular altitude δ (Fig. 4.9) above the optical horizon of a point of altitude h_2 seen at the distance D at the altitude h_1 is obtained by combining (4.13) and (4.22)

$$\delta = \epsilon_{\mathrm{H}} - \epsilon = \sqrt{\frac{2h_1}{R}\,(1 - \alpha\,R)} + \frac{h_2 - h_1}{D} - \frac{(1 - \alpha\,R)}{2}\,\frac{D}{R} \tag{4.24}$$

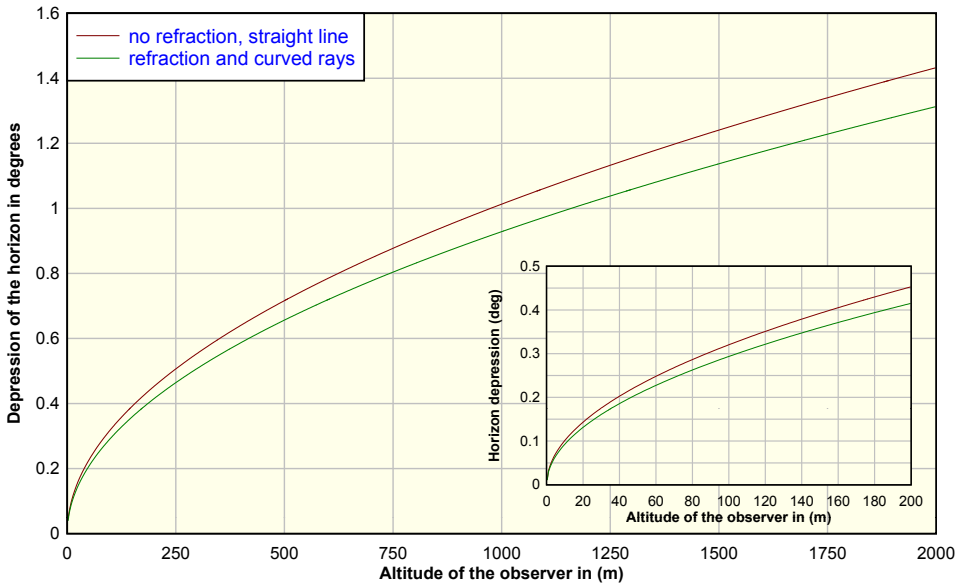


FIGURE 4.8: Comparison of the dips of the horizon edge for an observer at the height h according to the light propagation model. The horizon depression is smaller with curved rays than with straight lines. Inset: magnification around $h = 0$. When a sunrise (or sunset) is observed from an altitude higher than $\sim$ 200 m, the upper limb of the solar image is below the horizontal plane.

or numerically with δ in **arcmin**, altitudes in **m** and distance in **km**,

$$\delta = 1.761\,\sqrt{h_1} + 3.44\,\frac{h_2 - h_1}{D} - 0.225\,D \tag{4.25}$$

where δ is positive when h_2 is seen above the horizon.

Finally the distance of visibility shown in Fig. 4.10 between two points of respective altitudes h_1 and h_2 is obtained by adding the two horizon distances,

$$d = \sqrt{\frac{2Rh_1}{1-\alpha\,R}} + \sqrt{\frac{2Rh_2}{1-\alpha\,R}} \tag{4.26}$$

For Nice and Corsica with $d = 200$ km, and the altitudes in metres this gives the visibility condition,

$$51.0 < \sqrt{h_1} + \sqrt{h_2} \tag{4.27}$$

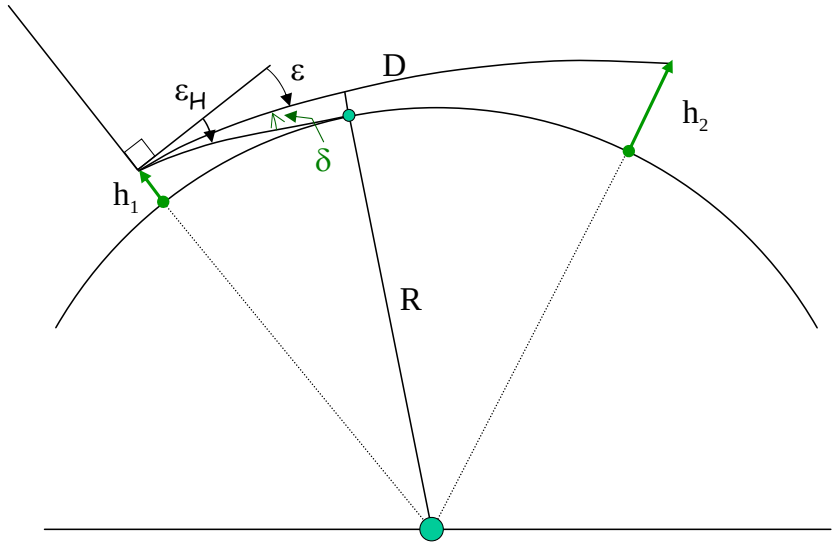


FIGURE 4.9: Elevation δ above the optical horizon of a feature at altitude h_2 seen from the distance D and altitude h_1. The analytical expression of δ is given in (4.24) and is applied in Sect. 13 to the Corsica landscape features visible from Nice.

When the distance d is given, as between Nice and Corsica, one can use (4.26) to find the smallest altitude h_2 visible from Nice for an observer located at an altitude h_1. One has

$$h_2 > \left(d\sqrt{\frac{1-\alpha\,R}{2R}} - \sqrt{h_1} \right)^2 \tag{4.28}$$

which with again d in **km** and h in **m** yields,

$$h_2 > (0.257\,d - \sqrt{h_1})^2 \tag{4.29}$$

or for Corsica with $d = 200\,\mathrm{km}$,

$$h_2 > 2634(1 - 0.0195\sqrt{h_1}) \tag{4.30}$$

4.2.1 Terrestrial refraction

The term *terrestrial refraction* refers to the displacement (upward in general) of the images of terrestrial objects from their geometric direction by the atmospheric refraction.

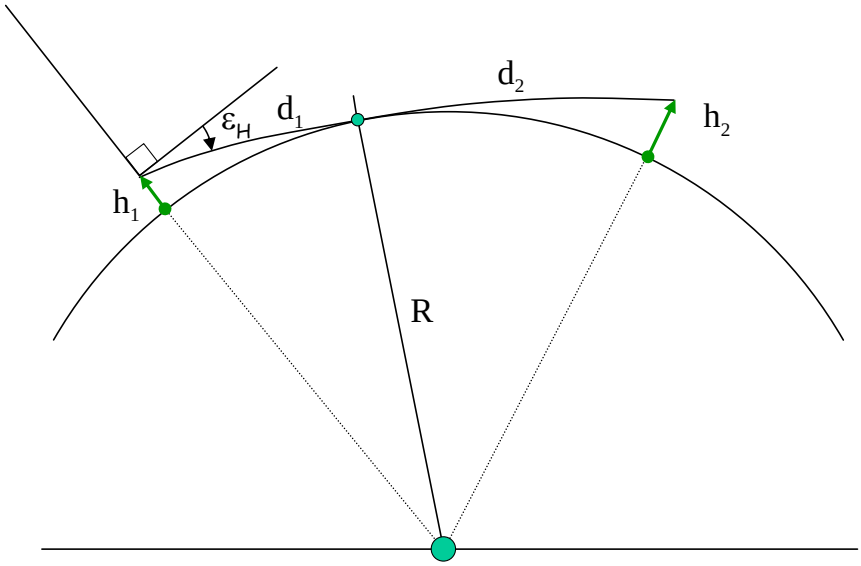


FIGURE 4.10: Maximum distance of visibility between two points at respective altitude h_1 and h_2 when refraction bends the light ray.

This is a very important topic in surveying and terrestrial geodesy and concerns primarily directions near the horizontal plane. It differs from astronomical refraction which deals with sources outside the atmosphere, with rays crossing the atmosphere in any direction and reaching the top of the atmosphere. The approximations made to compute terrestrial refraction, do not allow to extend the distance to infinity with the hope of ending with astronomical refraction. This simply does not work.

Therefore the terrestrial refraction is the angle between the directions of the incoming refracted ray and the straight line ray between an object and the observer. This is then the difference between (3.17) and (4.13) or,

$$r = \frac{\alpha D}{2} \tag{4.31}$$

a very simple expression with a simple interpretation with the help of Fig. 4.11. One might be tempted to define the terrestrial refraction by the total deflection of the tangent (how much it has rotated) along the ray between its starting direction at h_2 and its final direction at h_1. This is clearly an effect of refraction, but something not measurable and of little interest for the observer. Nonetheless for the regular rays I have considered, with nearly constant curvature, this angle is easily determined: since the distance between the

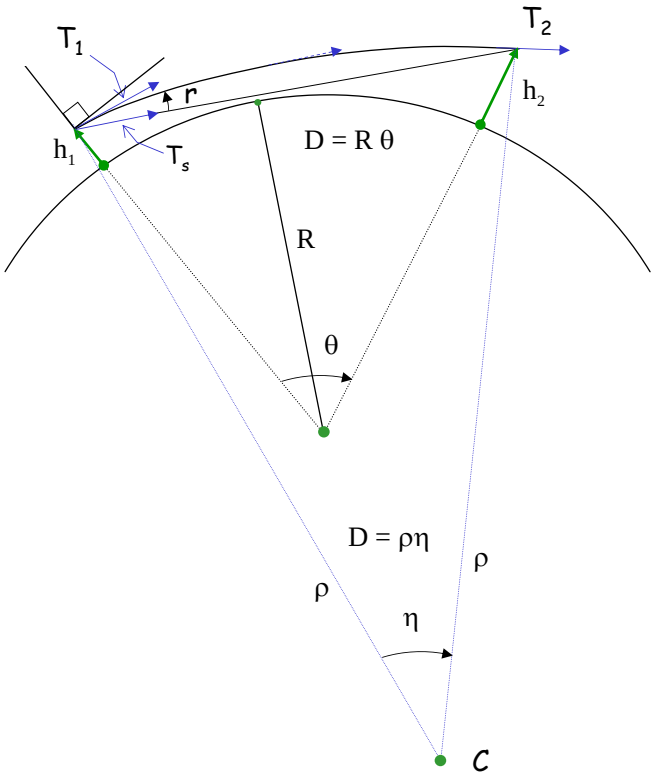


FIGURE 4.11: The terrestrial refraction is the angle r between the direction of the tangent $\mathbf{T}_1$ along the refracted ray and the direction $\mathbf{T}_s$ along the geometric straight line to the object. The centre of curvature of the light ray is C and the corresponding radius ρ.

two end-points is D and that the ray is an arc of circle whose radius is $\rho = 1/\alpha$, the angle between the tangents at the arc ends is just, $\eta = D/\rho = \alpha\, D$. Now the tangent on the ray at about $D/2$ is parallel to the geometric straight line, which gives exactly the expression (4.31). Essentially the terrestrial refraction is half the light deflection over the distance travelled between the object and the observer. Conversely, in astronomical refraction, this is equal to the total deflection along the light ray from outside the atmosphere to the observer. This is a significant difference that must be kept in mind. This difference is very similar to the one in the relativistic light deflection of a light ray by the sun, according as it refers to a star at very large distance compared to the astronomical unit, or to a minor planet within the solar system.

The application of (4.31) to a Nice-Corsica ray gives $r \sim 8.5'$. The mountains are raised by about $8'$ above their geometric directions, but this cannot be evidenced and is of no im-

portance for the visibility conditions (since the optical horizon shares a large part of this effect). What matter have been discussed earlier, namely where the optical horizon lies and how large the angular height of the object above this line is. With the same formula we can estimate the astronomical refraction at the horizon with a simple argument. An atmosphere with constant density would have a height of about $h_a \sim 8.5\,\mathrm{km}$, and an horizontal ray would have to cross an atmospheric depth of $\sqrt{2Rh_a}$ to reach its border. Now the deflection of the ray in the course of its journey would be $\alpha\sqrt{2Rh_a} \sim 28.5$ arcmin, a surprisingly good result, since the true value is $33'$, when computed by integrating the ray with a comprehensive atmospheric model and from the exact propagation equation derived in Sect. 5.

TABLE 4.1: *Visibility of Corsica from Nice at the altitude h with* **curved light rays** *due to the variation of the refractive index with the altitude. Distances between the two end points from 190 to 205 km. The columns give the altitude of the observer, the distance to its optical horizon, the depression of the horizon below the horizontal plane and the lowest altitude visible for each distance. The figures must be compared to those in table 3.1 to see the role of the refraction to enhance the visibility. The Monte Cinto (2700 m, ∼ 200 km) is visible, albeit marginally, from the coastline thanks to refraction and is not in straight line.*

h observer	horizon	depression	h visibility			
m	km	arcmin	m	m	m	m
			190 km	195 km	200 km	205 km
0	0.0	0.0	2379	2505	2635	2769
5	8.7	3.9	2165	2287	2411	2539
10	12.3	5.6	2080	2199	2321	2446
25	19.5	8.8	1916	2030	2147	2268
50	27.5	12.5	1739	1847	1959	2075
100	39.0	17.6	1503	1604	1709	1817
200	55.1	25.0	1199	1290	1383	1481
300	67.5	30.6	989	1071	1157	1246
400	77.9	35.3	828	903	982	1064
550	91.4	41.4	641	708	778	851
750	106.7	48.3	457	514	574	637
1000	123.2	55.8	294	340	389	441
1250	137.7	62.4	180	216	255	298
1500	150.9	68.4	101	128	159	193
2000	174.2	78.9	16	28	44	62
2500	194.8	88.2	0	0	2	7

TABLE 4.2: *Lowest altitude in m of a* **refracted light ray** *between a point in Corsica at altitude h_2 in m (columns) and an observer in Nice at altitude h_1 in m (line) and separated by a distance of 200 km. Values < 0 indicates the ray goes under the sea and that there is no mutual visibility. The light ray from the top of the Monte Cinto (~ 2700 m) observed at an altitude of 200 m near Nice goes as low as 198 m above the surface of the sea.*

h_1 \ h_2	0	500	1000	1250	1500	1750	2000	2250	2500	2700
0	-659	-433	-254	-182	-122	-74	-38	-14	-2	0
5	-656	-430	-250	-178	-118	-70	-34	-9	3	5
10	-654	-427	-247	-175	-114	-66	-30	-5	8	10
25	-646	-418	-237	-164	-103	-54	-16	9	23	25
50	-634	-403	-219	-145	-83	-33	5	32	47	50
100	-610	-374	-186	-109	-45	8	49	78	95	100
200	-563	-317	-120	-38	31	88	134	167	189	198
300	-517	-263	-55	31	105	167	217	255	282	295
400	-474	-210	7	98	176	243	298	341	373	389
550	-413	-134	97	195	281	355	417	467	505	528
750	-337	-40	210	317	413	496	568	628	676	705
1000	-254	67	341	460	567	663	746	818	878	917
1250	-182	163	460	591	710	817	913	996	1068	1117
1500	-122	246	567	710	841	960	1067	1163	1246	1305
2000	-38	378	746	913	1067	1210	1341	1460	1567	1645
2500	-2	462	878	1068	1246	1413	1567	1710	1841	1937

TABLE 4.3: *Dip below the horizon in arcmin of the initial direction of* **refracted light ray** *between a point in Corsica at altitude h_2 in m (columns) and an observer in Nice at altitude h_1 in m (line)and separated by a distance of 200 km. Value larger than the horizon depression of table 4.1, means that the ray goes under the sea level. Negative values means the direction is above the horizontal plane. The light ray from the top of the Monte Cinto ($\sim$ 2700 m) observed at an altitude of 200 m near Nice starts 2′ below the horizontal plane, and then the top of the Monte Cinto is below this plane.*

h_1 \ h_2	0	500	1000	1250	1500	1750	2000	2250	2500	2700
0	45	37	28	24	20	15	11	7	2	-1
5	45	37	28	24	20	15	11	7	2	-1
10	45	37	28	24	20	15	11	7	3	-1
25	46	37	29	24	20	16	11	7	3	-1
50	46	38	29	25	20	16	12	7	3	0
100	47	38	30	26	21	17	13	8	4	1
200	49	40	32	27	23	19	14	10	6	2
300	50	42	33	29	25	20	16	12	7	4
400	52	44	35	31	26	22	18	14	9	6
550	55	46	38	33	29	25	20	16	12	8
750	58	50	41	37	32	28	24	20	15	12
1000	62	54	45	41	37	32	28	24	20	16
1250	67	58	50	45	41	37	32	28	24	20
1500	71	62	54	50	45	41	37	32	28	25
2000	80	71	62	58	54	50	45	41	37	33
2500	88	80	71	67	62	58	54	50	45	42

TABLE 4.4: *Angular height (in arcmin) above the optical horizon of a* **refracted light ray** *between a point in Corsica at altitude h_2 in m (columns) and an observer in Nice at altitude h_1 in m (line), situated 200 km apart. Values < 0 indicates the ray goes under the sea and that there is no mutual visibility. The top of the Monte Cinto ($\sim$ 2700 m) observed at an altitude of 200 m near Nice is seen $23'$ above the optical horizon, but below the horizontal plane.*

h_1 \ h_2	0	500	1000	1250	1500	1750	2000	2250	2500	2700
0	-45	-37	-28	-24	-20	-15	-11	-7	-2	1
5	-41	-33	-24	-20	-16	-11	-7	-3	2	5
10	-40	-31	-23	-18	-14	-10	-6	-1	3	7
25	-37	-28	-20	-15	-11	-7	-3	2	6	10
50	-34	-25	-16	-12	-8	-4	1	5	9	13
100	-29	-21	-12	-8	-4	1	5	9	14	17
200	-24	-15	-7	-2	2	6	11	15	19	23
300	-20	-11	-3	2	6	10	14	19	23	27
400	-17	-8	0	5	9	13	17	22	26	30
550	-13	-5	4	8	12	17	21	25	30	33
750	-10	-1	7	12	16	20	25	29	33	37
1000	-7	2	11	15	19	23	28	32	36	40
1250	-4	4	13	17	21	26	30	34	39	42
1500	-3	6	14	19	23	27	32	36	40	44
2000	-1	8	16	21	25	29	34	38	42	46
2500	0	9	17	21	26	30	34	39	43	46

5 Curved light rays: full derivation

5.1 General equation

The basic equation for the propagation of light rays can be derived from the Fermat principle, stating that the actual path followed by the light in a medium of refractive index $n(\mathbf{r})$ has the shortest optical path among all the other rays joining the same end points. It is shown in advanced textbooks in optics, *e.g.* Born and Wolf, Sect. 3.2, that this leads to the second order differential equation,

$$\frac{d(n\mathbf{T})}{ds} = \nabla n(\mathbf{r}) \tag{5.1}$$

where $\mathbf{T}$ is the tangent vector at $\mathbf{r}$ on the ray. For a homogenous medium with constant refractive index n, the general solution of (5.1) reduces to,

$$\mathbf{r} = s\,\mathbf{u} + \mathbf{v} \tag{5.2}$$

$\mathbf{u}$ and $\mathbf{v}$ being two constant vectors. The path represented by (5.2) is a straight line parallel to $\mathbf{u}$ and going through $\mathbf{r} = \mathbf{v}$ at $s = 0$.

5.2 Spherical symmetry

When the expression of $n(\mathbf{r})$ is without symmetry or has a complex behaviour, numerical methods, known as ray tracing in optical instrument trade, are used to compute the trajectory of the light, nominally between the object and the image. We are interested here in the case of a spherically symmetric system where the refractive index depends only on the distance to the centre of the earth, that is to say $n(\mathbf{r}) = n(r)$. It is very general that to an invariance under a symmetry is associated a conservation law, which for differential equations takes the form of a first integral. Guided by the conservation of angular momentum in the motion under central forces it is natural to look at the quantity,

$$n\mathbf{r} \times \mathbf{T} \tag{5.3}$$

Its variation along the ray is given by,

$$\frac{d\mathbf{r}}{ds} \times n\mathbf{T} + \mathbf{r} \times \frac{d(n\,\mathbf{T})}{ds} \tag{5.4}$$

Since $\mathbf{T} = d\mathbf{r}/ds$, the first term vanishes, and with the propagation equation (5.1) and $n = n(r)$, the second term is also equal to zero. Therefore in the propagation in a spherically symmetric medium one has

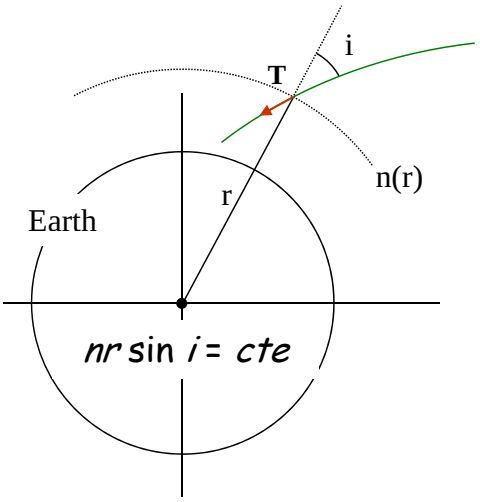


FIGURE 5.1: The Bouguer invariant based on the first integral (5.5).

$$n\mathbf{r} \times \mathbf{T} = \mathbf{C} \tag{5.5}$$

where $\mathbf{C}$ is a constant vector determined by the initial conditions. This is equivalent to the Bouguer [3] invariant along the ray, (Fig. 5.1),

$$n\, r\, \sin i = C \tag{5.6}$$

Now in polar coordinates with origin at the centre of the earth, the components of the unit tangent vector are,

$$T_r = \frac{r'}{(r^2 + r'^2)^{1/2}} \tag{5.7}$$

$$T_\theta = \frac{r}{(r^2 + r'^2)^{1/2}} \tag{5.8}$$

with $r' = dr/d\theta$. Inserting in (5.5) this yields,

[3] Pierre Bouguer, French hydrographer and mathematician $(1698 - 1758)$ who worked on the theory of ships and navigation and participated in the mission sent by the French Academy of Sciences to Peru to determine the length of a degree of meridian near the equator in order to assess the overall shape of the Earth. He is also one the founders of the science of photometry, with his treatise *Traité d'Optique sur la Gradation de la Lumière, Paris 1760.*

$$\frac{nr^2}{(r^2+r'^2)^{1/2}} = C \tag{5.9}$$

which can be resolved in r' to obtain the differential equation of the trajectory,

$$\frac{dr}{d\theta} = \eta\, r \left[\frac{n^2 r^2}{C^2} - 1\right]^{1/2} \tag{5.10}$$

where $\eta = \pm 1$. The solution reduced to a quadrature [4]

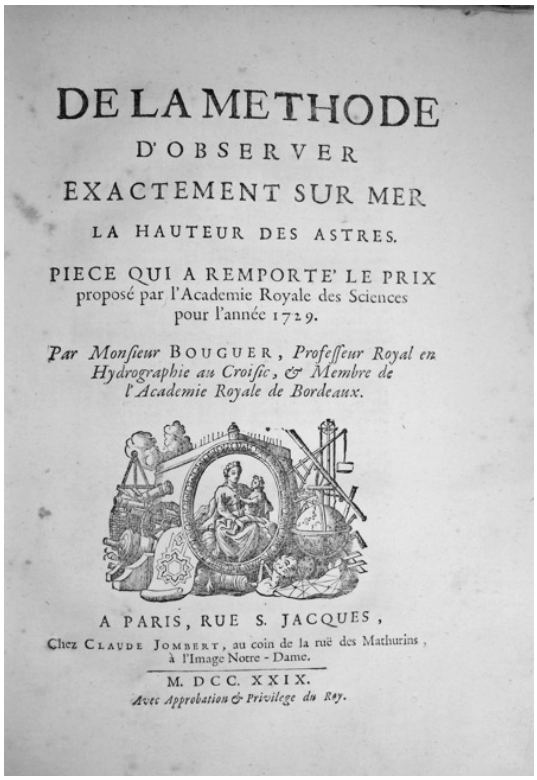
$$\boxed{\int_0^\theta d\theta \quad = \quad \eta \int_{r_0}^{r} \frac{dr}{r\left(\frac{n^2r^2}{C^2} - 1\right)^{1/2}}} \tag{5.11}$$

The presence of a sign indetermination in η follows for a root taking and the necessity to chose the branch with positive or negative sign of $dr/d\theta$. Eventually a square will appear later removing this ambiguity, but it's better to keep track of the exact procedure in the analytical development with η. The only approximation in Eq. 5.11 is the radial symmetry of the refractive index $n(r)$. Even in this case, no general solution can be obtained analytically without further simplification. But for a constant gradient of the refractive index, altitudes h small compared to the radius of the earth and near horizontal rays, a solution is readily obtained. We put,

$$r = R + h (h/R \ll 1) \tag{5.12}$$
$$n = n_0(1 - \alpha h) \tag{5.13}$$
$$\cos\epsilon = 1 - \epsilon^2/2 \tag{5.14}$$

where h is the altitude of the ray above the earth surface and ϵ its initial inclination on the horizontal plane. Then we have for the optical invariant,

[4] There is a considerable literature on the theory and practice of astronomical refraction. Regarding the theoretical and physical approaches and the establishment of equations very similar to (5.10), the first sound investigation upon physical principles is due to the British mathematician Brook Taylor (the one of the Taylor expansion) at the end of a treatise devoted to the introduction of finite differences *Methodus Incrementorum Directa et Inversa* published in 1715. See for an English translation `http://www.17centurymaths.com/contents/taylorscontents.html` . P. Bouguer investigated the same problem in his prize winning essay in 1729 *La Meilleure manière d'observer la hauteur des astres en mer* in which he introduced the equivalent of the invariant (5.6) and reduced the problem of the path into a quadrature. This became the first general method to be used by astronomers to compute refraction tables resting on a physical model. There is an extensive note on this topic by M. Mathieu inserted at the end of Delambre's *Histoire de l'Astronomie au XVIIIe siècle*, Paris, 1827.



DE LA METHODE
D'OBSERVER
EXACTEMENT SUR MER
LA HAUTEUR DES ASTRES.

PIECE QUI A REMPORTE' LE PRIX
proposé par l'Academie Royale des Sciences
pour l'année 1729.

Par Monsieur BOUGUER, *Professeur Royal en Hydrographie au Croisic, & Membre de l'Academie Royale de Bordeaux.*

A PARIS, RUE S. JACQUES,
Chez CLAUDE JOMBERT, au coin de la ruë des Mathurins, à l'Image Notre-Dame.
M. DCC. XXIX.
Avec Approbation & Privilege du Roy.

FIGURE 5.2: Title page of the Memoir of P. Bouguer printed in 1729 and containing a theory of astronomical refraction based on physical principles, where the equivalent of (5.6) is derived.

$$C = n(h_1)(R + h_1)\cos(\epsilon) \sim n_0 R\left(1 - \alpha R - \frac{h_1}{R} - \frac{\epsilon^2}{2}\right) \tag{5.15}$$

and the integral becomes

$$\frac{\eta}{\sqrt{2}}\int_{h_1}^{h} \frac{d(h/R)}{\left(\frac{h-h_1}{R}(1-\alpha R) + \frac{\epsilon^2}{2}\right)^{1/2}} \tag{5.16}$$

and using $U = \frac{h-h_1}{R}$ as integration variable, one has

$$\frac{\eta}{\sqrt{2}}\int_{0}^{\frac{h-h1}{R}} \frac{dU}{\left((1-\alpha R)\,U + \frac{\epsilon^2}{2}\right)^{1/2}} \tag{5.17}$$

which integrates as,

$$\theta = \frac{\eta}{\sqrt{2}} \left[\frac{2}{1-\alpha\, R} \left\{ (1-\alpha\, R)\, U + \frac{\epsilon^2}{2} \right\}^{1/2} \right]_0^{\frac{h-h1}{R}} \tag{5.18}$$

or,

$$\theta = \eta \frac{\sqrt{2}}{1-\alpha\, R} \left[\left((1-\alpha\, R)\, \frac{h-h_1}{R} + \frac{\epsilon^2}{2} \right)^{1/2} - \frac{\sqrt{\epsilon^2}}{\sqrt{2}} \right] \tag{5.19}$$

This can be resolved in $h(\theta)$ by straightforward algebra, taking into account that $\eta = \pm 1$ and the $\sqrt{\epsilon^2} = \pm\epsilon$. One obtains,

$$\boxed{\frac{h}{R} = \frac{1-\alpha\, R}{2}\, \theta^2 - \epsilon\, \theta + \frac{h_1}{R}} \tag{5.20}$$

and knowing that the distance d and the polar angle θ are related by $d = R\theta$, (5.20) is identical to (4.12), based on less general arguments. This equation of the light ray assumes (i) $h/R \ll 1$ and (ii) the rate of change of the refractive index with altitude is constant. The η factor has vanished in the process with the appearance of $\eta^2 = 1$, showing that the trajectory (5.20) covers the whole domain, one either side of the minimum altitude.

5.3 Differential equation for the light ray

While the quadrature is useful to find the analytical expression of the ray, we have seen that it is not so easy to handle properly the two branches appearing with the square root. This becomes an incontrovertible problem for numerical integration, since the trajectory must be integrated separately on each branch, with negative and then positive $dr/d\theta$. The sign problem vanishes by using a second order differential equation giving $d^2r/d\theta^2$ as a function of r. One can rewrite (5.10) as,

$$\frac{dr}{d\theta} = \pm r \left[\frac{n^2 r^2}{C^2} - 1 \right]^{1/2} \tag{5.21}$$

and then differentiating, the second derivative is regular over the whole domain,

$$\frac{d^2r}{d\theta^2} = \frac{d}{dr}\left(\frac{dr}{d\theta}\right) \frac{dr}{d\theta} = \frac{1}{2}\frac{d}{dr}\left(\frac{dr}{d\theta}\right)^2 \tag{5.22}$$

which removes the sign ambiguity and leads to,

$$\boxed{\frac{d^2r}{d\theta^2} = r\left[\frac{2n^2\,r^2}{C^2} + \frac{n\,r^3}{C^2}\,\frac{dn}{dr} - 1\right]} \tag{5.23}$$

where the refractive contribution will arise only from the vertical gradient dn/dr. This can be illustrated by computing the curvature given for a curve in polar coordinates $r(\theta)$ by the following expression (to be found in any textbook of elementary differential geometry),

$$K = \frac{r^2 + 2r'^2 - r\,r''}{(r^2 + r'^2)^{3/2}} \tag{5.24}$$

which leads to the curvature along the trajectory,

$$K = -\frac{n'}{n^2}\frac{C}{r} \sim n'\frac{C}{r} \tag{5.25}$$

confirming that there is no curvature in an homogeneous medium. In the lower atmosphere one has always $r \sim R$ and $C \sim R\cos\epsilon$ and the curvature of a light ray making an angle ϵ with the horizontal is,

$$K \sim -\frac{dn}{dh}\cos\epsilon. \tag{5.26}$$

Using $u = 1/r$ to describe the path, (5.23) with (5.10) takes a very simple form,

$$\boxed{\frac{d^2u}{d\theta^2} = -u + \frac{n}{C^2}\,\frac{dn}{du}} \tag{5.27}$$

With a constant refractive index, $dn/du = 0$ and the general solution of (5.27) is

$$u = \frac{1}{r} = A\,\cos(\theta - \phi) \tag{5.28}$$

which is a straight line. One would establish easily that $\phi = \epsilon$ and $1/A = r_0\,\cos\epsilon$.

For a constant gradient, the last term in the right hand side, is very close to a constant nearly equal to $-dn/dh = \alpha$ (same α as before), and the integration can be performed in closed form to give,

$$u = \frac{1}{r} = A\,\cos(\theta - \phi) + \alpha \tag{5.29}$$

where A and ϕ are determined by the initial conditions. Since $A \sim 1/R$, the curvature of the earth, and α is the curvature of the rays, one has $A/\alpha > 1$, and the curve is a branch of hyperbola with an eccentricity $A/\alpha \simeq 7$.

Using the differential equation of the light-ray as in (5.27), one can use the above straight line (5.28) as a reference solution to determine the actual path from perturbation theory by constructing the two first order differential equations for the variation of the constants A and ϕ,

$$\frac{dA}{d\theta} = -\sin(\theta - \phi)\,\frac{n}{C^2}\,\frac{dn}{du} \tag{5.30a}$$

$$A\frac{d\phi}{d\theta} = \cos(\theta - \phi)\,\frac{n}{C^2}\,\frac{dn}{du} \tag{5.30b}$$

This amounts to describing the ray with an osculating straight ray with variable parameters (initial height and direction) as one moves along the ray, in the same way as planetary motions are represented by an osculating ellipse. In this case the osculating straight ray is simply the tangent to the curved ray.

Equations 5.23- 5.27 are very general and contain no other approximation than the spherical symmetry. They include already one constant of motion derived from the first integral. As soon as the refractive index vertical profile is known, the light ray path can be determined by numerical integration with specified initial conditions. For the path between two end-points, one has to deal with a boundary values problems, which can be solved by searching the initial direction ϵ of the ray, by solving iteratively a non linear equation. By putting $r = R + h$, (5.23) is transformed into an equation for the altitude,

$$\boxed{\frac{d^2h}{d\theta^2} = (R+h)\left[\frac{2n^2\,(R+h)^2}{C^2} + \frac{n\,(R+h)^3}{C^2}\,\frac{dn}{dh} - 1\right]} \tag{5.31}$$

with $n = n(h)$. All the numerically computed rays of this note follow from a numerical integration of (5.31), in initial conditions or boundary conditions mode, with $n(h)$ from (11.20) for standard conditions or (6.5) to investigate the inferior mirages, or the general atmospheric model for the astronomical refraction.

The path constrained by boundary conditions, namely the altitudes of the ray h_1 and h_2 and a distance d between the end-points, is determined by searching the initial direction of the ray ϵ so that one has exactly

$$h(d, \epsilon, h_0) = h_1 \tag{5.32}$$

where $h(x, \epsilon, h_0)$ is the initial values solution of (5.31). This is achieved by solving iteratively this non-linear equation in ϵ with a Newton-Raphson scheme with,

$$\epsilon_{n+1} = \epsilon_n - \frac{h(d, \epsilon_n, h_0) - h_1}{\frac{dh}{d\epsilon}} \tag{5.33}$$

One can take ϵ_0 to start the iterations from the boundary conditions found for the straight line ray or the analytical solution with curved ray. The convergence is reached in one or two iterations.

5.4 Accuracy of the constant curvature path

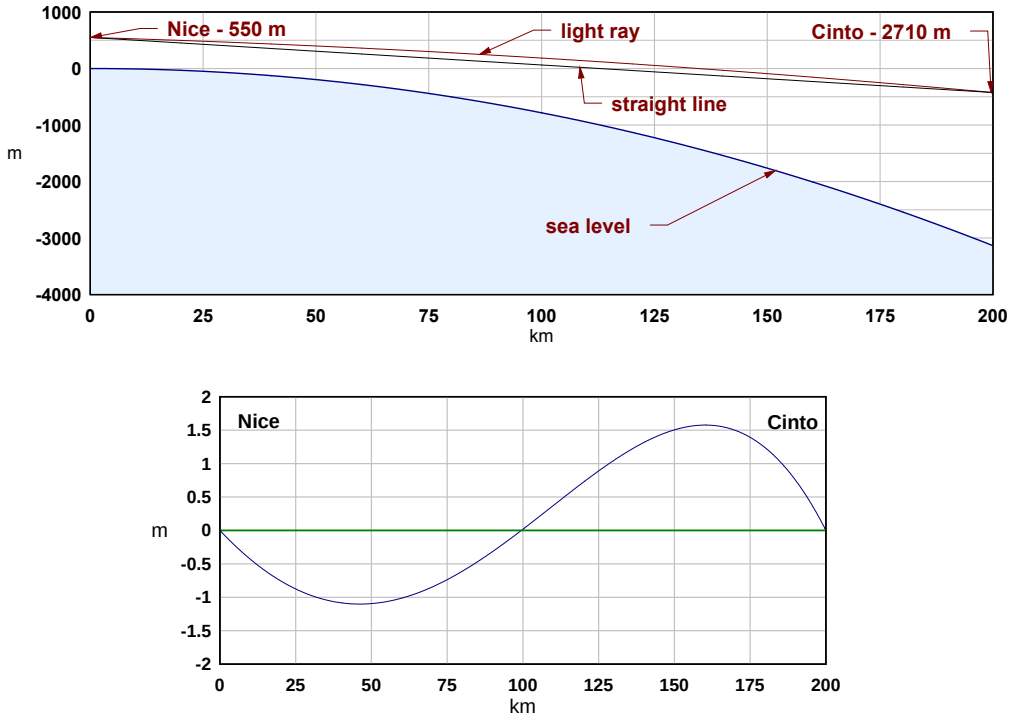


FIGURE 5.3: Light ray propagation between the Col d'Eze, near Nice at an altitude of 550 m, and the Monte Cinto in Corsica. The top panel gives the light ray propagation with refraction, based on numerical integration and from the analytical expression with constant curvature (the two are superimposed at this scale) and the geometric straight line joining the two end-points. The bottom plot shows the difference ($\sim$ 1 m) between the numerical and analytical solution with constant curvature, computed at the average altitude given by (5.34).

To check the accuracy of the approximate expression for the trajectory given in (4.12) with initial conditions or (4.14) with boundary conditions, I have computed a ray between

a point in Nice at altitude 500 m and the top of the Monte Cinto in Corsica, 200 km away at an altitude 2710 m. For the analytical solution, one needs to select a value of the gradient of the refractive index, or equivalently a value for the radius of curvature of the ray. A reasonable approach is to take the value of the gradient at some intermediate altitude between the two end points. The easiest is to take the average altitude along a straight line, given by,

$$< h >= \frac{h_1 + h_2}{2} - \frac{1}{12}\frac{D^2}{R} \tag{5.34}$$

where the first term is just the flat earth approximation and the second the correction due to the earth curvature.

For this particular application, this gives $< h >= 1100$ m and then $\alpha = 2.45 \times 10^{-5}$ km^{-1}. Results are shown in Fig 5.3 for the trajectories (top) and for the difference in altitude above the sea between the two solutions (bottom). In the first plot, the trajectories are superimposed, and one cannot see the small difference between the two solutions reaching just above one metre. This difference is plotted in the bottom diagram with the scale in metres. Therefore, at least for ray travelling in lower atmosphere over few hundred kilometres and with a smooth gradient of the refractive index, the approximation with constant curvature is remarkably accurate and can be used for accurate modelling very easily. One metre difference is hardly noticeable for virtually all the applications using nearly horizontal rays. Had I used the gradient at the starting point, the error would have been less regularly distributed, in this case always positive, and slightly larger (~ 3.5 m max).

6 Mirages

6.1 True position and refracted position

It is rather commonplace in discussions about the visibility of Corsica from Nice to hear statements like *yes, it is visible, but not at its true place*, or *this a mirage, and it works thanks to a temperature inversion*. The first statement refers implicitly to the curved nature of the light ray which is responsible for the upward shift of the direction where one can see Corsica, or more precisely its image. This viewpoint is roughly correct and refers to the description of the perceived world through our senses. This issue belongs to the philosophical realm rather than to science. There is somewhere an object, in the distance, and we have no immediate access to this object, but just to the impression made by lightray on our retina (or photographic plate or any image recorder). At a particular point, light rays arrive from various directions and this set of directions and intensities make the image (a virtual image for an optician) of a source. There is no point of telling that *it is not at the right place or in the right direction*. It is there, where we see it, and in normal conditions, unique. Now we may think that the source has an existence and a place independent of its image and this realistic stance is a generally accepted description, so that one can speak of the *true direction* of the source. Without further assumption of geometric nature, one cannot conclude on this true direction, and the usual way is to consider euclidean geometry in the 3D space (whereas we are on a the surface of a spheroid). Then by idealising the light propagation, one may consider a straight line propagation with rays ending in our eye from a direction different from what we actually see through the atmosphere. In these normal circumstances, the image is so similar to the object, that in the ordinary language one does not make the distinction between the two. We call *fish* the little orange moving thing with fins we see in the bowl on the furniture in the living room, although one sees just an image in a direction much different from where the fish actually swims.

6.2 Is the vision of Corsica a mirage?

It depends on the definition accepted for a mirage. If your definition of mirages encompasses every propagation effect through an inhomogeneous medium, then ordinary refraction produces mirage everywhere. The fish you see in its glass bowl is a mirage, the tiny stamp on your table magnified with a powerful lens is a mirage, the refracted reddish sun setting at the horizon is a mirage, etc. The usual image of Corsica produced by the refraction of light rays in a quiet atmosphere with temperature falling smoothly with altitude, is the normal situation, and in no case an anomaly: light does not propagate in straight

line in the real world, even with a standard atmosphere. There is no point of qualifying this image, essentially undistorted for usual atmospheric conditions, as being a mirage. We are offered not option of seeing it in another direction, in better agreement with our Euclidean ideal. Therefore it is better to reserve the word *mirage* to anomalous refraction, producing unexpected images, often multiples and distorted, and hard to interpret. But even when one has multiple images, they have all the same status, none being *truer* than the other. This is particularly clear for astronomers, when they see the light of a multiply lensed quasar: the two, three or more images look more of less the same, and none can be said as *the one* representing the object, while the others would be only copies through the lens. The mirage is the global optical phenomenon, stemming from the departure of light propagation from the usual nearly rectilinear and smooth lines, which produces an unusual light distribution compared to the vast majority of the cases. Sometimes the images are clearly unconnected to each other allowing to refer to them as *individual images*, but for extended sources these images may overlap into a single pattern, more or less fuzzy, that cannot be broken down into simpler structures.

Hereafter I reserve the word *mirage* to this unusual situation with complex light distribution, split or not into individualised images, although it is not possible to specify a clear borderline between the normal and anomalous refractions. It is tied to our previous experiences and how much the structure departs from what we refer to as the *normal situation*.

6.3 True mirages with Corsica

As we have seen in the earlier sections, in the standard situation the light propagates on rays having a nearly constant curvature equal to the gradient of the refractive index dn/dz. When $n(z)$ decreases with altitude the ray is curved toward the ground, where the air density is higher. In this usual situation the density variation of the air results primarily from the change of pressure with altitude while the temperature is a small correcting factor. The atmospheric refraction under discussion for the mirages near the horizon takes place in the very lower part of the atmosphere (between 0 and $\sim 20 - 50$ m), to the extent that over such a small layer there is no pressure variation and no density change due to the pressure. Here the temperature variations become the main factor, while they are negligible compared to pressure changes at higher altitude.

It is now useful to return to the expression of the refractive index as a function of the altitude to see how all this can happen. We know that $n - 1$ is proportional the air density, which in turn is determined by the temperature and the pressure, giving:

$$\frac{n-1}{(n-1)_0} = \frac{P}{P_0}\frac{T_0}{T} \tag{6.1}$$

As we move up in the atmosphere (below 10km) both the temperature and pressure decrease. The refractive index $n-1$ is proportional to the pressure but inversely proportional to the temperature. A pressure decrease at constant temperature yields a decrease in the refractive index, while a decrease in temperature at constant pressure ends with a larger refractive index. The sign of the actual gradient of the refractive index depends on which of the two factor is larger. In normal conditions, the pressure effect dominates the temperature's by a factor about five and $dn/dz < 0$.

It is useful at this point to feed the discussion with the analytical expression of (11.22) giving the refractive index gradient to the first order as,

$$\frac{dn}{dz} = -(n-1)_0 \left[\frac{Mg}{RT_0} - \frac{\gamma}{T_0}\right] \tag{6.2}$$

where $\gamma = -dT/dz \sim 6.5$ K km^{-1} (the sign has been so selected that γ is positive in the standard conditions). The first term in the brackets is the pressure term ~ 0.118 km^{-1} and the second term is directly proportional to the temperature gradient and is $\sim 0.023\,\mathrm{km}^{-1}$ in normal condition, giving at the end $dn/dz \sim -2.6 \times 10^{-5}$ km^{-1} when $(n-1)_0 \sim 0.000275$. The pressure term being linked to the local mechanical equilibrium, remains fairly constant, whatever the conditions and any departure is quickly restored. On the other hand, the temperature gradient, can be, on short scale, very different from its standard value. This is the usual case over a heated road with a dark surface whose temperature can be 30 to 40 °Celsius higher than that of the atmosphere few metres above. In this situation, if we take 10 m before the temperature is stabilised, one has $\gamma \sim 30/10 = 3$ K m^{-1} and $dn/dz \sim 2.6 \times 10^{-3}$ km^{-1}, or a refractive index growing with altitude. In fact, from (6.2) one sees that this the case as soon as

$$\gamma > \frac{Mg}{R} \sim 0.035\mathrm{K\ m}^{-1} \tag{6.3}$$

a temperature gradient just five times larger than the standard atmosphere value. One should notice, that sign of the temperature gradient has not changed, the temperature still decreases with altitude, but the gradient is very large close to the ground before it reaches its equilibrium value few metres above ground. There is no temperature inversion here, but just a density inversion: the temperature factor in (6.1) dominates the pressure, or equivalently the air density increases over the first few metres above the ground, before

returning to its steady decrease with altitude. Temperature inversions may happen, but they are normally of no importance for the visibility of Corsica. This happens, when at some altitude one has $\gamma < 0$ (with my sign convention, this means the temperature increases with altitude), then in (6.2), the pressure and temperature factors go in the same direction and the consequence of a temperature inversion is to increase the absolute value of dn/dz and also that of the curvature of the lightrays, without changing the fact the bending is toward the ground, as the rays in standard atmosphere. The bending is just larger, and could match that of the earth curvature to guide the light ray over a very long distance in the atmosphere, making very distant objects visible.

Here I focus only on the density inversion and its consequences on the light propagation. When the temperature gradient is large enough to lead to a density inversion, the ray curvature given by dn/dz is positive and the rays are bent *upwards*, at least those rays which during their journey between an object and the eye of the observer go through altitude below $\sim 10\,\mathrm{m}$, when possible density inversions may occur. The most common case is, as I mentioned before, the overheated tar on a road under sunshine which leads to so called *inferior* mirage. But this can also happen in much colder situations and typically when observing Corsica in winter, when the air temperature is of few degrees Celsius, while the sea level temperature is at about $12 - 14\,^{\circ}\mathrm{C}$. The temperature gradient is then large during the few metres above the sea, larger than one degree per metre, sufficient to produce a density inversion and changing the direction of the curvature of the rays. The consequences in terms of image formation are not trivial, but can be explained qualitatively with few drawings.

6.4 Ray tracing in the atmosphere

6.4.1 Refractive index with density inversion

For the purpose of simulating light rays with anomalous curvature, I modified the standard expressions of the refractive index in the lower atmosphere of Eqs. (11.20) -(11.21) (just repeated here for convenience):

$$n = 1.000277 - 2.644 \times 10^{-5}\, h + 8.70 \times 10^{-7}\, h^2 \tag{6.4a}$$

$$\frac{dn}{dh} = -2.644 \times 10^{-5} + 1.74 \times 10^{-6}\, h \tag{6.4b}$$

where h is in km. I have added a term giving a strong positive gradient on the lowest layers, up to $\sim 10 - 20\,\mathrm{m}$. This is an ad-hoc mathematical formula, without physical

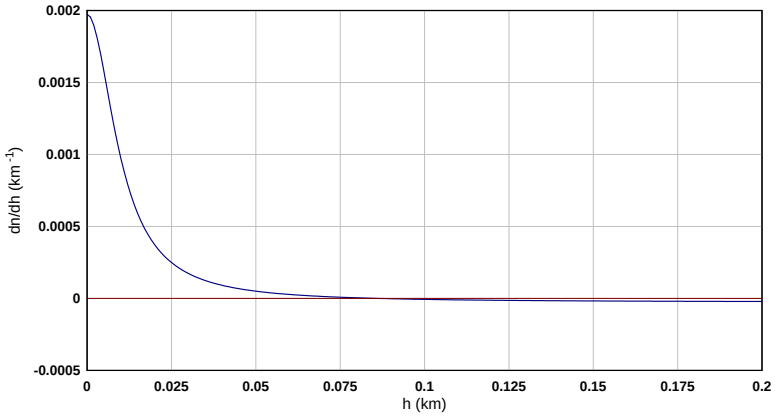


FIGURE 6.1: Rate of change of the refractive index near the earth surface, when a strong density inversion is included. Over the first ~ 50 m, the refractive index increases strongly with altitude, and after ~ 100 m one recovers the slow standard decrease of the refractive index with altitude, with $dn/dh \sim -2.5 \times 10^{-5}$ km $^{-1}$.

foundation, just able to produce the density inversion with a smooth transition toward the standard refractive index at higher altitude.

Analytically, the new expressions have the form,

$$n = 1.000277 - 2.644 \times 10^{-5}\, h + 8.70 \times 10^{-7}\, h^2 + 2 \times 10^{-5} \arctan \frac{h}{0.01} \tag{6.5a}$$

$$\frac{dn}{dh} = -2.644 \times 10^{-5} + 1.74 \times 10^{-6}\, h + 2 \times 10^{-3}/(1 + (h/0.01)^2) \tag{6.5b}$$

with a typical scale-height of few 0.01 km where the additional terms are significant. All the simulations of this section with density inversions are based on these formulas. The strong gradient extends over a wider range of altitudes than for a typical density inversion above the sea. This amplifies the curvatures and permits to draw more readable diagrams to show the main features of the inferior mirage.

6.4.2 Diagrams with light rays

The discussion below of the inferior mirages formation is based on several diagrams showing the curved light rays and the correspondance between the object and image spaces. Usually, the rays originate at the object and one shows that the two rays with different curvature and starting at some point of the object may reach the observer, leading to the duplication of the vision by the observer. I found that taking the observer perspective is much more illuminating to account in a simple manner for the effect. The

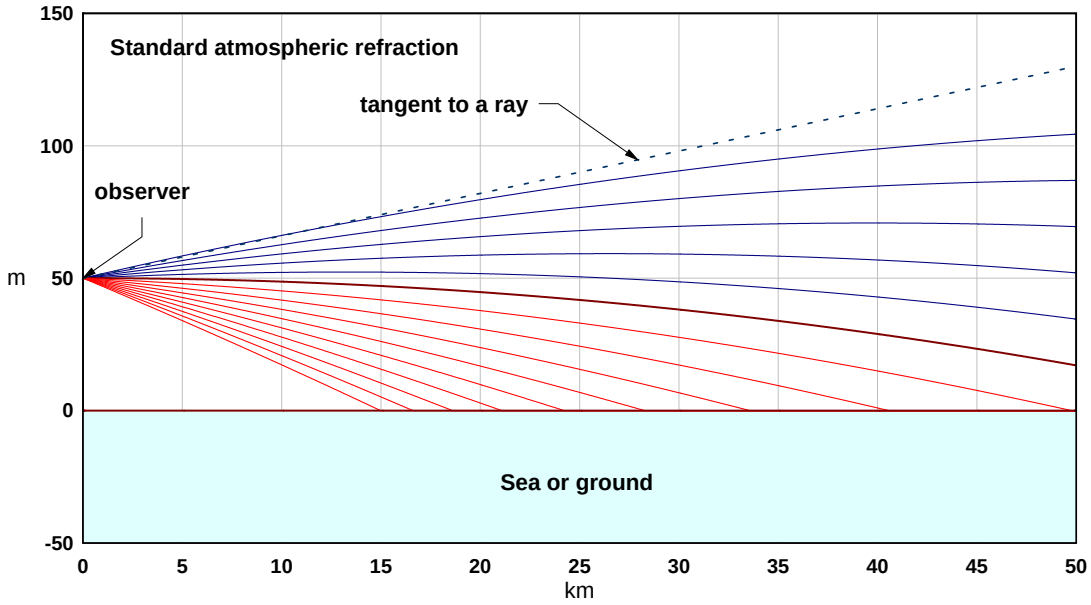


FIGURE 6.2: Light ray propagation on a plane stratified atmosphere without density inversion near the ground. The earth curvature is neglected and the ray propagates with the refraction of the standard atmosphere. The horizontal scale is in km and the vertical in m.

typical diagram is shown in Fig. 6.2, showing rays leaving the observer (or reaching the observer with the conventional description), heading in different directions, above or below the horizontal plane. The curvature of the earth will be introduced later, since it is just an additional geometrical element not connected to the refraction. The ray starting off horizontally is the brown and thicker line. The rays heading down reach the sea (or the ground) and these are the directions where the observer sees the surface of the sea, in the direction of the tangent along the ray reaching his/her eye. The upper ray, if not hindered by an obstacle will show the sky background. All the subsequent diagrams of this section are designed on the same model, with flat or curved earth, using an horizontal scale in km and a vertical in m. The light rays are computed with a numerical integration of (5.31) with initial conditions determined by the height of the observer and the starting direction of the ray referred to the local horizontal plane. The refractive index $n(z)$ is taken either from (6.4) or (6.5) according to the simulation, with or without density inversion.

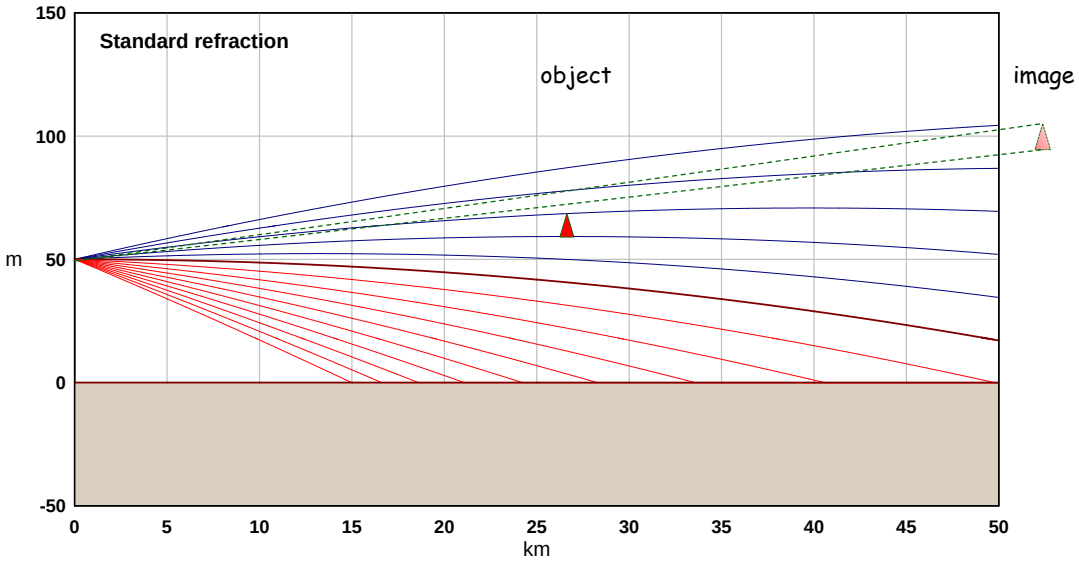


FIGURE 6.3: Light ray propagation on a plane stratified atmosphere. The earth curvature is neglected and the ray propagates with the refraction of the standard atmosphere. Small objects are seen undistorted, with a single image from an higher elevation in the sky than their geometric position.

6.4.3 Plane geometry and standard refraction

I start with the simpler case, of a flat earth, meaning that the optical phenomenon of interest takes place at a small distance from the observer compared to the earth radius, typically few kilometres up to few tens kilometres. When one has no density inversion the ray propagation, is shown with a bundle of lightrays in Fig. 6.3 for an observer elevated about the horizontal plane of the ground level. One must notice that in this simplified geometry, there is no optical horizon and all the space above the ground is optically accessible to the observer. The rays do not intersect each other and there is a one-to-one correspondance between the geometric directions and the refracted directions. An object, displayed as a red cone, is seen in the directions determined by the tangent to the rays at the observer's eye. In this configuration the image is seen shifted upward with respect to the geometric direction of the object, but, unless the observer is informed of the actual position of the object, the only information at his disposal is based on the directions of the optical rays, and normally does not call what he sees an *image*, but simply says that he sees the object in this particular direction.

6.4.4 Plane geometry and anomalous refraction

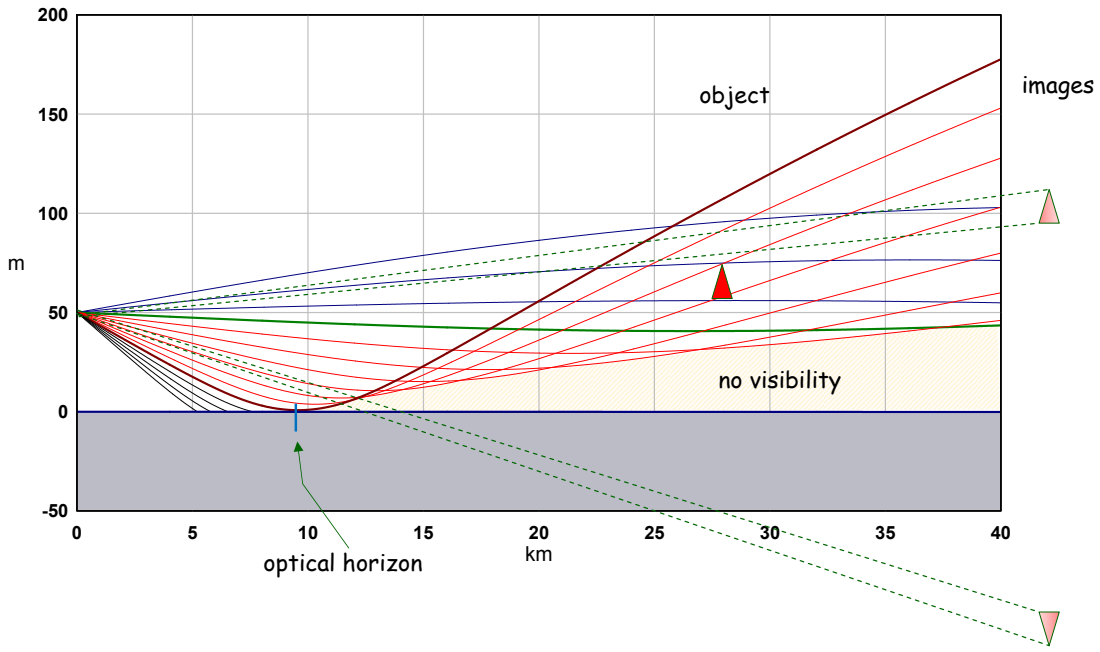


FIGURE 6.4: Light ray propagation on a plane stratified atmosphere. The earth curvature is neglected and the ray propagates with the refraction including density inversion near the ground.

In the second case, I still use the simple plane geometry approximation, but introduce a density inversion in the lower atmospheric layers, very close to the ground. The rays are shown in Fig. 6.4. The upper part of the diagram is similar to the standard refraction with a downward curvature, while for the rays approaching the ground there is locally an upward curvature. The two groups of ray intersect each other and the image of a small object is duplicated with two well separated images, one above the geometric direction, the other below and turned upside down. Given the non linearity of the gradient of the refractive index in the lower layer, this inverted image is also distorted, because the magnification is not constant over the size of the object. In both cases the directions where the images are seen by the observer is determined by the tangent to the lightrays connecting the object and the observer eye or detector. Naturally the observer has no idea of the actual route followed by the light, and cannot infer from what he sees the actual geometric position of the object. Without previous experience about the nature of the source, he even cannot say which of the two images is inverted or distorted, although his/her conclusion will be that there is a reflection as though there were an horizontal mirror or still water on the ground.

As in the previous example, the images are virtual and no distance can be associated to the image perception and to the true size of the object.

One must also stress the fact that one refers naturally to *two images* because they are well separated and easily isolated from each other. But more generally, it is more correct to consider the two images as a *single complex* image of a source. For extended objects considered later, where direct and inverted images overlap, there is no such distinction and just a localised and connected distribution of light. A conspicuous feature in this diagram is the appearance of an optical horizon, where there is the transition between rays hitting the ground (left part) and those going up toward the sky. Also, beyond the horizon, there is a connected region of the space not visible. An object small enough to remain entirely in this area won't be visible for our observer placed at the convergence point of the rays. This is a pure optical fact and happens even with flat geometry.

6.4.5 Spherical earth and simple object

The earth curvature plays a minor role in the image formation, either with standard atmosphere or when density inversion occurs. This is shown in the next two plots with a similar small conical object. The refractive index gradient has been increased by a factor five, to enhance the ray curvature. The main difference in Fig. 6.5 with the planar case is the presence of an optical horizon due to the finite radius of curvature of the earth. It has nothing to do with the light bending by refraction, but would exist, as discussed in detail at the start of this paper, with rectilinear propagation. The distance to the optical horizon agrees fairly well with (4.20) with $\alpha R \sim 0.8$ instead of 0.16 for the standard atmosphere.

For the second case shown in Fig. 6.6, with inverted curvature of the rays, the optical horizon owes very little to the curvature of the earth and its distance is much smaller than without density inversion (Fig. 6.5). Beyond this optical horizon, there is always an area above the earth surface which is not visible, below a *vanishing line*, whose altitude is typically less than 100 m for the strongest temperature gradient one may find above the sea surface in winter. Above this line one recovers quickly the visibility condition expected with standard atmosphere, and described in the previous sections. For usual density inversion above the sea, this angular extension of this mirage zone is a matter of few minutes of arc above the optical horizon.

6.4.6 Images formation with extended objects

No particular problems are expected for the image of an extended object in the case of standard refraction. Conversely for inferior mirages, one expects that with an object of

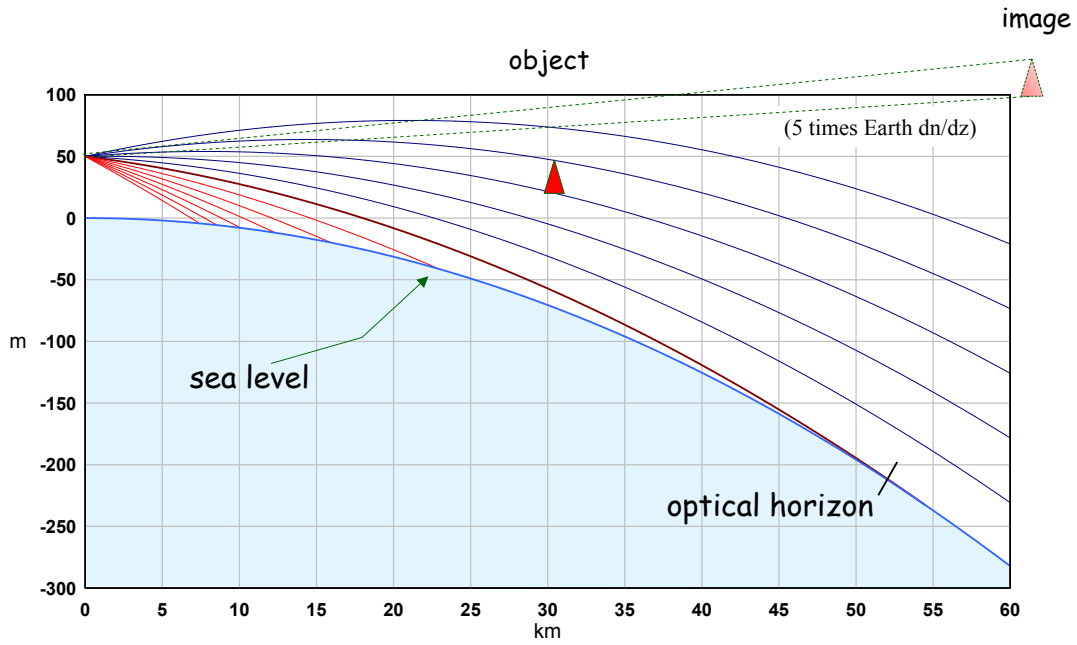


FIGURE 6.5: Light ray propagation with regular atmospheric conditions (no density inversion, but dn/dh increased by a factor 5) for an observer at about 50 m above the sea. The figure can be interpreted as the ray emanating from a point source and propagating from left to right, or as the rays coming from different places in the space above the sea and reaching an observer. The tangent to the rays at $x = 0$ indicate the directions from where the light seems to come for the observer. The optical horizon is the line on the sea separating the sea and sky visibility. In this simulation, the refractive gradient is about ten times larger than its value for the standard atmosphere.

angular vertical size comparable to the angular distance separating the direct and inverted images of a point-like source, the two images will merge into a single and complex image, since the direct and inverted images will overlap.

The first case is illustrated in Fig. 6.7 for a plane-stratified atmosphere and the discussion would be similar with a spherical earth. The object is seen with a colour coding of its height, so than one can see how the image forms. The image is a one-to-one mapping of the object, and with a constant gradient of the refractive index, there is no distortion and no magnification. The image is just shifted upward compared to the geometric position of the object.

The discussion is more involved when the lower part of the object is subjected to distortion by inferior mirage. There is no particular problem, but distortion, when the object is

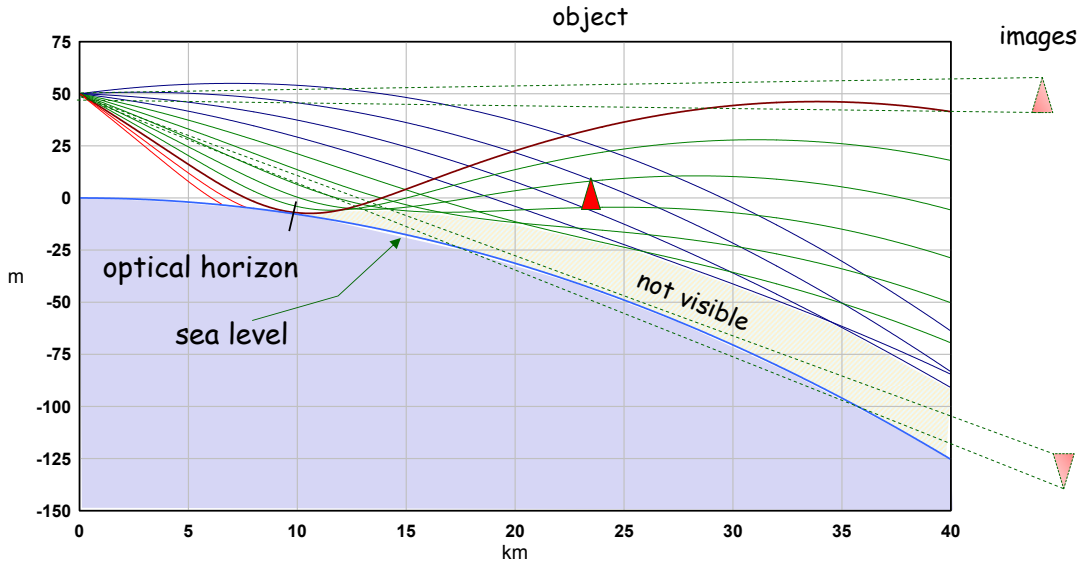


FIGURE 6.6: Light ray propagation in standard atmospheric conditions for an observer at about 50 m above the sea. The figure can be interpreted as the ray emanating from a point source and propagating from left to right, or as the rays coming from different places in the space above the sea and reaching an observer. The tangent to the rays at $x = 0$ indicate the directions from where the light seems to come for the observer. The optical horizon is the line on the sea separating the sea and sky visibility.

between the observer and the optical horizon. The problems starts when the object is beyond this horizon as shown in Figs. 6.8 and 6.10. In the first case the object is high enough to have its upper part above the rays with upward curvature. The lower part in deep blue and purple lies in the non visibility zone, below the vanishing line and this part will not be imaged. The upper part, in yellow, orange, red lies in a region where the light rays do not intersect, and is singly imaged, with little distortion. The intermediate part is twice imaged, with one direct and not distorted image finishing down just above the vanishing line, and an inverted image down from the vanishing line to the optical horizon. The lowest ray corresponding to the horizon imaging the highest part of this section of the object with two images. This is displayed in the plot with the colour coding. There is no more this simple separation between an upper and a lower image, as the two images merge into a single one with the lower part highly distorted. Strictly speaking the two images do not overlap, since the inverted image started at the vanishing line, where the upper image ends. The lower image fills the room left empty by the lower part of the object hidden below the vanishing line.

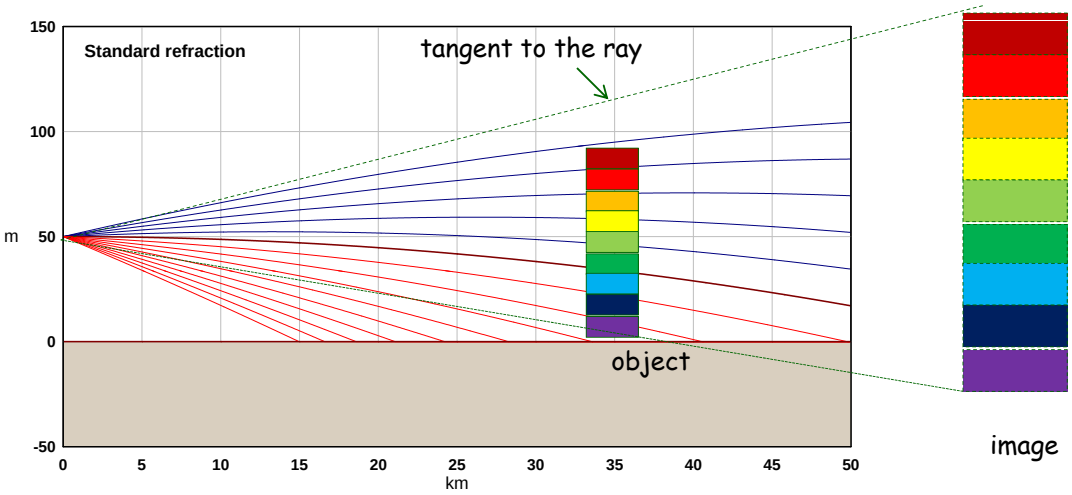


FIGURE 6.7: Image formation for a light propagation on a plane stratified atmosphere. The earth curvature is neglected and the ray propagates with the refraction of the standard atmosphere.

An exemple of this inferior mirage image structure for an extended object is given in Fig. 6.9, during a winter sunrise above the sea, few seconds before the lower solar limb crosses the optical horizon in the upward direction. The two images are taken 11 s apart, and the sun is more than 95% above the horizon. One sees a little zone at the bottom, smaller than 1.5 arcmin where the limb is not visible and a less distinct light distribution takes over. This is the inverted and compressed image of a small part of the sun with a vertical size of about 1-2 arcmin, seen between the vanishing line and the optical horizon. This is in winter and the air temperature was lower than that of the sea surface and the temperature gradient over the first few metres was large enough to yield a density inversion.

The next diagram shown in Fig. 6.10 deals with the situation of an object small enough to fit entirely below the ray delimiting the optical horizon. As before, the lower part, below the vanishing line is not visible and then the three lower cells of the tower are not imaged at all. All the rest of the object, above the vanishing line is twice imaged, with a direct image shifted upward and a lower symmetrically inverted and compressed downward. The two meet exactly at the vanishing line. But since the space with double image extends higher than the top of the object, the lower part of the image just above the horizon, is an image of the background near the top of the object. Eventually the image of the object is seen floating somewhat above the horizon, and a strip of sky is seen between

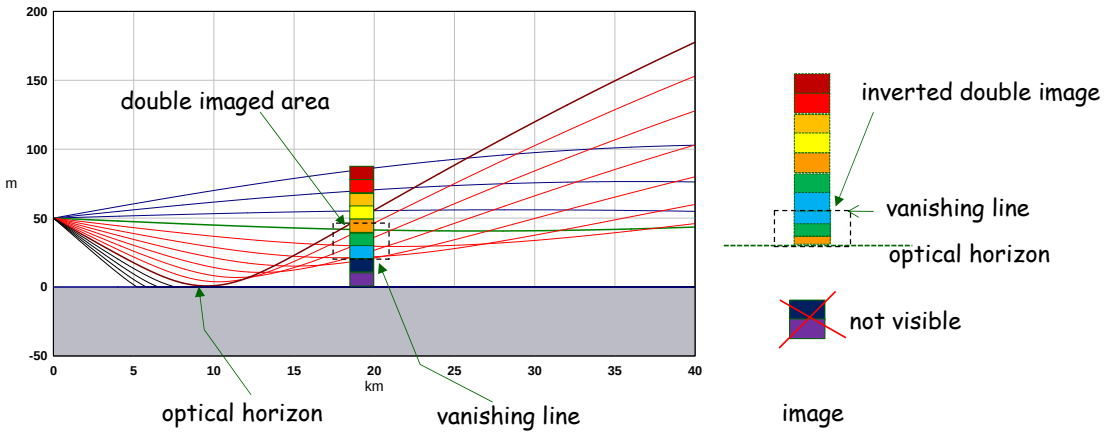


FIGURE 6.8: Image formation for a light propagation on a plane stratified atmosphere. The earth curvature is neglected and the ray propagates with the refraction including density inversion near the ground. The height of the object is higher than the area with duplicated images. The observer sees *the object* with a double imaging of its upper part, upside down and distorted

the horizon and the bottom of the image. This strip is not the sky in this direction, but an image of a strip of sky lying just above the top of the object.

These various instances are illustrated in Fig. 6.11, where a virtual island is observed from the coast at difference distance, with or without density inversion. The top panel shows more or less what corresponds to Corsica (discarding here the curvature of the earth which is well understood) when the air temperature is similar to that of the sea surface, typically in October or early November. Then later in winter, there is a density inversion, and inferior mirages show up.

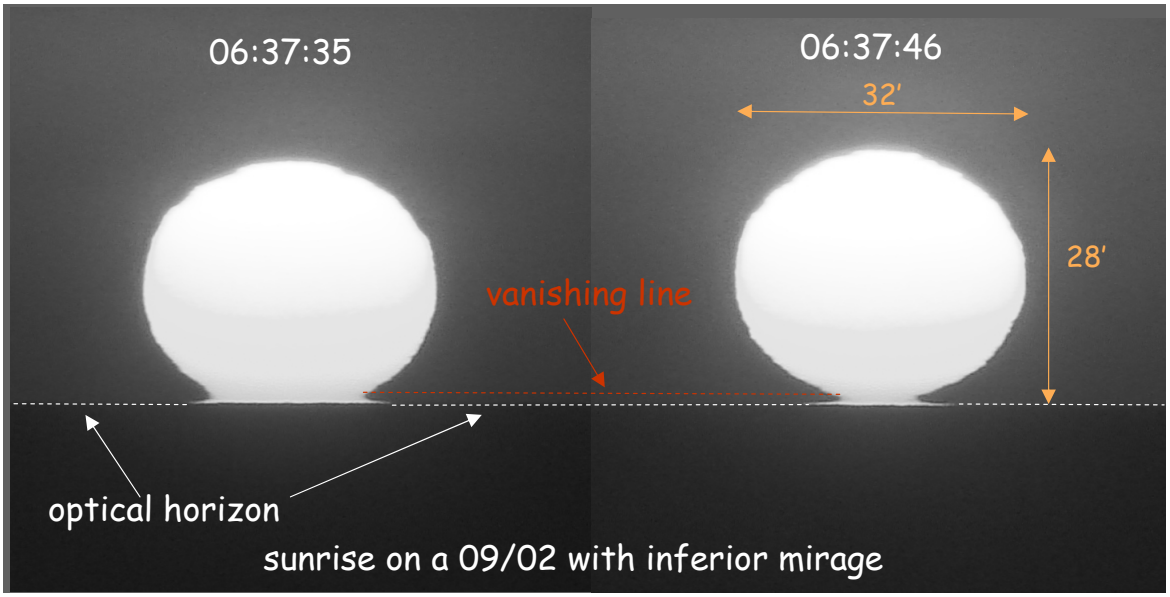


FIGURE 6.9: Image of a winter sunrise above the sea with an inferior mirage near the optical horizon. The very lower part of the image, widening toward the horizon, is the inverted image of the lower limb seen just above the vanishing line.

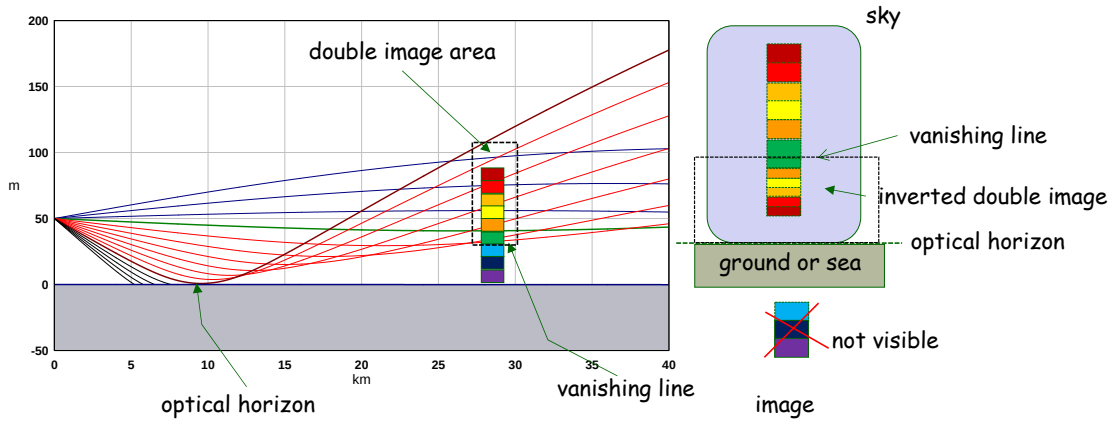


FIGURE 6.10: Image formation for a light propagation on a plane stratified atmosphere. The earth curvature is neglected and the ray propagates with the refraction including density inversion near the ground. The height of the object is smaller than the area with duplicated images. The observer sees *the object* floating above the horizon on the background sky. There is a double imaging with the upper part of the object upside down and distorted. The sky one sees at the bottom is the image of the true sky above the object and not the direct background.

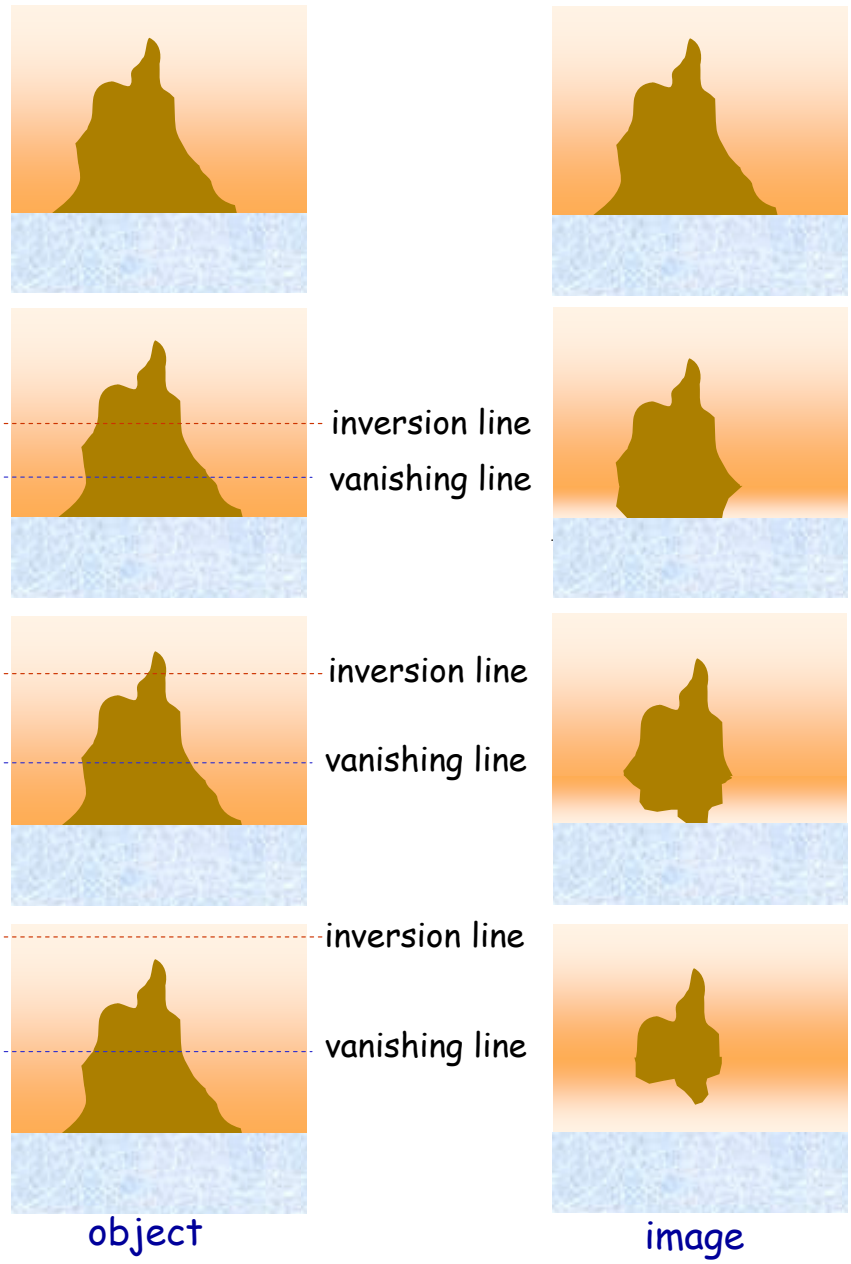


FIGURE 6.11: An island seen in standard refraction condition (top) and then through an inferior mirage as a function of the distance beyond the optical horizon. Nothing is visible below the vanishing line while the area comprised between the vanishing line and the inversion line is imaged twice, with the second image inverted and distorted below the vanishing line. In the bottom panel, the island is seen floating above the optical horizon on the inverted background sky.

7 Contrast and visibility

7.1 Qualitative description

Visibility is the term used in the context of meteorology or navigation to indicate if it is possible to sight something, a lighthouse or a landscape feature, in the distance. Visibility is always the combination of a geometric condition (light rays must be possible between the light source and the observer) and transparency of the air (meteorological visibility). This general principle applies to full extent to the visibility of Corsica from the Nice area. However, any casual observer of Corsica in the morning twilight would not fail to notice the drastic change in visibility as soon as the sun appears above the horizon: a beautiful and dark ridge line silhouetted on the horizon transforms quickly into a blueish-whitish, rather indistinct outline as the sky gets brighter. Later in the morning or during the day, the visibility of Corsica is hardly possible, at least from moderate altitude, and even from the highest locations in Mercantour, the daylight visibility never compares to what is easily achievable from Nice surroundings ~ 30 mn before sunrise. Obviously the atmospheric transparency does not change all of a sudden at sunrise and the culprit is elsewhere and linked to the change of contrast brought about by the scattered sunlight in the direction of the observer. The scattered sunlight in this direction is negligible before sunrise and becomes very significant as soon as the sun illuminates the intervening atmosphere between the observer eye and Corsica. This is exactly similar to what happens in a hilly or mountainous area when the sun sets (or rises) behind the ridge line: the line stands out neatly, very well delineated, against the sky background, until the sky becomes very dark. The whole issue can be summarised in a single catchword: contrast. Visibility is just a matter of contrast, in luminosity or colour, or both, between two neighbouring areas. What happens just after sunrise is a sudden drop of contrast due to the sharp increase of amount of light coming from the direction of Corsica, rather than from the slighter increase of luminosity of the sky.

7.2 Visibility during daylight

This can be expressed mathematically with a rather simple model comparing the light entering the observer's eye according as it comes from the sky or from the distance landscape. In both cases the light has been attenuated by its passage through the air, but provided the general transparency is good (no haze, no clouds), this has little effect on the visibility. Let's consider the case shown in Fig. 7.1, during daytime, with two pencils of light reaching the observer, one from the sky at an undefined distance, and the other one

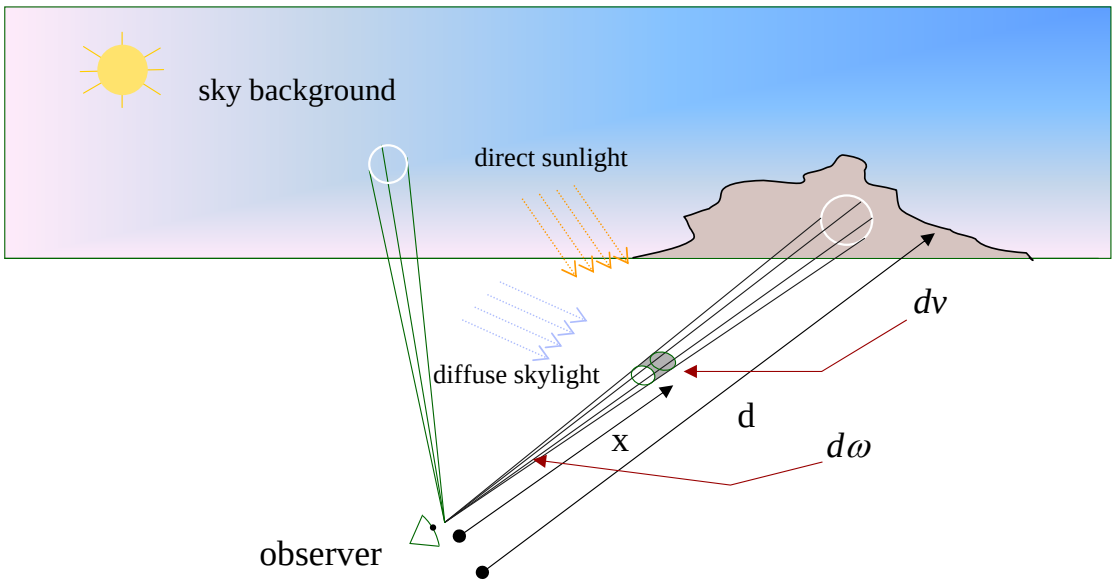


FIGURE 7.1: Visibility of a landscape feature against sky background just after the sunrise.

from a finite distance d where Corsica lies.

The flux E transported by a beam of light decreased as light is absorbed or scattered in different directions. The loss dE in a small slab of length dx along the beam chief ray is proportional to the flux with,

$$\frac{dE}{E} = -\sigma dx \tag{7.1}$$

where σ is the total scattering coefficient. The remaining flux after thickness x follows the exponential law (Bouguer-Lambert law),

$$E = E_0 \exp(-\sigma x) \tag{7.2}$$

for a collimated beam and

$$E = E_0 \frac{\exp(-\sigma x)}{x^2} \tag{7.3}$$

for a converging beam.

Now, due to scattering, each volume element illuminated by the sun becomes itself a source of secondary light, such that the amount of light produced in the volume element dv in the solid angle $d\omega$ is,

$$dI = A\sigma x^2 d\omega dx \tag{7.4}$$

where A is a proportionality factor. The illumination produced at the observer by this scattered light is,

$$dE = dI \frac{\exp(-\sigma\, x)}{x^2} \tag{7.5}$$

or finally for the contribution of the slab dx to the brightness along the line of sight,

$$dB = A\sigma \exp(-\sigma\, x) dx \tag{7.6}$$

In the direction of the sky, the line of sight extends through the entire atmosphere, and the sky brightness is given by integrating (7.6) to infinity,

$$B_s = A \int_0^\infty \sigma \exp(-\sigma\, x) dx = A \tag{7.7}$$

Come now to the beam interrupted at distance d by a landscape feature like a mountain in Corsica. Let B_0 the brightness of the landscape at zero distance, and B the brightness at the observer's eye. The latter is the sum of the brightness B_0 attenuated by the travel in the atmosphere over a distance d, and the brightness produces by the scattered light along the pencil up to the distance d.

Therefore,

$$B = B_0 \exp(-\sigma\, d) + A \int_0^d \sigma \exp(-\sigma\, x) dx \tag{7.8}$$

which reduces to (with $B_s = A$ from (7.7)),

$$B = B_0 \exp(-\sigma\, d) + B_s \left[1 - \exp(-\sigma\, d)\right] \tag{7.9}$$

The landscape-background contrast is then,

$$C = \frac{B - B_s}{B_s} = \frac{B_0 - B_s}{B_s} \exp(-\sigma\, d) \tag{7.10}$$

or equivalently,

$$C = C_0 \exp(-\sigma\, d) \tag{7.11}$$

showing that the contrast is attenuated by air in the same way as the light is absorbed. If the object is black, $B_0 = 0$, then $C_0 = -1$, the black object will vanish in the distance with

the brightness of the beam in its direction gradually rising to match that of the background sky when $\sigma\, d \gg 1$.

The value of the extinction coefficient σ, measured in km^{-1}, depends very much on the state of the atmosphere, the number of dust particles and aerosols in suspension, the amount of water vapour. For the visibility of Corsica, this must be evaluated at low altitude because the observation takes place near the horizon. When observing from the Nice area, at a maximum altitude of 500 m, and for a ray reaching Corsica at 1500 m leaving the possibility to see the main mountain tops, the lowest altitude of the ray (4.2) is 250 m above the sea. More generally the average altitude above the sea of a ray joining two end-points of altitude h_1 and h_2 at a distance D of each other, is given by averaging (4.14) and yields,

$$\frac{< h >}{R} = \frac{1}{D}\int_0^D h(x)dx = \frac{h_1 + h_2}{2R} - \frac{1-\alpha R}{12}\frac{D^2}{R^2} \tag{7.12}$$

where the first term is just the altitude of the mid point for a straight propagation with a flat earth, and the second combines the effect of the Earth curvature and the ray bending. For a given distance D, the average height of the ray grows like half of the increase of the observer altitude. Again take as an illustration 1500 m in Corsica, 500 m in Nice at 200 km, this gives $< h > \sim 560$ m, with the lowest point at 250 m. Now observing from one of the summits in the inland Mercantour, say at an altitude of 2500m, where several are of easy reach. The distance increases modestly from 200 km to $230 - 250$ km, according to the place. With the worse case of 250 km, the average altitude of the ray becomes 1300 m and the minimum 900 m. Although the distance is larger, there is a great advantage in terms of air transparency. It increases quickly with altitude (less molecules and aerosols to scatter the light), and globally the contrast will be higher than at lower altitude. Good pictures of Corsica during the day would be easier to shoot from the distant mountains in the north of Nice than from the hills near the coastline. See for example several such pictures at `http://emmanuel.varoquaux.free.fr/corse.php`, where, however, one can see that even in this favorable configuration, the contrast remains very low.

7.3 Visibility before sunrise

Move now to the case sketched in Fig. 7.2 when the sun is below the horizon and not direct sunlight reaches any part of the atmosphere between the observer and the distance landscape. The background is still illuminated as before, as long as the sun is not deep

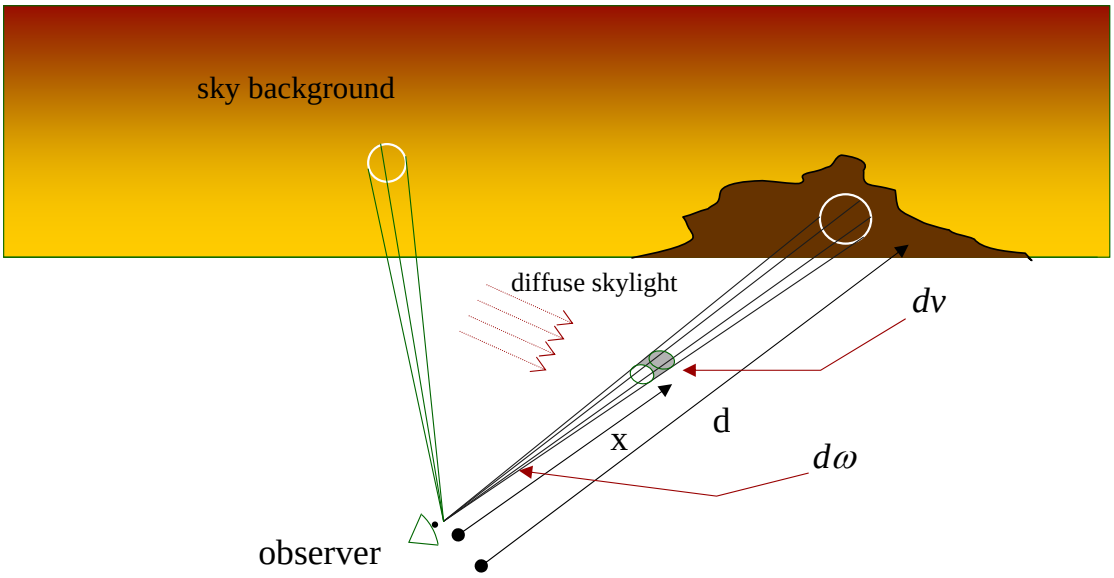


FIGURE 7.2: Visibility of a landscape feature against sky background when the sun is below the observer horizon.

below the horizon and illuminates the upper atmosphere above the observer in the direction of the sunrise. The contribution of the background is again given by (7.7) with an integration starting above the geometric shadow as shown in Fig. 7.3 and extending to infinity giving,

$$B'_s = A \int_{x_0}^{\infty} \sigma \exp(-\sigma\, x) dx = B_s\, \exp(-\sigma\, x_0) \tag{7.13}$$

The main change arises in the brightness from the landscape, since there is no contribution from the scattered light (neglecting other sources of diffuse light than that of solar origin or secondary diffusion from the skylight) and then (7.9) reduces to,

$$B' = B_0 \exp(-\sigma\, d) \tag{7.14}$$

giving for the contrast,

$$C' = \frac{B' - B'_s}{B'_s} = \frac{B_0\, \exp(-\sigma\, d) - B'_s}{B'_s} \tag{7.15}$$

If the object is dark, with $B_0 \sim 0$, the contrast remains close to -1 and the visibility, in terms of contrast, is *not affected* by the distance. The projection of the landscape along the

line of sight remains distinctly dark, well contrasted against a bright background produced by the sunlight scattered in the upper atmosphere, or that part of the lower atmosphere away from the direction of the distant landscape. In the case of Corsica, even in winter when the snow covers most of the visible peaks, given the direction of the sunrise and the distance, there is no part of the visible Corsica under the sun when one observes in the morning twilight, and the approximation $B_0 \sim 0$ remains valid as long as the snow covered cap are in the shadow.

When the sun is too low under the horizon, $B'_s \rightarrow 0$ and, even if mathematically the contrast is not changed, the sky background gets as dark as the landscape, and nothing can be seen. This explains why the timing to see Corsica in the morning is rather narrow and limited to about 30 mn before sunrise, with a sharp decrease in contrast within minutes after apparition of the sun above the horizon. But during this favorable window, the contrast is no match for any other time during the day and Corsica appears almost black against the glowing morning sky.

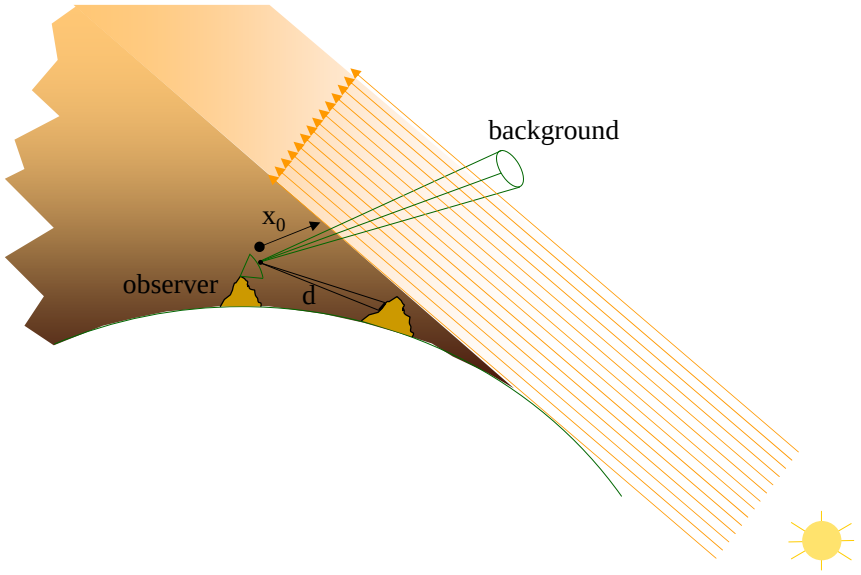


FIGURE 7.3: Geometry of the sky illumination during morning twilight, when the sun is still below the horizon of the observer, but casts light on the upper atmosphere.

7.4 Visibility after sunset

The above principles can be used now to explain why the observations are also difficult just after sunset. All the light coming from the atmosphere in the direction of Corsica, at that time more or less opposite to the sun, is indirect and results from single or multiple

scattering in the atmosphere still above the earth shadow. The rays reaching the observer on the ground are primarily scattered in the backward direction, as illustrated in Fig. 7.4, where the height of the atmosphere is greatly exaggerated in comparison with the earth's radius. The top mountains of Corsica are faintly illuminated by the scattered light, as is the background atmosphere. The evaluation of the contrast between the landscape at distance d and the sky background is similar to the derivation of 7.2, by replacing the direct sunlight as main source by the scattered light. The result is then,

$$C = C_0 \, \exp(-\sigma \, d) \tag{7.16}$$

with a contrast vanishing with the distance. In addition, due to the secondary source of light, both the sky and landscape are strongly dimmed and the general visibility decreases quickly in this direction opposite to sunset. Corsica can be visible, with a very low contrast within 10 to 20 minutes after sunset.

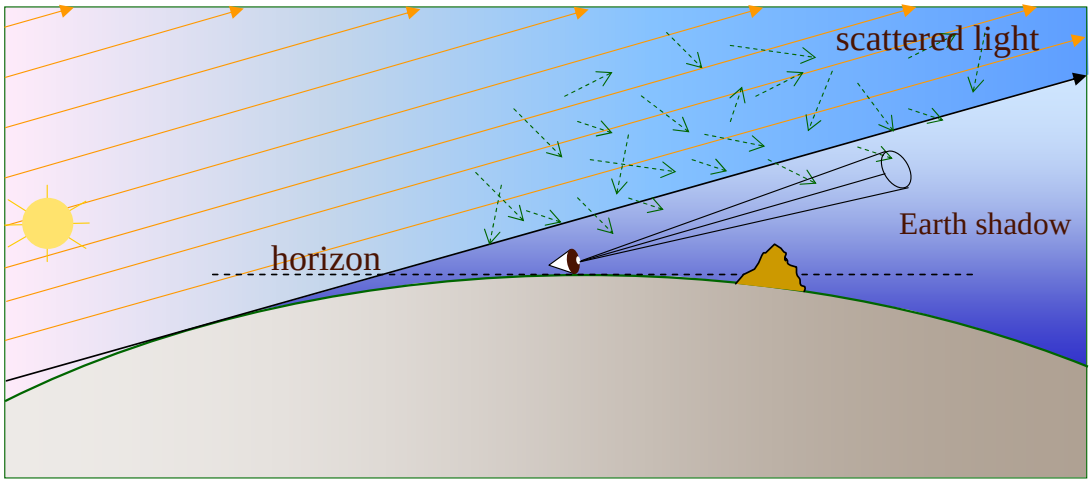


FIGURE 7.4: Geometry of the sky illumination during evening twilight, when the sun is below the horizon of the observer, but illuminates the part of the atmosphere not yet plunged in the shadow of the earth. Scattered light in this region keeps the shadow bright enough for at least 30 to 45 mn after sunset.

8 Rising sun above the Cap Corse



FIGURE 8.1: Sunrise behind the Cap Corse on January 3 from the Col d'Eze. The sun gives the scale of the landscape on the picture. It rises here above the Bocca Santa Maria, between the Stello and the Capra, in agreement with the data in table 8.1.

The highest peaks of the Cap Corse are all below 1300 m, and one needs to observe from an altitude higher than 400 m to see them. In the immediate vicinity of Nice this can only be achieved from the east of the city, on the upper Corniche between Eze and la Turbie. From these places the azimuths are between 119 deg to 122 deg. The precise figures for the Folicce given in table 12.1 shows the quick variations with the observer position and the conclusions of this sections are correct for an observer close to the col d'Eze on the upper Corniche. It happens that the sun rises precisely in this range of azimuths few weeks per year between $\sim$ 30 November and $\sim$ 10 January, respectively at $\sim$6 h 40 m and $\sim$07 h 00 m TU (add one hour to get legal winter time). It is then possible, when meteorological conditions are favorable, to see the sun rising behind the major landscape features of the Cap Corse. Detailed numerical values are given in table 8.1, and the phenomenon is illustrated in Fig.8.1.

If we wish to compute sunrise times and directions behind the ridge line of the Cap Corse, one should not refer directly to the usual definition of sunrise using the first appearance of light on the horizon. This is the rise of the upper limb, normally used in almanachs.

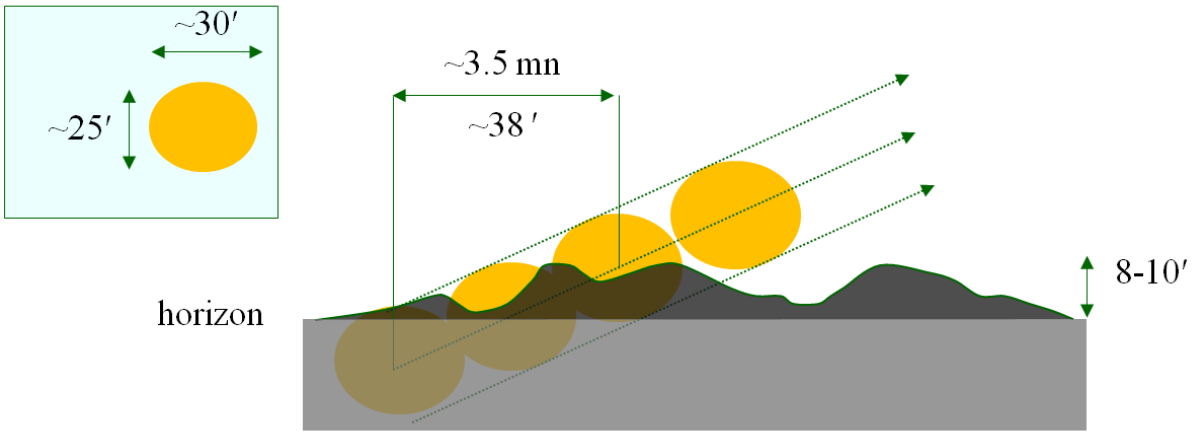


FIGURE 8.2: Sketch of the rising sun behind a projected ridge line similar to the Cap Corse. The inclination of the path of the sun to the horizon is 42 deg in winter time and it takes about three and half minutes for the sun to move vertically of an angle equal to its angular diameter. For this inclination, the motion in azimuth is nearly the same as the motion in altitude. Given the apparent height of the mountains above the horizon, it is relevant to compute the phenomenon for the rise of the lower solar limb, whereas the usual definition of the sunrise refers to the upper limb, when the first sunlight becomes visible on a free horizon. An horizontal displacement of 36′ is equivalent to 2.5 km along the nearly north-south oriented Cap Corse (corrected for the projection on a plane normal to the line of sight).

Given the height of the crest line, one sees the sun when it is already several arcmin above the horizon. In addition, given the inclination of the trajectory of the sun to the horizon, about 42 deg in December at the latitude of Nice, the actual direction when the sun just appears above the top of the mountains is shifted southward by several ten arcmins from the direction of the upper limb rise. This is sketched in Fig. 8.2 with the scale based on the observation of the Cap Corse peaks from an altitude of 550 m on the east of Nice. Using both the azimuth and time of the rise of the lower limb of the sun would be much closer to the reality.

Therefore I computed in Table 8.1 the relevant parameters of the phenomenon within the six weeks when it is observable, with the time of the rise of the lower limb of the sun. From year to year the times of sunrise and azimuth reproduce more or less identically at the same date and for the same geographical location, within 10-20 seconds, thus times have been rounded to the nearest minute. Around the two end-points of the visibility pe-

riod, the daily change in azimuth is large enough to be easily observed on two successive mornings.

TABLE 8.1: *Period of visibility of the sunrise behind the Cap Corse for an observer located near the col d'Eze on the east of Nice at an altitude of* ~ 500 *m. The landscape feature seen projected on the solar disk is given in the last column.*

day	month	sunrise TU	azimuth deg	landscape
29	November	6h 41m	119.4	Alticcione
01	December	6h 43m	119.9	Bocca di a Serra
03	December	6h 46m	120.4	Folicce
05	December	6h 48m	120.7	Canetto
07	December	6h 50m	121.1	Stello
09	December	6h 52m	121.4	Bocca Sta Maria
11	December	6h 53m	121.6	Capra
15	December	6h 56m	122.0	Bocca di Antigliu
19	December	6h 59m	122.2	Foscu
23	December	7h 01m	122.2	Foscu
27	December	7h 02m	122.1	Bocca di Antigliu
31	December	7h 03m	121.7	Capra
02	January	7h 04m	121.5	Bocca Sta Maria
04	January	7h 03m	121.2	Stello
06	January	7h 03m	120.9	Cibiolla
08	January	7h 03m	120.5	Folicce
10	January	7h 02m	120.1	Bocca di a Serra
12	January	7h 01m	119.4	Alticcione



FIGURE 8.3: Sunrise behind the Cap Corse on December 1st, from the Col d'Eze. The sun rises here behind the Croce a Viezza, very close to the Bocca di a Serra, in agreement with the data in table 8.1, computed for the rising of the lower limb. At the time of the picture, the lower limb is still below the optical horizon and is then located few arcmin more to the north than expected from the table.



FIGURE 8.4: Sunrise behind the Cap Corse on December 13, from the Col d'Eze. The sun rises here behind the Capra, close to the Bocca di Antigliu.

9 Application to the Pic of Canigou



FIGURE 9.1: Picture from A. Origné showing the Mont Canigou (on the right) and adjacent peaks standing up on the setting solar disk on 09 February 2008, observed from Allauch in the north of Marseille. The angular height of the Canigou measured on that picture is $4.3'$, in excellent agreement with the prediction of (4.24).

This section deals with a very similar case of limiting visibility, not connected to Corsica but well explored and then supplying an excellent basis to test the validity of the principles developed in the previous sections.

The Pic of Canigou is a prominent peak on the eastern border of the Pyrenees, well visible from the distance and particulary from the sea. It has been known for more than two centuries that few weeks per year the Canigou is visible from Marseille area silhouetted against the sunset. This can happen only around the 10 th February or 1st November, when the sun sets in the proper direction. The phenomenon is well documented and attracts groups of amateurs every year equipped with camera fitted with big lenses to picture the black outline of the mountain on the solar disk, as shown in Fig. 9.1.

Much detail about the history and the physics of the phenomenon can be found in the authoritative and well designed Website of A. Origné at `http://canigou.allauch.free.fr/` and I will add nothing really new to the wealth of information available there. I just want to apply the general visibility conditions derived in this paper to this very ex-

treme case, where, unlike the visibility of Corsica from Nice, the Canigou would not be visible at all from moderate elevation around Marseille without refraction, which makes the application of the general theory more interesting.

The Canigou tops at 2785 m and the distance from Marseille area is about 260-270 km. Observations have been successfully carried out from several observing sites from Notre Dame de la Garde (altitude 160 m, distance 253 km) to the Mont Faron in the north of Toulon (altitude 584 m distance 292.5 km).

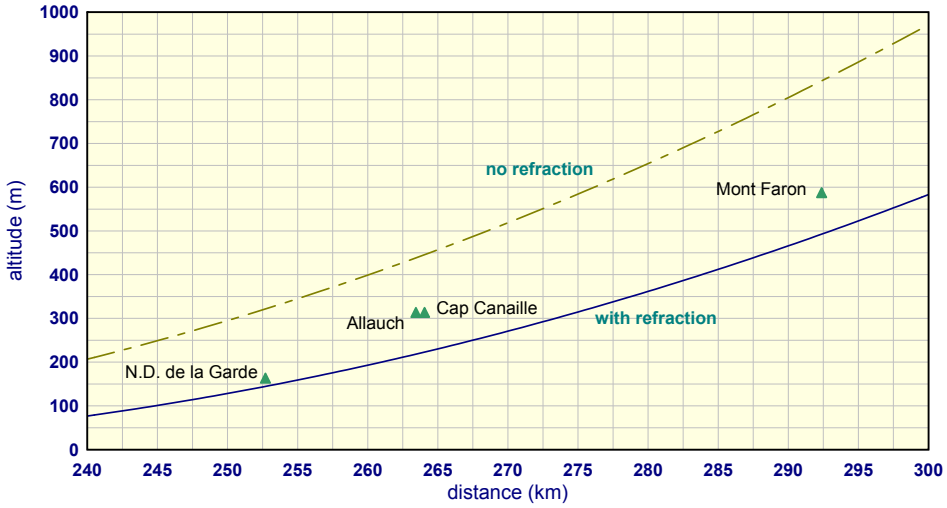


FIGURE 9.2: Lowest possible altitudes for an observer near Marseille to see the Canigou at sunset. The dashed curve is computed with light propagation on straight lines, while the solid line includes the refraction. Four sites are also mapped, showing that the visibility is only possible thanks to the curvature of the light rays and could be even marginal for N.D. de la Garde.

From the azimuths in Table 9.1 one finds that the observations are achievable on the $\sim$ 30 th October or $\sim$ 10 th February from N.D. de la Garde, on the $\sim$ 1 st November or $\sim$ 9 th February from Allauch, on the $\sim$ 24 th October or $\sim$ 17th February from Cap Canaille, on the $\sim$ 18th October or $\sim$ 23rd February from the top of the Mont Faron, with a margin of $\pm$ 1 day from year to year. One should also notice that both in November and February, the daily change of the azimuth of the sunset is nearly equal to the sun angular diameter, restricting the observation from a given place to a single evening or two within each favorable period. This is again a major difference with the visibility of Corsica and is more akin to searching a sunrise behind a particular peak of the Cap Corse.

The actual paths of the light ray, with or without refraction, are shown in Fig. 9.3 for

TABLE 9.1: *Visibility conditions of the Canigou ($\phi = 42.5189$ deg, $\lambda = 2.4567$ deg) from three sites around Marseille. The columns give the latitude, longitude and altitude of the sites, the arc-length and the azimuth to the Canigou, the earth local radius of curvature in this direction, the projected distance on the earth surface between a site and the Canigou and the lowest altitude visible near the Canigou with refracted rays. See explanation in the text. I have used a constant gradient for the refractive index of $\alpha = -dn/dh = 2.5 \times 10^{-5}$ km^{-1}. Changing this value by about $\pm 10\%$, decreases or increases the lowest altitude visible by about 60 m. For all this sites, a direct sight along a straight line would go under the sea (Eq. 3.20) at a depth between 70 m (Allauch) to 166 m (Mont Faron).*

Site	ϕ_1 deg	λ_1 deg	alt. m	θ deg	Az deg	R_c km	D km	$h_{\min}$ m
N.D. de la Garde	43.2839	5.3711	160	2.268	251.28	6385.7	252.7	2720
Allauch	43.3367	5.4864	310	2.364	250.80	6385.6	263.5	2495
Cap Canaille	43.1989	5.5528	310	2.369	254.38	6386.4	264.1	2510
Mont Faron	43.1503	5.9297	584	2.624	257.26	6386.9	292.5	2580

an observation from Allauch, in the north of Marseille, at an altitude of 310 m and a distance from the peak of 263 km. The light ray has been determined from the numerical integration of (5.31), using for the scale $R_c = 6385.6$ km. A standard atmosphere with temperature at sea level of 15 °C was used to compute the refractive index in the lower atmosphere. The extreme configuration for the visibility is striking on this plot, as only the fully refracted ray remains above the sea level between the Canigou and Allauch and is nearly grazing the surface of the sea. At the same location, but 100 m lower in altitude, the refracted ray would go under the sea, as shown in Fig. 9.2. Likewise, keeping the same altitude of 310 m but moving the station away by 12 km would be sufficient to make the observation impossible.

As a vivid proof, selected among the wide sample of pictures on A. Origné Webpages, the image of Fig. 9.1 has been taken from Allauch on February 9, 2008. The horizontal diameter of the sun of $\sim 32'$ provides a scale applicable to the vertical direction. If we assume that the bottom of the picture is aligned with the optical horizon, a crude measurement with a ruler shows that the angular altitude of the Canigou above the optical

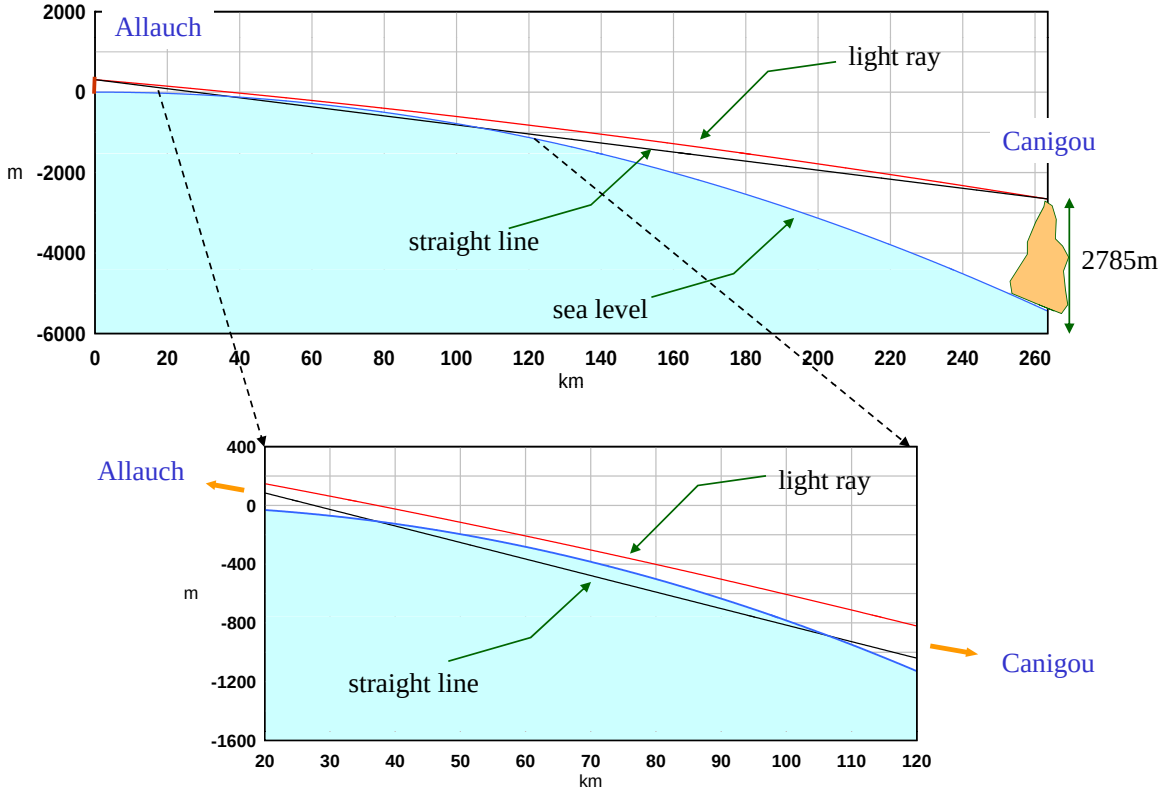


FIGURE 9.3: Light ray propagation between the top of the Canigou in the Pyrenees and Allauch, in the North of Marseille at an altitude of 310 m. The straight line goes about 93 m below the surface of the sea, while in normal atmospheric condition the refracted ray remains 74 m above at its lowest point. The vertical axis refers to the position of the earth or of the ray with respect to the horizontal plane at the sea level on the vertical of Allauch.

horizon is $4.3'$. Now the prediction based on (4.24) with the parameters of Table 9.1 yields $4.0'$. Changing the altitude of the observing site from 310 m to 320 m, raises this angle to $4.4'$. Thus, the mathematical prediction, and then the details of the phenomenon itself, are very sensitive to the precise location of the observer. In fact I consider this agreement as fortunate, since there are in general anomalous refractions on a ray grazing the surface of the sea, making the theory with standard temperature lapse rate questionable for these ultimate rays. Note that for the ray travelling from the top of the Canigou to Allauch, the minimum height above the sea computed with (4.17) is 70 m (74 m with numerical integration of (5.31)), above the thin layer in the first few metres above the sea where strong temperature gradients produce mirages and the standard model is normally

applicable.

10 The apparent shape of the sun

Basically this section dealing with the solar flattening brings nothing directly relevant for the visibility of Corsica from Nice. However, these observations of Corsica in the morning, or that of the Canigou in the evening, are clear opportunities to make snapshots of the sun rising or setting just on the optical horizon and then to investigate its flattened shape. Since one attempts to observe normally from elevated places, the depression of the optical horizon below the horizontal plane is significant, often larger than 0.5 degrees, and the flattening is larger than what one can see with an observation near the horizon from a sailing boat or from a beach. The astronomical tables never give the refraction below the horizontal plane, and the sun flattening resulting from the differential refraction is likewise never estimated below the astronomical horizon. In this section, I derive numerical and analytical formulas to fill this gap with range of validity extending to depressions as large as one degree, or equivalently for an observer able to see the optical horizon from an altitude of about 1000 m.

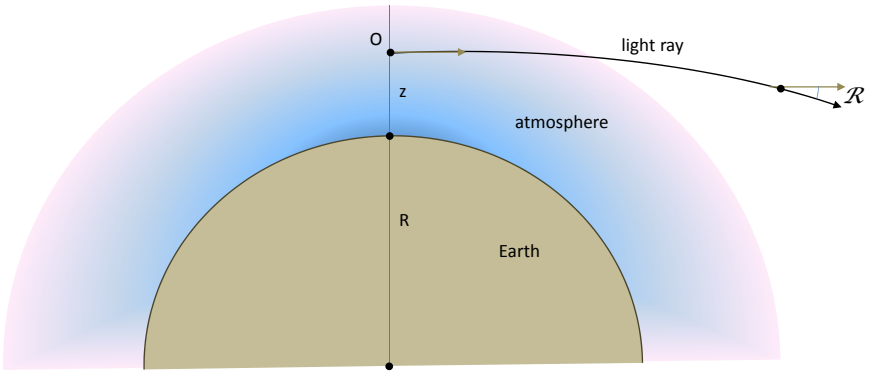


FIGURE 10.1: Astronomical refraction for an horizontal ray. The astronomical refraction $\mathcal{R}(h, z)$ is the angular difference between the initial direction of the ray (here in the horizontal plane) and that outside the atmosphere.

I establish first several numerical results based on the computation of the astronomical refraction in the vicinity of the horizontal plane (above and below), including an expression for the sun flattening as a function of its apparent position. Then I show how the main terms of these polynomials can be obtained from physical and analytical considerations from simple expressions using only the physical parameters of the atmosphere.

In this section, to stick with some traditional astronomical practices, I denote the altitude (height in metres or km) of an observer above the earth with z and the altitude (angular, in

degrees or radians) of a the direction along a light ray above the observer horizontal plane as h. This angle is positive when the ray starts above the astronomical horizon of the observer, and negative below, which happens when the observer optical horizon is below the astronomical horizon. Compared to the earlier sections one has $h = -\epsilon$. The altitude h at the observer where an astronomical source is seen is called the *apparent altitude* while the geometric altitude, hereafter denoted ζ, is referred to as the *true altitude*.

Regarding the overall shape of the apparent sun, the earth's atmosphere can be considered as an optical system, mapping a source lying in the object space into an image in the image space. One considers here only the case of a standard atmosphere, with a regular and small atmospheric gradient of the refractive index, so that the mapping between the object and image spaces is one-to-one, meaning that the optical system is stigmatic for an extended area. A point source is mapped onto a single point-like image, with a slowly varying magnification. In real conditions, the lower layers of the atmosphere departs from this ideal situation and often what one sees is a seriously distorted image of the solar disk, with lower or superior mirages. However, occasions to see a perfect flattened shape down to, or up from, the horizon are not so exceptional that investigating the phenomenon in detail is less academic than one may think at first glance.

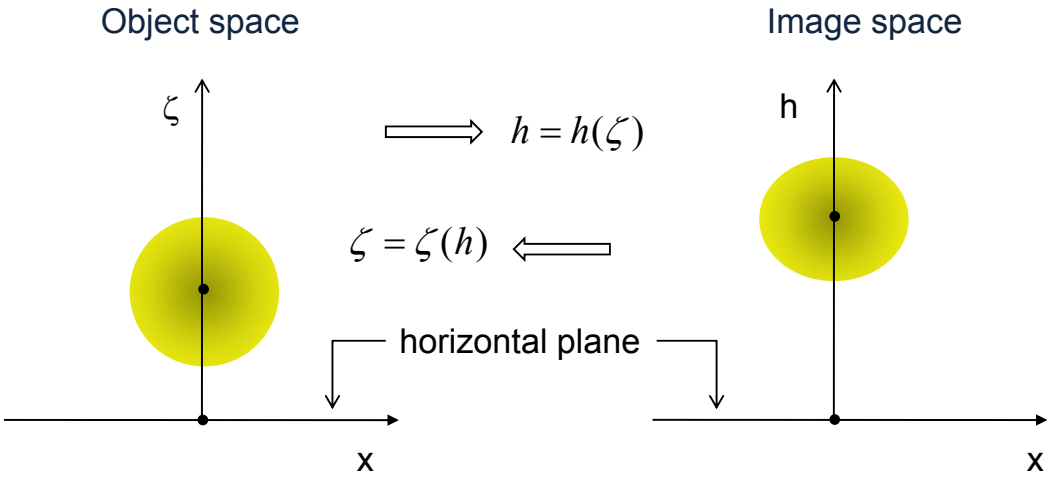


FIGURE 10.2: Correspondence between the object and the image in the optical mapping by the atmosphere. Unlike in most image forming systems, the reference systems are identical in both spaces, being tied to the horizontal plane and the local vertical of the observer.

10.1 Astronomical refraction

.

10.1.1 Defining equations

The astronomical refraction is the change in altitude resulting from the light bending through the atmosphere for a source placed outside the atmosphere. The difference with the terrestrial refraction has been already stressed in Sect. 4.2.1. Let h be the apparent altitude of a source and ζ its geometric altitude. The optical mapping by the atmosphere provides the relationships,

$$h \quad \rightleftarrows \quad \zeta \tag{10.1}$$

or

$$\zeta = \zeta(h) \tag{10.2}$$

from a computation of the path of the ray starting along the initial direction h. The direction of the tangent outside the atmosphere being precisely the geometric direction ζ. Then one defines the refraction angle as the difference between the two directions as,

$$\mathcal{R}(h) = h - \zeta \tag{10.3}$$

As this depends also on the observer altitude z above the sea level, I also use $\mathcal{R}(h, z)$ when needed. The horizontal refraction illustrated in Fig. 10.1 is the refraction for $h = 0$, when the ray starts in the observer's horizontal plane. In (10.3), the refraction is an explicit function of the apparent direction h, but it can also be considered as an implicit function of the geometric direction ζ, since one has,

$$\zeta = h - \mathcal{R}(h) \tag{10.4}$$

which is a non linear equation which can be solved in h for a particular ζ. Then the refraction $\mathcal{R}$ can be evaluated as a function of ζ with (10.3).

In the following developments, two quantities would be of particular importance and are introduced in this defining section. The optical mapping between the object and image spaces produces a vertical magnification (in the present case always < 1) of a small object. If the object is large enough in the vertical direction, the magnification cannot be considered constant over its size and there is also a distortion, meaning the image (only in the vertical direction) is not simply an expanded or compressed copy of the object. The magnification is responsible for the overall flattening of the sun, and the distortion

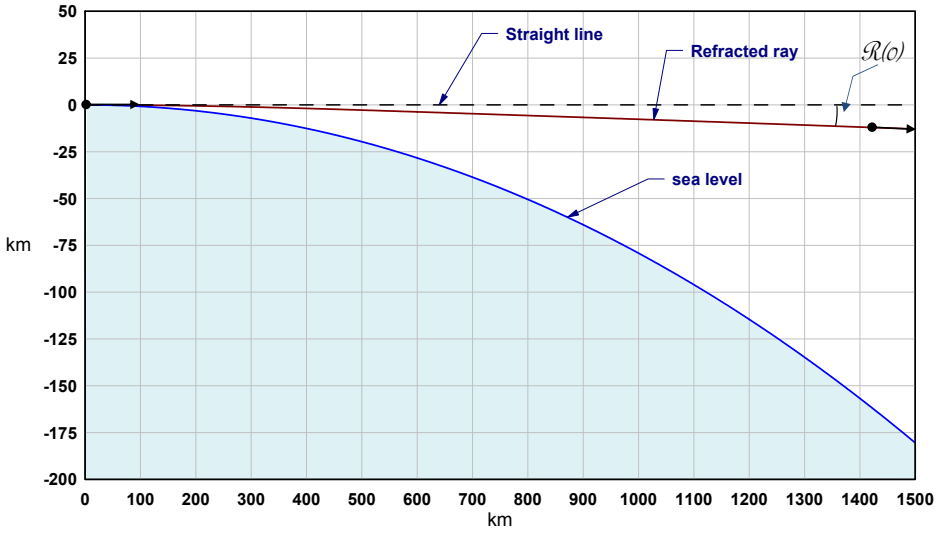


FIGURE 10.3: Path of an initially horizontal light ray in the earth atmosphere compared to a propagation in the vacuum. The horizontal astronomical refraction $\mathcal{R}(0) \simeq 33'$ is the amount of deflection along the ray until it reaches the external boundary of the atmosphere. The horizontal path is about 1000 km to reach the altitude of 100 km, where the refraction becomes totally negligible. At this distance the ray is just 7.5 km below the straight line. The light ray has been numerically integrated with the refractive index derived from the standard atmosphere model introduced in Sect. 11.2.

accounts for the very small asymmetry between the upper and lower half of the solar image.

Let Γ be the magnification,

$$\Gamma = \frac{dh}{d\zeta} \tag{10.5}$$

giving the ratio between the vertical size of the image (δh) of a small object to its true size ($\delta\zeta$). Then one has,

$$\Gamma = \frac{1}{\dfrac{d\zeta}{dh}} = \frac{1}{1 - \dfrac{d\mathcal{R}}{dh}} \tag{10.6}$$

which can be explicitly computed as soon as one has a numerical method to compute the refraction or an analytical representation as a function of the apparent direction.

The distortion Δ is just the rate of change of the magnification

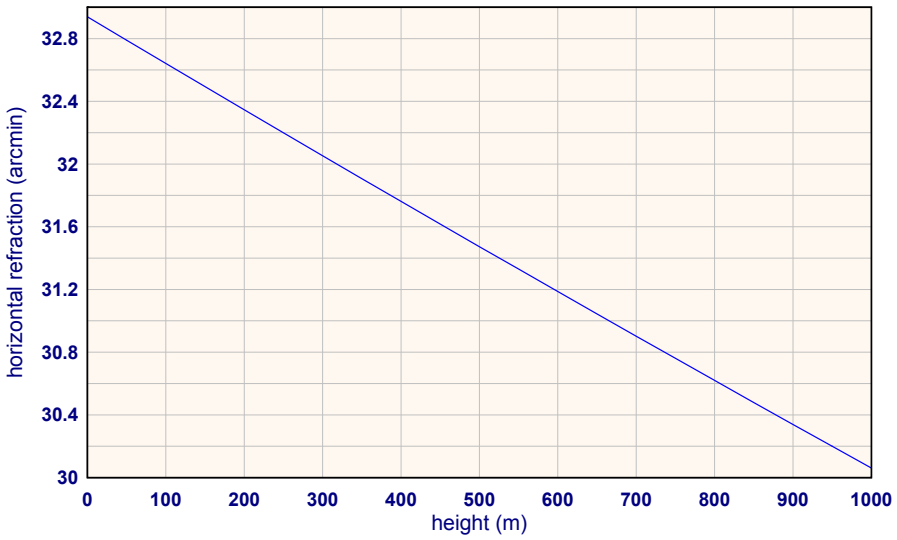


FIGURE 10.4: Variation of the astronomical horizontal refraction (i.e referred to the astronomical horizon) with the observer's altitude.

$$\Delta = \frac{d\Gamma}{dh} \tag{10.7}$$

and can be evaluated explicitly with the derivatives of $\mathcal{R}$ with (10.6),

$$\Delta = \Gamma^2 \frac{d^2\mathcal{R}}{dh^2} \tag{10.8}$$

10.1.2 Numerical integration

For normal atmospheric conditions at sea level ($P = 1013$ hPa, $t = 15°$C), I have integrated numerically the path of the light ray starting in different directions in the vicinity of $h = 0$ and for different altitudes of the observer. Table 10.1 gives the horizontal refraction $\mathcal{R}(0, z)$ at different altitudes, while the refraction near the horizon at $z = 1000$ m is tabulated in Table 10.3, down to the optical horizon depression, which in this case is about 1 deg (4.1. The horizontal refraction $\mathcal{R}(0, z)$ will be used later to derive an analytical expression for the sun flattening.

10.1.3 Polynomial fitting

As shown in Fig. 10.4 the decrease of the horizontal refraction with the altitude of the observer is nearly linear and easily fitted by polynomial. The numerical expression is

TABLE 10.1: *Horizontal refraction at different altitude above sea level and for standard atmospheric conditions at $z = 0$. The values expressed in arcmin have been computed by integrating the path of light through the atmosphere up to an altitude of 100 km, equivalent to a path length of about 1000 km. This is the refraction for a ray reaching the observer in the horizontal plane (altitude = 0 deg) and not the refraction of ray grazing the optical horizon, which is larger as soon as $z > 0$, as seen in Table 10.3.*

z	$\mathcal{R}(0)$	z	$\mathcal{R}(0)$
m	arcmin	m	arcmin
0	32.939	550	31.330
50	32.790	600	31.187
100	32.642	650	31.044
150	32.494	700	30.902
200	32.346	750	30.761
250	32.199	800	30.620
300	32.053	850	30.479
350	31.907	900	30.339
400	31.762	950	30.200
450	31.617	1000	30.061
500	31.473	-	-

given in (10.9), with z in km and the refraction in arcmin. The first two coefficients (in z and z^2) of this polynomial will be related to physical parameters in Section 10.2.

$$\mathcal{R}(0, z) = 32.94 - 2.989\, z + 0.117\, z^2 - 6.4 \times 10^{-3}\, z^3 \tag{10.9}$$

As for the general polynomial representation of the refraction as a function of the apparent direction h in the range -1 deg to 4 deg, including the effect of the observer's altitude is amazingly and unexpectedly simple, since it can be factored with two polynomial in h and z as,

TABLE 10.2: *Astronomical refraction for altitudes from 0 degrees to + 4 degrees. It is computed for an observer at sea level down to his horizontal plane. Γ is the magnification of the atmospheric optical system and $1 - \Gamma$ would be the solar flattening.*

h	$\mathcal{R}$	Γ	h	$\mathcal{R}$	Γ
arcmin	arcmin	-	arcmin	arcmin	-
240.00	11.463	0.9657	85.00	20.769	0.9104
230.00	11.829	0.9638	80.00	21.271	0.9072
220.00	12.216	0.9617	75.00	21.793	0.9038
210.00	12.626	0.9595	70.00	22.336	0.9002
200.00	13.061	0.9571	65.00	22.901	0.8966
190.00	13.522	0.9545	60.00	23.490	0.8927
180.00	14.014	0.9518	55.00	24.104	0.8887
170.00	14.537	0.9488	50.00	24.743	0.8845
160.00	15.095	0.9455	45.00	25.410	0.8801
150.00	15.691	0.9420	40.00	26.106	0.8755
140.00	16.328	0.9382	35.00	26.833	0.8707
130.00	17.010	0.9340	30.00	27.592	0.8657
120.00	17.742	0.9295	25.00	28.385	0.8604
115.00	18.128	0.9271	20.00	29.214	0.8550
110.00	18.528	0.9246	15.00	30.082	0.8492
105.00	18.943	0.9220	10.00	30.990	0.8432
100.00	19.374	0.9193	5.00	31.942	0.8370
95.00	19.822	0.9164	**0.00**	**32.939**	**0.8304**
90.00	20.286	0.9135	-	-	-

TABLE 10.3: *Astronomical refraction for altitudes from -1 degree to + 4 degrees. It is computed for an observer at 1000 m to have the horizon depression as large as one degree. Changing the refraction column with a constant offset taken from Table 10.1 would give the refraction from another height above sea level with sufficient accuracy, as can be checked by straight comparison to Table 10.2.* Γ *is the magnification of the atmospheric optical system and* $1 - \Gamma$ *would be the solar flattening. The slight change with altitude can also been assessed with Table 10.2 at* $h = 0$.

h	$\mathcal{R}$	Γ	h	$\mathcal{R}$	Γ
arcmin	arcmin	-	arcmin	arcmin	-
240.00	10.459	0.9687	55.00	21.984	0.8973
230.00	10.791	0.9670	50.00	22.568	0.8934
220.00	11.143	0.9651	45.00	23.178	0.8893
210.00	11.516	0.9630	40.00	23.814	0.8850
200.00	11.911	0.9608	35.00	24.478	0.8805
190.00	12.331	0.9585	30.00	25.172	0.8758
180.00	12.778	0.9559	25.00	25.897	0.8709
170.00	13.254	0.9531	20.00	26.655	0.8657
160.00	13.762	0.9501	15.00	27.449	0.8603
150.00	14.305	0.9469	10.00	28.279	0.8547
140.00	14.886	0.9433	5.00	29.149	0.8488
130.00	15.508	0.9395	**0.00**	**30.061**	**0.8427**
120.00	16.175	0.9353	-5.00	31.017	0.8362
115.00	16.527	0.9331	-10.00	32.021	0.8295
110.00	16.893	0.9308	-15.00	33.074	0.8224
105.00	17.271	0.9283	-20.00	34.181	0.8151
100.00	17.665	0.9258	-25.00	35.345	0.8073
95.00	18.073	0.9232	-30.00	36.569	0.7993
90.00	18.497	0.9204	-35.00	37.857	0.7909
85.00	18.938	0.9175	-40.00	39.214	0.7821
80.00	19.396	0.9145	-45.00	40.645	0.7729
75.00	19.873	0.9114	-50.00	42.154	0.7633
70.00	20.369	0.9081	-55.00	43.747	0.7533
65.00	20.885	0.9047	-60.00	45.430	0.7429
60.00	21.423	0.9011	-65.00	47.210	0.7321

$$\mathcal{R}(h,z) = \mathcal{R}(0,z) + \left[-12.42\,h + 3.570\,h^2 - 0.6963\,h^3 + 0.06155\,h^4\right](1 - 0.086\,z) \tag{10.10}$$

where $\mathcal{R}(h,z)$ is in arcmin, h in degrees and z in km. The units have been so chosen as to have coefficients close to unity. The accuracy is better than $10'$ over the domain ($-1 < h < 3$ deg) and sufficient for all the applications, considering the high variability of the refraction near the horizon. Obviously it makes non sense to apply this formula at the altitude z below the corresponding optical horizon, since the ray goes under the sea level. Most of the numerical coefficients will be given a physical explanation in the next section.

By expressing first $\mathcal{R}$ in (10.10) in degrees and then differentiating with respect to h, one obtains the magnification (10.6) as,

$$\Gamma(h) = \frac{1}{1.207 - 0.119\,h + 0.0348\,h^2 - 0.0041\,h^3} \tag{10.11}$$

whose validity is limited to $h < 3$ deg. A more accurate expression from $h = -1$ deg up to $h = 4$ deg is given below with a third order polynomial fitted to the magnification directly determined with the numerical integration of the ray associated to an accurate numerical differentiation. The first coefficient includes the small effect resulting from the observer altitude:

$$\Gamma(h) = 0.8302(1 + 0.015z) + 0.080\,h - 0.0195\,h^2 + 0.00192\,h^3 \tag{10.12}$$

where, as before, h is in degrees and z in km. The complement to the magnification $1-\Gamma(h)$ is plotted in Fig. 10.5 as a function of the altitude of the image (apparent altitude), for an observer at the sea level and another at 500 m. The curves are nearly identical and the extrapolation below the optical horizon gives the magnification for an observer with a higher depression below the astronomical horizon. The value around $h = 0$ is equivalent to the sun flattening at rise or set.

10.1.4 Overall shape of the solar image

Uniform flattening The simplest approach consists in taking the sun as a small circular luminous object of radius $\delta = 16'$. When its centre is in the geometric direction ζ, it is seen by an observer in the apparent direction $h(\zeta) = \zeta + \mathcal{R}(h)$. We know that the vertical magnification of the image in that direction is $\Gamma(h)$ and can be computed with (10.12).

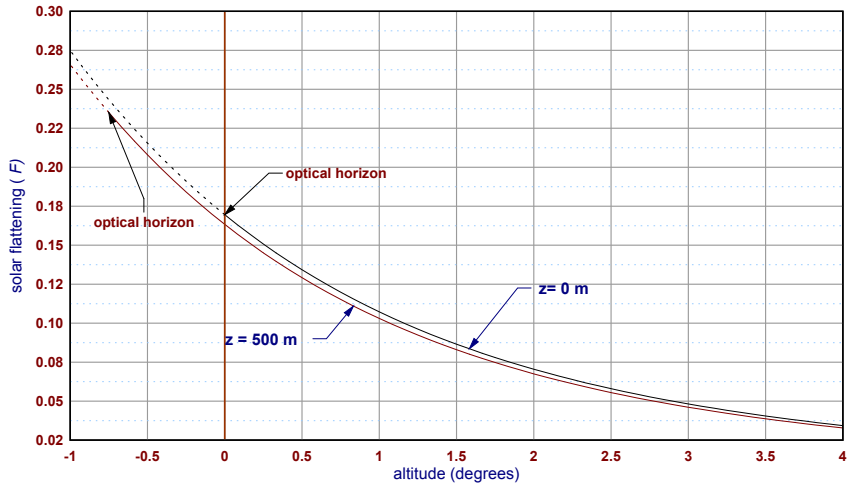


FIGURE 10.5: Overall solar flattening through the standard atmosphere considered as a stigmatic optical system. A vertical object is shrunk (magnification < 1) by the differential refraction. The curves are given for an observer at sea level or at an height of $500\,\mathrm{m}$, to show that the flattening is not very sensitive to the observer altitude. The flattening is meaningful down to the optical horizon and the extrapolation appear in dotted lines. When the lower limb of the solar image just touches the horizon, the flattening is about 17% at sea level while at $500\,\mathrm{m}$, with a depression of the optical horizon of $45'$, the flattening reaches 23%. In real conditions, these factors are highly variable.

Therefore when the lower limb is seen just in the horizontal plane when $h = 0$, the centre is at the altitude $h_c \sim \Gamma(0)\delta \sim 13'$ and finally the vertical magnification of the disc is $\Gamma(h_c) \sim 0.84$. The vertical diameter is then shorter than the horizontal one, and the sun looks shrinked or flattened.

The ratio between the two axes is equal to $\Gamma(h_c)$ and is usually referred to as the *solar flattening*, although this is not a good terminology: this flattening factor is equal to one, when there is no *flattening* at all and the number decreases as the flattening gets larger. I prefer to use the same definition as for the earth with $\mathcal{F} = (a - b)/a$, where a, b are the equatorial and polar axes. Then the flattening of the solar image is $1 - \Gamma(h)$, when h is the altitude of the image of the centre of the sun, very similar to what we spontaneously refer to as *the centre of the image*, although, due to the asymmetry of the image, its centre has no obvious definition. Anyway, the flattening of the circular sun, high above the horizon, is zero and increases as the sun approaches the optical horizon and gets more flattened.

Mathematically the flattening can be expressed as a function of the first derivative of the

refraction angle $\mathcal{R}(h)$ as,

$$\mathcal{F} = \frac{-\dfrac{d\mathcal{R}}{dh}}{1 - \dfrac{d\mathcal{R}}{dh}} \tag{10.13}$$

and with (10.12), this leads to the polynomial representation of the flattening for altitude in the range $-1° < h < 4°$, with z in km:

$$\boxed{\mathcal{F}_\odot = 0.1698(1 - 0.073z) - 0.080\,h + 0.0195\,h^2 - 0.00192\,h^3} \tag{10.14}$$

The position and shape of the solar image and the geometric position of the sun are sketched in Fig. 10.6 for observations near the optical horizon and for nominal atmospheric conditions. The two leftmost cases refer to an observer at about 500 m observing the sunrise and few minutes later the sun about half degree above his optical horizon. The other cases are for an observer at sea level, with the rising sun and few other altitudes.

Differential flattening The sun is not infinitely small, and the change of magnification over its size is not negligible, giving rise to a slight asymmetry between the upper and lower half. I derive now the equation of the apparent rim through the refraction, from which one can easily derive the asymmetry factor.

Let $\tilde{x} = 0, \zeta_0$ the centre of the sun in the object space. The rim is a circle of radius $\delta = 32'$, of equation

$$(\zeta - \zeta_0)^2 + \tilde{x}^2 = \delta^2 \tag{10.15}$$

in which one can plug the imaging transformation,

$$\tilde{x} = x \tag{10.16a}$$

$$\zeta = h - \mathcal{R}(h) \tag{10.16b}$$

$$\zeta_0 = h_0 - \mathcal{R}(h_0) \tag{10.16c}$$

where the last sub-equation is introduced for convenience to use the image of the centre of the sun as a reference in the image space, since the constant ζ_0 is in practice not accessible.

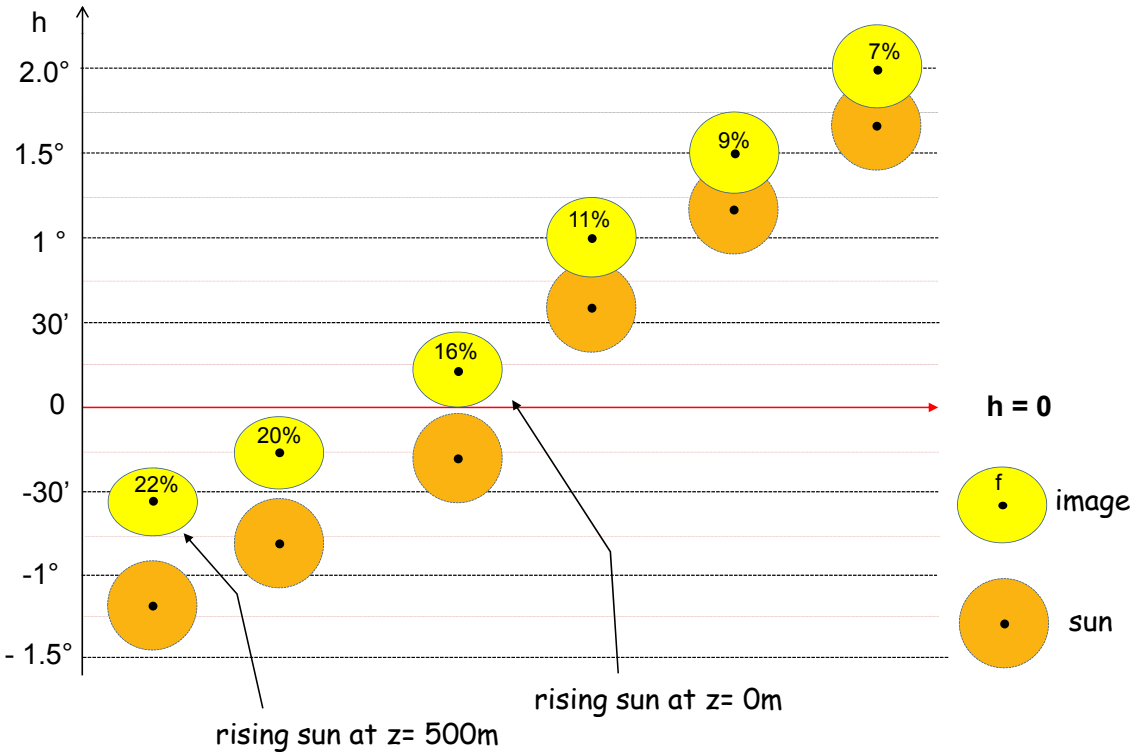


FIGURE 10.6: The diagram shows the geometric position of the sun and that of its flattened image at different altitudes and for standard atmospheric conditions. The two examples on the left are for an observer seing the sun from an altitude of 500 m, including the sunrise, while the others are from the sea level. The flattening in % is given within each image.

By inserting (10.16) into (10.15) one gets the equation of the external boundary of the image of the sun as,

$$(h - h_0 - (\mathcal{R}(h) - \mathcal{R}(h_0)))^2 + x^2 = \delta^2 \tag{10.17}$$

and considering the small size of the sun, the refraction terms in the parenthesis can be expanded to the second order in $h - h_0$. The equation becomes,

$$\left[(1 - \frac{d\mathcal{R}}{dh})(h - h_0) - \frac{1}{2}\frac{d^2\mathcal{R}}{dh^2}(h - h_0)^2\right]^2 + x^2 = \delta^2 \tag{10.18}$$

and with (10.6) and (10.8) this becomes,

$$\left[\frac{h-h_0}{\Gamma}-\frac{\Delta}{2}\left(\frac{h-h_0}{\Gamma}\right)^2\right]^2+x^2=\delta^2 \tag{10.19}$$

where the magnification Γ and distortion Δ are taken at h_0.

Ignoring first the distortion, which has a very small contribution over the size of the sun disk, (10.19) reduces to,

$$\frac{(h-h_0)^2}{\Gamma^2}+x^2=\delta^2 \tag{10.20}$$

that is to say that of an ellipse centred at $x=0, h=h_0$ with the large axis δ in the horizontal direction and a small vertical axis $\Gamma\,\delta$. At this level of approximation, the overall shape of the sun is elliptical with a flattening determined by the magnification taken at its centre. This is equivalent to the conclusion reached above from simpler arguments.

Let see now the next approximation with the differential effect between the upper and lower limb taken into account. With $\Delta\sim 0.08$ deg^{-1} near the horizon, the term involving the distortion in (10.19) is a correction not larger than 2%. Then one can rewrite the equation of the shape in the following form,

$$\frac{(h-h_0)^2}{\Gamma^2}\left(1-\Delta\frac{h-h_0}{\Gamma}\right)+x^2=\delta^2 \tag{10.21}$$

which is that of a slightly distorted ellipse with more flattening in the lower part than in the upper's. Considering now the position of the lowest and highest points at $x=0$, by denoting h_u for the upper limb, h_l for the lower limb, and as before h_0 remains the apparent altitude of the image of the centre of the sun. It is not necessarily identical to the centre of the actual image, since with a figure lacking horizontal symmetry this is loosely defined.

Solving for h when $x=0$ one finds with $(h-h_0)/\Gamma\sim\delta$,

$$h_u=h_0+\Gamma\delta\left(1+\frac{\Delta\delta}{2}\right) \tag{10.22a}$$

$$h_l=h_0-\Gamma\delta\left(1-\frac{\Delta\delta}{2}\right) \tag{10.22b}$$

and finally

$$h_u - h_l = 2\Gamma\delta \tag{10.23}$$

and the flattening,

$$1 - \frac{h_u - h_l}{2\delta} = \mathcal{F} \tag{10.24}$$

Equation (10.23) shows that the global shape of the sun, defined as the ratio between the vertical to the horizontal extension, is given by the magnification taken at its apparent centre. One the other hand, (10.22a) - (10.22b) give the asymmetry between the two halves of the solar image. The interpretation is obvious: the extension of the upper half is the radius shrunk by the magnification taken at the mid point between the centre and the upper rim, while this is just the opposite for the lower half.

For the sun observed at sea level with the lower limb just touching the horizon, one has $h_l = 0$ and then with (10.22b), $h_0 = \Gamma\delta(1 - \Delta\delta/2)$ and for the upper half $h_u - h_0 = \Gamma\delta(1 - \Delta\delta/2)$. With $\Gamma(h_0) = 0.84$ and $\Delta = 0.08$ deg^{-1}, and $\delta = 16'$, one obtains,

$$h_u - h_0 = 13\farcm58 \tag{10.25a}$$

$$h_0 - h_l = 13\farcm30 \tag{10.25b}$$

$$h_u - h_l = 26\farcm88 \tag{10.25c}$$

The asymmetry is really very small, of the order of 17 arcsec and the plot of the true shape cannot be distinguished from an ellipse. A plot with much stronger distortion far from the standard conditions can be seen in Fig. 10.9. It is useful to introduce an asymmetry coefficient, or a skewness factor,

$$\mathcal{S} = \frac{(h_u - h_0) - (h_0 - h_l)}{(h_u - h_0) + (h_0 - h_l)} = \frac{\Delta\,\delta}{2} \tag{10.26}$$

as the ratio of the difference between the size of the upper and lower half, scaled to the apparent vertical diameter. It is essentially the variation of the magnification over the image of the solar disk. This is a dimensionless quantity, which is zero for a symmetric shape, positive and < 1 when the lower half is shorter than the upper's. It would be negative if the opposite could happen. For the standard conditions and the lower limb of the sun at the horizon $\mathcal{S} \sim 1\,\%$.

A more realistic picture In general the image of the sun close to the horizon is much less regular as the light propagation near the horizon is more complex yielding images of a very distorted sun as it plunges (raises above) below the horizon. Due to the more or less horizontal stratification of temperature above the sea, complex mirage structures appear, notching the image of the solar disk. Typically in summer, the sea temperature is lower than the surrounding air just above its surface and the temperature gradient is positive over the few ten's metres. This is the source of upper mirages, raising the lower part of the solar disk in front of the image of the higher part which are less refracted. Since the horizontal width remains unchanged in this process, one sees an irregular shape until at least half of the solar image is below the horizon. This is well visible in the sequence of picture shown in Fig. 10.7 taken during a summer sunset, when the air temperature was higher than that of the sea surface. The whole sequence duration is 4 minutes.

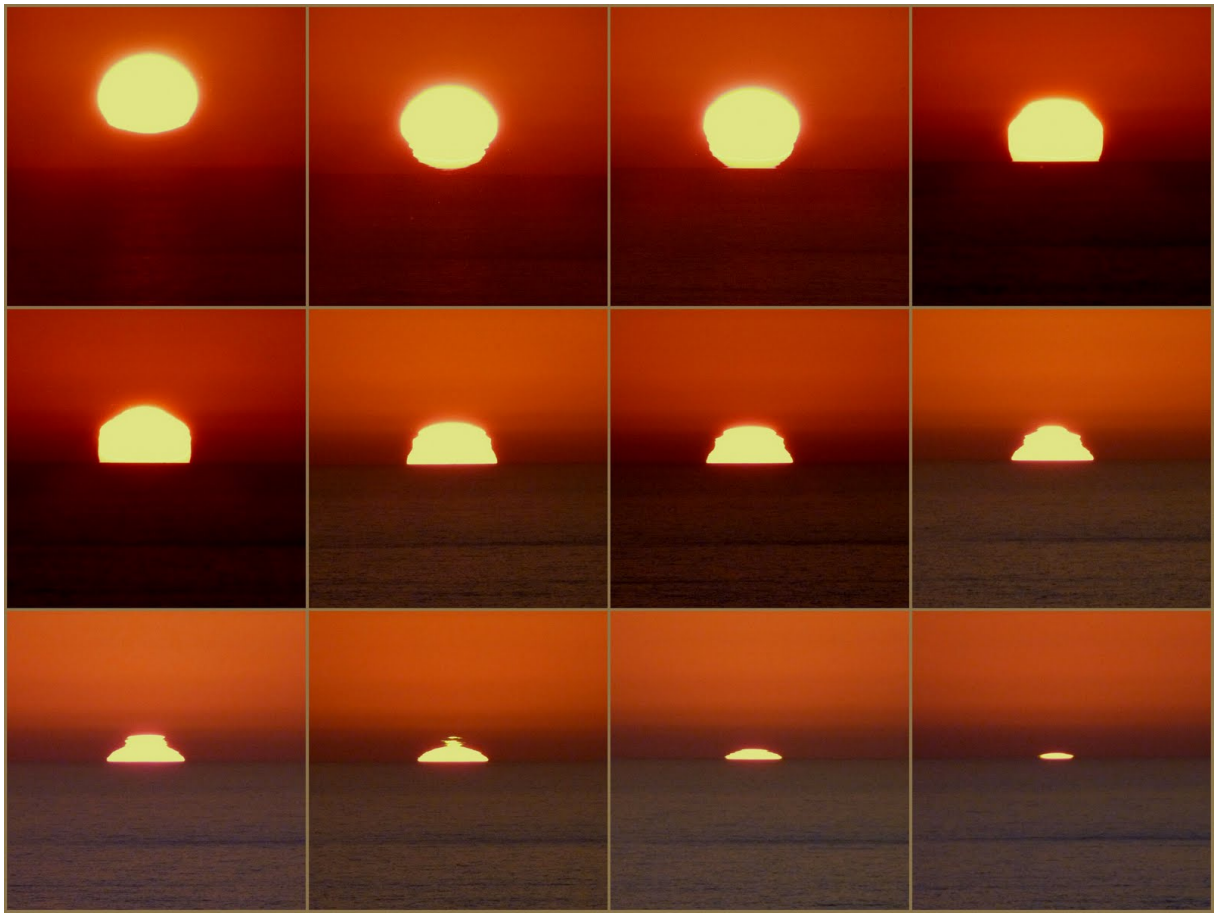


FIGURE 10.7: Images of a summer sunset above the sea showing the complex distortions resulting from layers with temperatures discontinuities. The observer (indeed me) stands at 80 m above the sea level, giving a distance to his optical horizon of about 30 km and a depression of 15 arcmin. The sequence covers 4 mn of time between the first and last image. The air temperature was about 5 degrees higher than the sea surface.

10.2 Physical approach

In this section I show how the differential refraction near the horizon, which is only what matters for the solar flattening, can be easily modelled with elementary geometry and physics, and then how the most important numerical coefficients in the polynomial representations used earlier can be accounted for with fundamental physical parameters.

10.2.1 Horizontal refraction at altitude z

The horizontal refraction $\mathcal{R}(0,z)$ has been listed in table 10.1 and fitted to a third degree polynomial in (10.9). The ray starting horizontally at altitude z is nearly identical to the ray at the sea level but for the pressure and temperature conditions prevailing at the starting point. It must be almost parallel to a ray starting at $z = 0$ with the physical conditions holding at z. Therefore one expects that,

$$\mathcal{R}(0,z) \simeq \mathcal{R}(0,0)\frac{P(z)}{P_0}\frac{T_0}{T(z)} \tag{10.27}$$

which is the same as,

$$\mathcal{R}(0,z) \simeq \mathcal{R}(0,0)\frac{(n-1)_z}{(n-1)_0} \tag{10.28}$$

studied in Sect. 11. The analytical expansion has been given in (11.22) with the corresponding numerical polynomial in (11.23). Using this equation and inserting into (10.28) one has for the horizontal refraction at z,

$$\mathcal{R}(0,z) \simeq \mathcal{R}(0,0)(1 - 0.09603z + 0.003514z^2 - 5.56\times10^{-5}z^3) \tag{10.29}$$

with z in km. Using now $\mathcal{R}(0,0) = 32.94'$, we end up with,

$$\mathcal{R}(0,z) \simeq 32.94 - 3.163\,z + 0.116\,z^2 - 0.002\,z^3 \tag{10.30}$$

which compares fairly well with the numerical fitting based on numerical integration given in (10.9)

$$\mathcal{R}(0,z) = 32.94 - 2.989\,z + 0.117\,z^2 - 6.4\times10^{-3}\,z^3 \tag{10.31}$$

meaning that the *change* of the horizontal refraction with the altitude up to $\sim$ 1000 m can be modelled with few physical parameters by formula given in (11.22). It is important to stress that the value $\mathcal{R}(0,0)$ cannot be determined without a full integration of the ray throughout the atmosphere, whereas the variations with z are almost entirely determined by the change of the local physical condition at low altitude. The linear coefficient in (10.9) based on the numerical integration is 5% smaller than the theoretical value, a discrepancy I have not been able to account for.

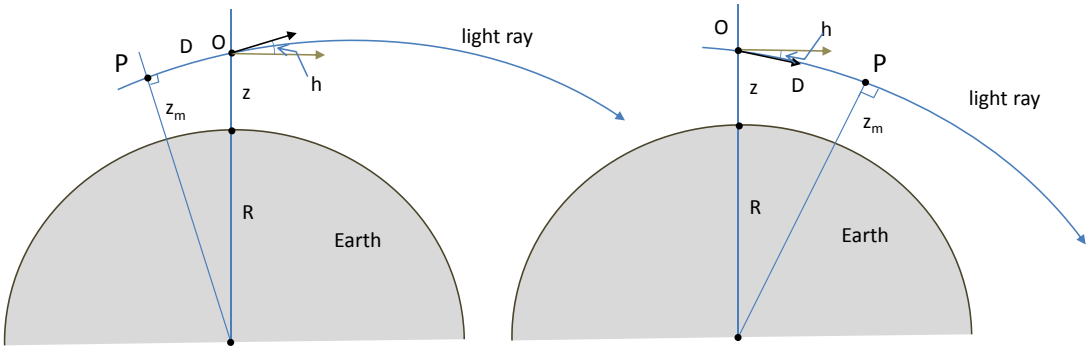


FIGURE 10.8: Astronomical refraction at O, $\mathcal{R}(h,z)$, is related to the horizontal refraction of the same ray at P, $\mathcal{R}(0,z_m)$. The difference is just the ray bending over the distance D between O and P.

10.2.2 Refraction near the horizontal

I consider now whether it is possible to relate in a simple manner the refraction $\mathcal{R}(h,z)$ to the horizontal refraction at the same altitude, namely to $\mathcal{R}(0,z)$, at least for small h, positive or negative. The answer to this issue is clearly positive as shown in Fig. 10.8, which shows the light ray starting from an altitude z above the earth with the initial direction h, upward (left panel) or downward (right panel). If h is small enough, there is a point P close to O where the ray is horizontal for an observer at P. Therefore the refraction at $\mathcal{R}(h,z)$ at O is equal the horizontal refraction at P, plus or minus a small angle due to the light bending between O and P over the distance D. This translates into the general relation,

$$\mathcal{R}(h,z) = \mathcal{R}(0,z_m) + \delta(h) \tag{10.32}$$

We have already computed the parameters z_m and D in Sect. 4.1, and more specifically

in the equations (4.16) for the distance to reach the minimum altitude and (4.18) for the minimum altitude. Given the use of astronomical notation here one must recall that $h = -\epsilon$ and the altitude above sea level noted h before is the same as z in this section. Therefore one has,

$$D = -\frac{Rh}{1 - \alpha\, R} \tag{10.33}$$

(it is in fact an abscissa with a sign and not purely a distance) and

$$z_m = z - \frac{Rh^2}{2(1 - \alpha\, R)} \tag{10.34}$$

where the refractive gradient α must be taken at some average point between z and z_m.

Solution to first order in h. To first order in h one has the very simple result that $\delta(h) = D/\rho = \alpha\, D$ where ρ is the radius of curvature of the ray along OP, that is to say,

$$\delta(h) = -\frac{\alpha R}{1 - \alpha\, R}\, h \tag{10.35}$$

yielding for the refraction to the same level of approximation,

$$\mathcal{R}(h, z) = \mathcal{R}(0, z_m) - \frac{\alpha R}{1 - \alpha\, R}\, h \tag{10.36}$$

and then

$$\left(\frac{d\mathcal{R}}{dh}\right)_{h=0} = -\frac{\alpha R}{1 - \alpha\, R} \sim 0.204 \tag{10.37}$$

with $\alpha = 2.65 \times 10^{-5}$ km^{-1} at sea level from (11.21). This is identical to the coefficient in h in the polynomial fit (10.10), (once divided by 60 because of the units).

Using now the definition of the solar flattening in (10.13) one gets immediately the flattening at horizon, (more exactly the flattening of the sun when the centre of the image of the sun crosses the horizon, which is a little larger than the flattening when the lower limb just rises),

$$\boxed{\mathcal{F} = \alpha\, R \sim 0.17} \tag{10.38}$$

a remarkable property linking the easily observed flattening to the refractive index gradient at the sea level. Since the gradient of the refractive index in the lowest layers of the atmosphere is highly dependent on the temperature gradient, one may also expect that the actual flattening will display a strong variability with local conditions, let alone the occurrence of discontinuity layers source of much stronger and less regular distortions with inferior and superior mirages. Even with slight departure from standard atmospheric conditions, with a temperature lapse rate significantly larger or smaller than the reference value of $6.5\,\mathrm{K\,km^{-1}}$, the outline of the solar image remains regular and smooth but showing variations from a nearly perfect disk to flattening above 20%.

This fact can be quantified with the expression of the refractive index gradient at sea level derived in (11.22) as,

$$\alpha = (n-1)_0 \frac{Mg}{RT_0}\left(1 - \frac{\gamma R}{Mg}\right) \tag{10.39}$$

where the factor in the right parenthesis includes the temperature lapse rate γ. In standard conditions the pressure term alone gives $\alpha\, R \simeq 0.21$, which would be the flattening for an isothermal atmosphere, or at least for conditions with constant temperature near the ground or sear level. Now the thermal gradient will change this flattening by a factor

$$1 - \frac{\gamma R}{Mg} \tag{10.40}$$

with $Mg/R \simeq 34\,\mathrm{K\ km^{-1}}$. In standard condition $\gamma = 6.5\,\mathrm{K\,km^{-1}}$ and the thermal factor is 0.81, giving the flattening of 0.17. Locally the thermal gradient over the first 10 to 100 m, can be much different from the standard one, and much larger where the ground is warmer than the surrounding air, without reaching the conditions with density inversion when the thermal factor becomes negative. So before reaching the mirage conditions, the temperature gradient may be larger than the standard value by a factor two or three, (meaning a decrease in temperature of just 0.2 K over the first ten metres of altitude!) generating a thermal factor of 0.4 instead of 0.8, reducing the flattening to 8%, with a regular image of the solar disk. On the other side, the flattening may increase to 20% is the temperature of the lower atmospheric layers is nearly constant and even to stronger flattening with temperature inversions ($\gamma < 0$ in (10.39)), provided they are smooth enough to allow regular image formation without strong distortions on angular scale smaller than the sun size. Anticipating the result of the next paragraph, it is shown that the skewness coefficient is also proportional to $\alpha\, R$, meaning that a strongly flattened sun tends to be also more asymmetric, in the same proportion. A plot is shown in Fig. 10.9, where the

shape given by (10.19) with $\Gamma = 0.7$, or a flattening of 30% and $\Delta = 0.75\,\mathrm{deg}^{-1}$, which may only occur with a severe temperature inversion.

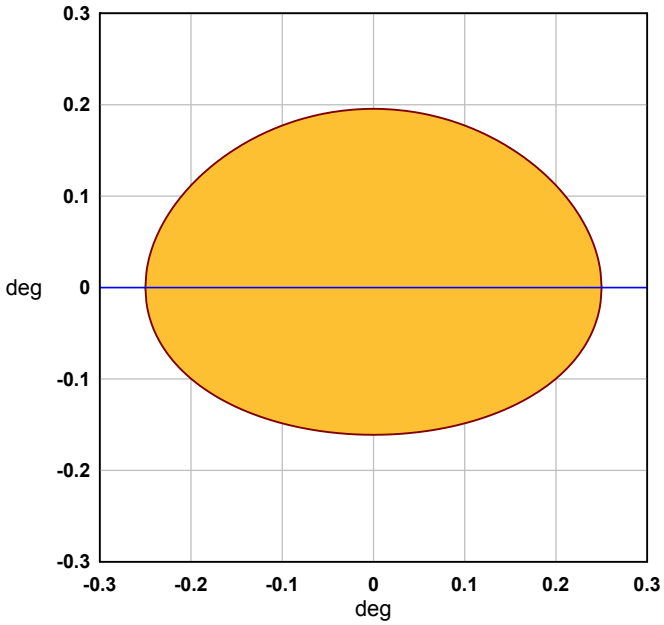


FIGURE 10.9: Plot of Eq. (10.19) in case of a strong temperature inversion, with a flattening of 30%, $\Gamma = 0.7$, and a skewness factor of 15%, corresponding to $\Delta = 0.75$ deg^{-1}. This shape is strikingly similar to the shape of the moon seen from the ISS in `http://www.atoptics.co.uk/atoptics/issmoon.htm`.

Expansion to higher orders in h The above expression for the flattening makes sense only very close to the horizon, and at least an expansion to the second order is needed to see how the flattening decreases with increasing h. We have now to combine Eqs. (10.32)-(10.34) and express $\mathcal{R}(0, z_m)$ as a function of h. This is done with (10.29), a polynomial form where the first two coefficients (in h and h^2) are related to the fundamental physical constant with (11.22). To keep track of the constants it is convenient to rewrite (10.28) as

$$\mathcal{R}(0, z) = \frac{\mathcal{R}(0, 0)}{(n-1)_0}\,(n-1)_z \tag{10.41}$$

with

$$(n-1)_z = (n-1)_0 - \alpha_0\, z + \frac{1}{2}\beta\, z^2 \tag{10.42}$$

where α_0 is as before $-dn/dz$ at sea level

$$\alpha_0 = (n-1)_0 \frac{Mg}{RT_0}\left(1 - \frac{\gamma R}{Mg}\right) \tag{10.43a}$$

$$\beta = (n-1)_0 \left(\frac{Mg}{RT_0}\right)^2 \left(1 - \frac{\gamma R}{Mg}\right)\left(1 - 2\frac{\gamma R}{Mg}\right) \tag{10.43b}$$

Numerical values are given in (11.20b) or (11.23b), with $\alpha_0 = 2.65 \times 10^{-5}$ km^{-1} and, $\beta = 1.95 \times 10^{-4}$ km^{-2}. Therefore,

$$\mathcal{R}(0,z) = \mathcal{R}(0,0) - \frac{\mathcal{R}(0,0)}{(n-1)_0}\,\alpha_0\, z + \frac{\mathcal{R}(0,0)}{2(n-1)_0}\beta\, z^2 \tag{10.44}$$

which relates immediately the expansion of the horizontal refraction at different heights to constants linked to the refractive index. A quick numerical check shows that (10.44) is the same as (10.30) (ignoring the term in h^3). Then with (10.34) one has,

$$\mathcal{R}(0,z_m) = \mathcal{R}(0,z) + \frac{\mathcal{R}(0,0)}{(n-1)_0}\,\frac{\alpha_0\, R}{2(1-\alpha_0\, R)}\left[1 - \frac{\beta}{\alpha_0}\, z\right] h^2 \tag{10.45}$$

The second term in (10.32) is given by (10.35), where α must be taken at about z_m, or with (10.42),

$$\alpha(z_m) = \alpha_0 - \beta\, z_m \tag{10.46}$$

giving for the light bending during the travel from P to O,

$$\delta(h) = -\frac{\alpha_0\, R}{1-\alpha_0\, R}\left(1 - \frac{\beta}{\alpha_0}\, z\right) h - \frac{\beta R^2}{2(1-\alpha_0\, R)^2}\, h^3 \tag{10.47}$$

and finally the refraction in the vicinity of the horizontal plane in analytic form with (10.32), (10.45) and (10.47),

$$\begin{aligned}\mathcal{R}(h,z) = \mathcal{R}(0,z) & \\ - \frac{\alpha_0\, R}{1-\alpha_0\, R}\left[1-\frac{\beta}{\alpha_0}\, z\right]\, h & \\ + \frac{\mathcal{R}(0,0)}{(n-1)_0}\, \frac{\alpha_0\, R}{2(1-\alpha_0\, R)}\left[1-\frac{\beta}{\alpha_0}\, z\right] h^2 & \\ - \frac{\beta R^2}{2(1-\alpha_0\, R)^2}\, h^3 &\end{aligned} \tag{10.48}$$

In fact for the last coefficient for h^3, it is more accurate to compute the gradient of the refractive index at the average height of the ray between P and O instead of z_m, and with (4.12) and (4.16) one has readily,

$$< z >= z - \frac{Rh^2}{3(1-\alpha\, R)} \tag{10.49}$$

instead of (10.34) and this changes the numerical coefficient $1/2$ into $1/3$.

One must now compare the numerical values of the coefficients of this polynomial to the numerical fitting (10.10), taking care of the units (refraction in arcmin and altitude in degrees). This yields,

$$\frac{\alpha_0\, R}{1-\alpha_0\, R} \simeq 12.25 \quad \text{arcmin/deg} \tag{10.50a}$$

$$\frac{\mathcal{R}(0,0)}{(n-1)_0}\, \frac{\alpha_0\, R}{2(1-\alpha_0\, R)} \simeq 3.70 \quad \text{arcmin/deg}^2 \tag{10.50b}$$

$$\frac{\beta R^2}{3(1-\alpha_0\, R)^2} \simeq 0.70 \quad \text{arcmin/deg}^3 \tag{10.50c}$$

$$\frac{\beta}{\alpha_0} \simeq 0.074 \quad \text{km}^{-1} \tag{10.50d}$$

in excellent agreement with the coefficients of the polynomial (10.10), ignoring the term in h^4.

The coefficient in h in (10.48) is directly proportional to the flattening while the skewness factor is proportional to the second derivative of the refraction with respect to the apparent direction, namely the coefficient of h^2. Both are primarily determined by the gradient of the refractive index α, which itself, near the horizon, is controlled by the temperature profile in the lowest layers of the atmosphere. As mentioned earlier, when the

sun (or the moon) is strongly flattened, it is then also strongly skewed, with the lower limb being pushed up by the refraction much more than the upper limb. See a very extreme case of flattening with this observation of the moonset from the ISS `http://www.atoptics.co.uk/atoptics/issmoon.htm`, where the refraction near the optical horizon is typically twice as large as for an earth-based observer.

11 Atmospheric parameters

In this section altitudes are in km and denoted by z instead of h. The most relevant parameter to determine the curvature of the light ray is the gradient of the refractive index along the photon trajectory, and is very simply related to the physical conditions expressed by pressure and temperature as a function of the altitude. I consider first a simple atmospheric model for the lower troposphere (below 5 km), accurate enough for most of the topics discussed in this document, and then I describe the parameters of a more general one needed to assess the astronomical refraction and investigate the solar flattening near horizon.

11.1 Tropospheric model

The atmosphere (up to 100 km) is remarkably homogeneous in composition with a constant proportion of molecular oxygen and nitrogen, plus other minor components. These are neutral molecules with no polarisation in the absence of electric field. In such medium there is a simple relationship established almost simultaneously by H.A. Lorentz and L. Lorenz in 1880, linking the molecular polarisability α (how much dipolar moment is created per molecule) and the refractive index (a macroscopic quantity) as,

$$\frac{n^2-1}{n^2+1} = \frac{N\alpha}{3\epsilon_0} \tag{11.1}$$

where N is the number of molecules per unit of volume and $\epsilon_0 = 8.85 \times 10^{-12}$ Fm^{-1} is the permittivity of the vacuum. For a gas one has, $n \sim 1$ and (11.1) reduces to

$$n - 1 \propto N \tag{11.2}$$

that is to say the refractive index $n-1$ of a gas is proportional to the its density (Gladstone law). Let for the air $\rho(h)$ be the density in kg.m^{-3} at an altitude h. One as,

$$n - 1 = (n-1)_0 \frac{\rho}{\rho_0} \tag{11.3}$$

Now within the troposphere, where the atmospheric composition is homogeneous, one can write,

$$\frac{\rho}{\rho_0} = \frac{P}{P_0}\frac{T_0}{T} \tag{11.4}$$

where P and T stand respectively for the atmospheric pressure and absolute temperature and the values at $h = 0$ are the standard values $T_0 = 288.16$ K, or a temperature of

15 °C, and $P_0 = 1013.25$ hPa. One has also $(n-1)_0 = 0.000277$. Note that with a different standard temperature at $h = 0$, $(n-1)_0$ is inversely proportional to the absolute temperature.

For rays in the troposphere, that is to say for altitude less than 10 km, a simple atmosphere in hydrostatic equilibrium can be used with a constant temperature gradient,

$$\frac{dT}{dh} = -\gamma = -6.5 \times 10^{-3} \text{K m}^{-1} \tag{11.5}$$

or equivalently,

$$T = T_0 - \gamma\, h \tag{11.6}$$

Inserting this gradient in the hydrostatic equation,

$$\frac{dP}{dh} = -\rho g \tag{11.7}$$

gives,

$$\frac{dP}{dT} = \frac{\rho g}{\gamma} \tag{11.8}$$

and with the perfect gas law,

$$P = \rho \frac{RT}{M} \tag{11.9}$$

we have

$$\frac{dP}{dT} = \frac{PMg}{\gamma\, RT} \tag{11.10}$$

where M is the molar mass of the air, $M = 28.97$ g/mol, $R = 8.3143$ J mol^{-1} K^{-1} for the gaz constant. Integrating (11.10) leads to,

$$P = P_0 \left(\frac{T}{T_0}\right)^{\frac{Mg}{R\gamma}} \tag{11.11}$$

and finally by inserting (11.6)

$$P = P_0 \left(1 - \frac{\gamma h}{T_0}\right)^{\frac{Mg}{R\gamma}} \tag{11.12}$$

The atmosphere density results from,

$$\frac{\rho}{\rho_0} = \frac{P}{P_0}\frac{T_0}{T} \tag{11.13}$$

and finally with (11.6) and (11.12),

$$\rho = \rho_0 \left(1 - \frac{\gamma h}{T_0}\right)^{\frac{Mg}{R\gamma}-1} \tag{11.14}$$

and also,

$$n - 1 = (n-1)_0 \left(1 - \frac{\gamma h}{T_0}\right)^{\frac{Mg}{R\gamma}-1} \tag{11.15}$$

Within the range of altitudes of interest for this study, one can restrict the formulas for the variation of pressure and temperature to $h < 5\,\text{km}$. I have derived convenient formulas from polynomial fits of tabulated values of the complete equation.

This yields for the pressure and absolute temperature as a function of the altitude h given in km:

$$P = P_0\,(1 - 0.1173\,h + 0.0048\,h^2) \tag{11.16}$$

$$T = T_0\,(1 - 0.02257\,h) \tag{11.17}$$

or equivalently with P in hPa and temperature in °C,

$$P = 1013.25 - 119.1\,h + 4.94\,h^2 \tag{11.18}$$

$$t = t_0 - 6.5\,h \tag{11.19}$$

The pressure decreases by about 120 hPa per km and the temperature of 6.5 °C for each elevation of one kilometer.

This is now combined with (11.3) to the different form of equivalent relationships for the refractive index as a function of the altitude in km as,

$$n - 1 = (n-1)_{h=0}\,(1 - 0.09547h + 0.003144h^2) \tag{11.20a}$$

$$n = 1.000277 - 2.644 \times 10^{-5}\,h + 8.70 \times 10^{-7}\,h^2 \tag{11.20b}$$

and for the gradient,

$$\frac{dn}{dh} = -2.644 \times 10^{-5} + 1.74 \times 10^{-6}\, h \tag{11.21}$$

or a typical average refractive index gradient of of $(2.4 - 2.6) \times 10^{-5}$ km^{-1}. This is also the mean curvature (in km^{-1}) of a light ray in the lower atmosphere due to the variation of the refractive index with altitude.

Comment: From the analytic expansion of (11.15), the Taylor expansion to second order is obtained as,

$$1 - \frac{Mg}{RT_0}\left(1 - \frac{\gamma R}{Mg}\right) h + \left(\frac{Mg}{RT_0}\right)^2 \left(1 - \frac{\gamma R}{Mg}\right)\left(1 - 2\frac{\gamma R}{Mg}\right) \frac{h^2}{2} \tag{11.22}$$

giving the gradient of the refractive index as a function of physical parameters. Numerically one gets $0.096\,\mathrm{km}^{-1}$ for the first term in excellent agreement with (11.20) and $0.0035\,\mathrm{km}^{-2}$ for the second order, somewhat different from 0.0031 in (11.20). But from a theoretical standpoint, (11.20) and (11.22) are not equivalent, since the fit is done on the exact formula and projects the $h^3, h^4, \cdots$ of a Taylor expansion to higher orders terms on the h, h^2 components of (11.20). The fit spreads the errors over its range, while the Taylor expansion is accurate in the vicinity of the origin. A nearly perfect agreement between the theoretical and numerical terms is found with a fit to h^3:

$$n - 1 = (n-1)_{h=0}\,(1 - 0.09603h + 0.003514h^2 - 5.56 \times 10^{-5} h^3) \tag{11.23a}$$

$$n = 1.000277 - 2.660 \times 10^{-5}\, h + 9.73 \times 10^{-7}\, h^2 - 1.54 \times 10^{-8}\, h^3 \tag{11.23b}$$

Therefore all the numerical results obtained in the different sections of this paper, could be traced back to simple physical parameters, like the air molecular mass, the temperature, lapse rate and gravity at the ground level. It remains only $(n-1)_{h=0}$ as empirical quantity, since its relation to polarisability (11.1) is normally used to determine this atomic quantity from the measurement of the refractive index.

11.2 Full atmospheric model

To investigate the shape of the rising or setting sun, one must follow the optical rays all the way through the atmosphere, over distances of nearly 1000 km and altitudes up to

TABLE 11.1: *Parameters of the International Standard Atmosphere. Pressure and temperature are given at the bottom of each layer. The pressure is propagated up to to the top of the layer with an isothermal or polytropic model according to the temperature gradient.*

-	layer	altitude	P	T	dT/dh
-	-	km	Pa	°C	K km^{-1}
0	Troposphere	0.0	101,325	+15.0	-6.5
1	Tropopause	11.000	22,6322	-56.5	+0.0
2	Stratosphere	20.000	5,474.9	-56.5	+1.0
3	Stratosphere	32.000	868.02	-44.5	+2.8
4	Stratopause	47.000	110.91	-2.5	+0.0
5	Mesosphere	51.000	66.939	-2.5	-2.8
6	Mesosphere	71.000	3.9564	-58.5	-2.0
7	Mesopause	84.852	0.3734	-86.2	0

100 km, when the refraction become negligible. We are then dealing with astronomical refraction and no more with terrestrial refraction.

The differential equation (5.31) can be used provided it is plugged to a routine giving the refractive index at any altitude. To this purpose I have implemented the International Standard Atmosphere (`http://en.wikipedia.org/wiki/International_Standard_Atmosphere`) which consists of a layered atmosphere alternating polytropic and isothermal models with continuity between successive layers. It gives the pressure and temperature as a function of the altitude, from which one can compute the density and the refractive index. The relevant parameters are given in Table 11.1 with the condition at the bottom of each layer and the value of the temperature gradient in this layer. When the gradient is zero, the layer is isothermal and the evolution of the pressure with altitude is the standard exponential pressure decrease. Otherwise on applies (11.12) from the bottom of this layer to the next. Then the density if computed with the perfect gas law (11.9) and finally the refractive index. The model is continuous at the crossing of each layer, but not smooth. There are cusps that could cause numerical instabilities during integrations. The implementation of the model is very easy in any programming language as a function

giving the refractive index as a function of the altitude. I also compute dn/dh numerically with central differences, with a step large enough to keep this rate continuous at the layer transitions.

11.2.1 A warning

The standard atmosphere is a very useful and handy model for the whole atmosphere perfect for numerical application. However one must be aware that this simplicity has a cost as it cannot represent the fine structure of lower layers of the atmosphere, that determine the actual behaviour of near-horizontal rays. It works well for astronomical refraction at altitudes of interest for astronomers (they never attempt accurate measurements below ~ 30 degrees of altitude) and allows us to compute standard refraction tables down to the horizon, without any guarantee that the results are meaningful. The smooth and unique thermal profile makes impossible to reproduce intricate mirage structures, let alone the complex notched rim of a distorted rising or setting sun.

12 Radius of Curvature of the earth

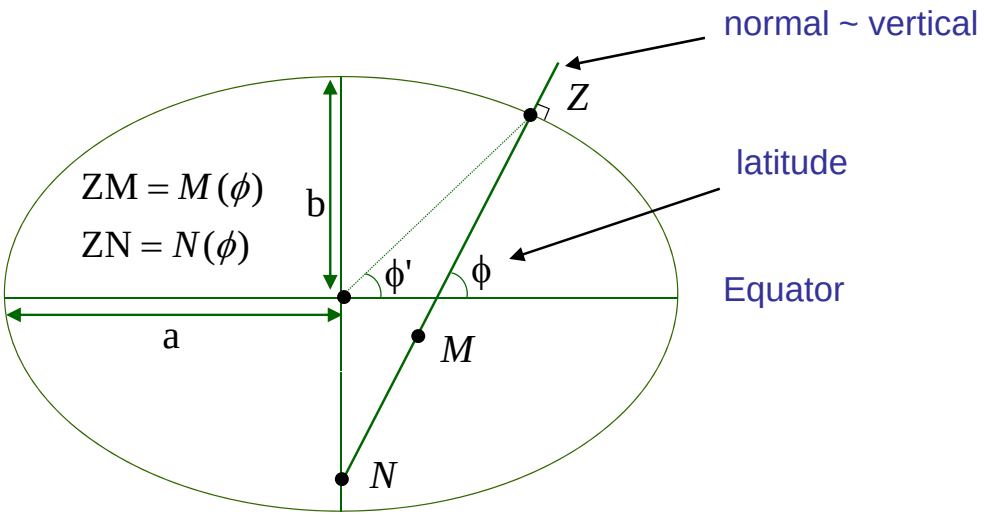


FIGURE 12.1: Meridian section of an axi-symmetric ellipsoid, with ϕ denoting the (geodetic) latitude and ϕ' the geocentric latitude. The meridian curvature at Z is $M(\phi)$ while $N(\phi)$ is the curvature of the east-west great circle (prime vertical) going through Z.

I have adopted in general a simple model of the earth as a sphere of radius R, with $R \sim 6400$ km, which is sufficient in many cases, although the Earth is spherical just to a first approximation since the difference between the equatorial and polar radii is 22 km. To illustrate the sensitivity of the numerical computations to the radius, the visible height in Corsica from Nice change by ~ 10 m when the radius is changed from 6370 km tm to 6400 km. Hence, this is not a major issue, but it can be handled properly without too much additional complications as explained in this section. It is fully independent of the rest of the document and can be skipped, although most of the numerical applications have in fact used the accurate value of the mean radius of curvature on the ellipsoid along the light ray.

As the rays considered travel over few hundred kilometres, it is not wrong to assimilate the local shape of the earth to a sphere. The true question is more about the value of the radius one should adopt, given the sensitivity of the distance or altitude of visibility to this single parameter. This parameter is used primarily to convert angular arc into distance, and acts primarily as scale parameter. The arc-length between two points defined by the geodetic latitude and longitude, does not depend on the precise model of the earth. This

is simply the angle between the two verticals. Using this angle to convert into a distance makes sense only with a model to represent a path on a surface, or in the 3D space, to join the two points.

Beyond the perfect spherical shape, the best approximation that has been used for more than two centuries is to assimilate the earth to a rotationally symmetric ellipsoid having a polar axis shorter than the diameter of the equatorial circle. The actual local curvature of a curve drawn on the ellipsoid depends on the location (longitude, latitude) and on the direction of the tangent vector to the curve (azimuth). Just to illustrate the importance of this local curvature, the smallest radius of curvature would be on the equator along the meridian with $\rho_{\text{min}} = 6335\,\text{km}$ and the maximum is reached at either pole with $\rho_{\text{max}} = 6400\,\text{km}$.

The ellipsoid has its origin at the barycentre of the earth and is defined by its equatorial radius (IERS, 1989) $a = 6\,378\,136\,\text{m}$ and its flattening $f = 1/298.257$. Then one obtains the polar radius $b = a(1-f) = 6\,356\,751.3\,\text{m}$. It is convenient to work also with the eccentricity $e = (a^2 - b^2)^{1/2}/a = 0.0818192$ and $e^2 = 0.00669438 \sim 2f$.

The earth is represented with this axi-symmetric ellipsoid whose meridian section is shown in Fig. ,12.1. The normal to the ellipsoid at a point Z on its surface is the local geodetic vertical (very close to the vertical materialised by the plumb line) and the latitude ϕ indicated in the figure is the geodetic latitude, that one finds on maps or in atlases. It is determined today by space geodesy or GPS techniques, while this was done by astronomical measurements in the past. The local vertical does not go (in general) through the centre of the Earth and the geodetic latitude ϕ is not identical to the geocentric latitude ϕ'. The latter is more a geometrical quantity than a physical one, not directly measurable, while the geodetic latitude is directly accessible thanks to its relation to the local vertical.

The local curvature of a curve drawn on the ellipsoid can be handled with classical formulas of differential geometry. For the ellipsoid one computes the two principal curvatures (Fig. ,12.1),

$$M = M(\phi) = \frac{a^2\,b^2}{(a^2\cos^2\phi + b^2\sin^2\phi)^{3/2}} = \frac{a(1-e^2)}{(1-e^2\sin^2\phi)^{3/2}} \tag{12.1}$$

$$N = N(\phi) = \frac{a^2}{\sqrt{a^2\cos^2\phi + b^2\sin^2\phi}} = \frac{a}{(1-e^2\sin^2\phi)^{1/2}} \tag{12.2}$$

for respectively the meridian curvature $M(\phi)$ and that in the perpendicular direction $N(\phi)$, with $e = \sqrt{a^2-b^2}/a$. In Fig. 12.1 the centres of curvatures are respectively M

and N. When the Z describes the meridian elliptical section, the locus of M is an astroid, an hypocycloid with four cusps of reduced equation $x^{2/3} + y^{2/3} = 1$, while N is always on the polar axis.

When the two principal curvatures are known on the surface, a famous theorem of differential geometry due to Euler gives the curvature of any regular curve, locally in a normal section, as a function of its bearing on the tangent plane as,

$$R_c = \frac{1}{\dfrac{\cos^2 A}{M} + \dfrac{\sin^2 A}{N}} \tag{12.3}$$

where A is the direction of the tangent to the curve measured from the north in the case of the earth ellipsoid, as shown in Fig. 12.2. To the first order of the flattening (or second order in eccentricity) one has the convenient formula,

$$R_c = a\left(1 + \frac{e^2}{2}(\sin^2\phi - 2\cos^2 A\,\cos^2\phi)\right) + \mathcal{O}(e^4) \tag{12.4}$$

This applies directly to the light rays to evaluate the most appropriate local curvature of the earth: the propagation takes place in a plane, and the Earth shape is locally that of the osculating circle in the direction of propagation, determined by the azimuth of a point in Corsica with respect to the observer in Nice.

It remains to determine the azimuth from the locations of the two end points. While this is an arduous task to do it rigourously on an ellipsoid (one needs to compute the geodesic connecting the two end-points), this is easy with a sphere and standard spherical trigonometry, as illustrated in Fig. 12.2.

$$\cos\theta = \sin\phi_2\,\sin\phi_1 + \cos\phi_2\cos\phi_1\cos\Delta\lambda \tag{12.5a}$$

$$\cos A\sin\theta = \sin\phi_2\,\cos\phi_1 - \cos\phi_2\sin\phi_1\cos\Delta\lambda \tag{12.5b}$$

$$\sin A\sin\theta = \cos\phi_2\sin\Delta\lambda \tag{12.5c}$$

where $\Delta\lambda = \lambda_2 - \lambda_1$. Eq. (12.5a) gives the length of the arc between the two locations and (12.5b)-(12.5c) provide the azimuth (reckoned from north) without quadrant ambiguity. For small distances, with $|\phi_2 - \phi_1| \ll 1$ and $|\lambda_2 - \lambda_1| \ll 1$ the above formulas are greatly simplified to,

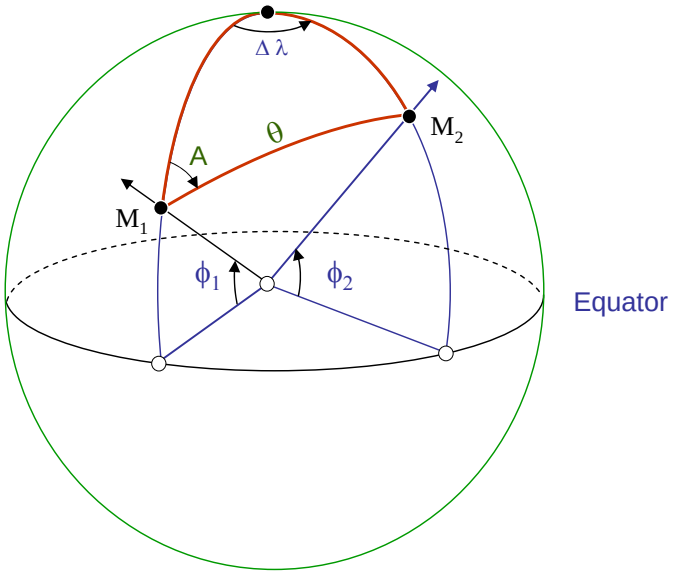


FIGURE 12.2: Angular distance θ and azimuth A on the great circle between two points on the earth, of respective latitude ϕ_1 and ϕ_2. The diagrams shows directions on the celestial sphere, and not points on the surface of the earth (which is not spherical).

$$\theta = (\Delta\phi^2 + \Delta\lambda^2 \cos^2\phi)^{1/2} \tag{12.6}$$

for the angular distance and

$$A = \arctan 2(\Delta\lambda \cos\phi, \Delta\phi) \tag{12.7}$$

for the azimuth. In these approximate formulas one should take $\phi = (\phi_1 + \phi_2)/2$, $\Delta\phi = \phi_2 - \phi_1$ and $\Delta\lambda = \lambda_2 - \lambda_1$. More generally, and to higher order, one has the more accurate expressions for the angular distance and the azimuth.

1. With $d = \phi_2 - \phi_1$ and $a = (\lambda_2 - \lambda_1) \cos\phi_1$

$$\theta = (a^2 + d^2)^{1/2} \left[1 - \frac{1}{2}\frac{a^2}{a^2 + d^2} \tan\phi_1\, d\right] + \mathcal{O}(a^2, d^2) \tag{12.8a}$$

$$A = \arctan 2(a, d) - \frac{1}{2}\frac{a^2 + 2d^2}{a^2 + d^2} \tan\phi_1\, a + \mathcal{O}(a^2, d^2) \tag{12.8b}$$

2. With $d = \phi_2 - \phi_1$, $\phi_\mathrm{m} = (\phi_1 + \phi_2)/2$ and $a = (\lambda_2 - \lambda_1)\,\cos\phi_\mathrm{m}$

$$\theta = (a^2 + d^2)^{1/2} \left[1 - \frac{1}{24}\,\frac{a^2}{a^2 + d^2}\,\frac{(2\sin^2\phi_\mathrm{m} + 1)d^2 + \sin^2\phi_\mathrm{m}\,a^2}{\cos^2\phi_\mathrm{m}}\right] + \mathcal{O}(a^4, d^4) \tag{12.9a}$$

$$A = \arctan 2(a, d) - \frac{1}{2}\,\tan\phi_\mathrm{m}\,a + \mathcal{O}(a^2, d^2) \tag{12.9b}$$

where one sees the interest of using the central latitude as reference, since the Euclidean distance is correct to third order.

TABLE 12.1: *Distance, azimuth and earth local radius of curvature for two Corsica landmarks (ϕ_2, λ_2) seen from Nice around the Mont Alban and on the upper Corniche around the Col d'Eze (ϕ_1, λ_1). See notations in text.*

	ϕ_1 deg	λ_1 deg	ϕ_2 deg	λ_2 deg	θ deg	A deg	R_c km	D km
from mont Alban to:								
Folicce	43.701	7.300	42.827	9.385	1.75	119.21	6382.76	195.17
Cinto	43.701	7.300	42.380	8.946	1.79	137.13	6375.78	198.85
from upper Corniche to:								
Folicce	43.727	7.336	42.827	9.385	1.74	120.39	6382.36	194.05
Cinto	43.727	7.336	42.380	8.946	1.79	138.33	6375.31	198.99

13 Identification of the summits of Corsica

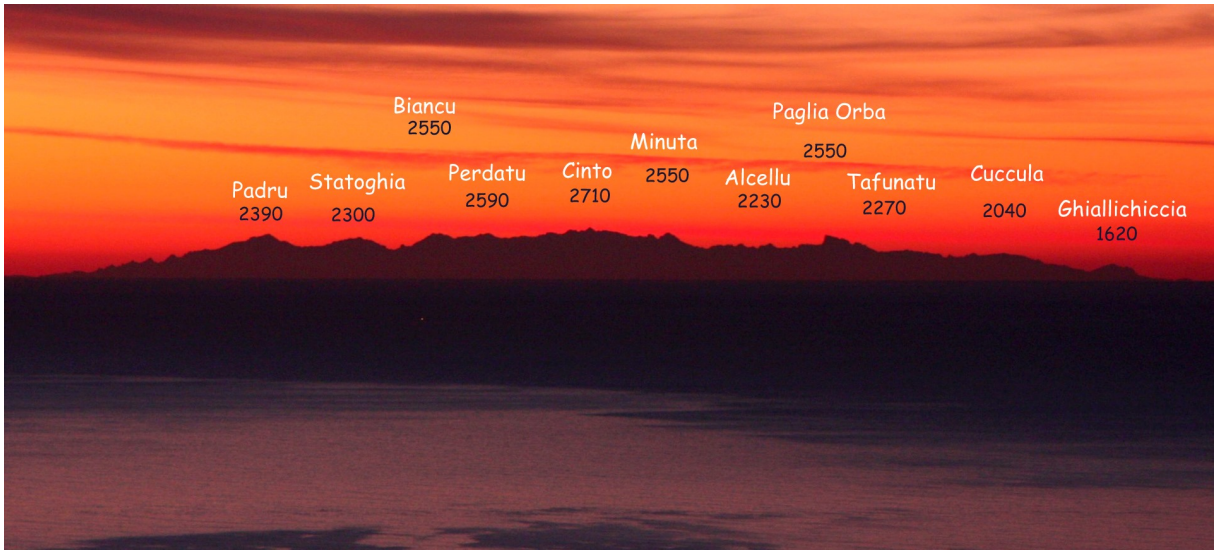


FIGURE 13.1: Identification of the major features in the central part of the Corsica visible from Nice. The picture has been taken from an altitude of 230 m in the east of Nice and the lowest altitude visible is of the order of 1300 m. See a more detailed panorama in Fig. 13.6.

13.1 Methodology

Identifying the landscape features of Corsica when one has just a projected line against the sky background is not an easy task. Lesser peaks in the foreground are usually not visible as they project against higher peaks more distant along the line of sight in a particular direction. Conversely, the angular height of a peak in the foreground my be larger than that of a higher peak at a larger distance. In a flat geometry this is easy to assess by computing the subtended angle as the ratio of the height to the distance (all relevant angles are small, less than half a degree). With the earth curvature, the angular height above the optical horizon is more difficult to compute, since the earth surface seems to fall behind the horizon, and the angle above the horizon decreases faster with the distance than in the case of a plane. Finally the bending of the ray must be taken into account in this computation. However, for standard refraction, the angular height of a peak of altitude h_1, separated from an observer at altitude h_0 by a distance d is a well defined quantity. So if we know the geographical coordinates of every summit or distinctive landscape feature, its altitude, one can determine its angular size above the optical horizon. If we have two, or more, peaks in the same direction, only the highest in angular measure will be visible

along the delineated crest line. Those smaller will be hidden if they are farther in distance, or invisible because of their being projected.

Then to map the projected summits seen as a 1-dimensional line to the true map of Corsica, one needs first to search all the possible hills, mountains, passes, ridges potentially visible, extract their coordinates and altitude. Then it is possible to compute their distance and azimuth from an observer near Nice, and finally their altitude (angular) above the optical horizon as a function of the altitude of the observer. At least this will give a list of those features above or below the horizon. Sorting that list by increasing azimuth will generate an ordered sequence of landscape marks (say from East to West), as they are actually seen on pictures. Hidden features in the background, or projected foreground peaks are readily spotted in a narrow azimuthal sector. Having the scale of the picture by the distance of two peaks, or the height above the horizon of the most conspicuous, it is not too difficult to assign a name to each feature.

13.2 Angular height

The angular height of an object of height h_2 above the optical horizon of an observer at distance d and altitude h_1 above the sea-level has been derived in (4.24), as the difference between the directions of the ray between the two end points and the one going to the optical horizon:

$$\delta = \sqrt{\frac{2h_1}{R}\,(1-\alpha\,R)} + \frac{h_2-h_1}{D} - \frac{(1-\alpha\,R)}{2}\,\frac{D}{R} \tag{13.1}$$

Numerical integration have shown that this simplified formula is in fact a remarkably good approximation for rays close to the horizon and angular height between 0 and 30 arcmin. The first term is the depression of the optical horizon referred to the horizontal plane, the second is the Euclidean formula for a flat earth and the last term represents the *fall* of the curved earth surface below the horizontal plane of the observer. Taking $\alpha = 0$ is the same as discarding refraction and reverting to straight line propagation. This assumes that the optical horizon does exist, and the condition is $\alpha R < 1$, meaning that the rays have a smaller curvature than the earth. In (13.1), one should use the local radius of curvature in the direction of the target for R.

13.3 List and coordinates of landscape features

I have used two main tools to select the relevant features and find their locations and names. A standard map of Corsica at the scale $1/100\,000$ with topographic details helped find the hilly or mountainous areas with altitude higher than ~ 700 m. Then these areas have been scanned with Google Earth (`http://earth.google.com`), using various resolution and inclination, to locate precisely each potentially interesting place. The coordinates and a preliminary altitude have been extracted for each place from the Google Earth images. Then using the French Géoportail (`www.geoportail.fr`), I consulted the high-resolution topographic maps to confirm the feature and extract the final altitude when indicated, or determine that altitude from the level lines. Names have been also taken generally from this source. Sometimes the local toponymy (in Corsican or *Corsu*) has been preferred and found from web sites related to tourism in these areas. While the name of the major landmarks is fixed, there are clearly regional or linguistic variations for the less important features. I found in several places, significant altitude differences between the maps and the value found with GoogleEarth, and, as a rule, I took the maps as reference source. Several checks have also been done from an existing identification (but less dense) here `http://www.nice-image.com/corse/identification-sommet-corse-vue-du-continent.php`.

13.4 Results in tabular form

Table 13.1 gives the relevant parameters for all the identified features visible or nearly visible from an altitude of 550 m, near Nice, sorted in increasing azimuths (from east to west), as if one were sighting the panorama. The quantities listed in the columns are the name, the latitude, longitude and altitude for the data extracted from the maps. The other columns contain computed data, namely the arc-length and the azimuth in degrees from (12.5), the distance in km based on the radius of curvature in the corresponding direction (Eqs. (12.1), (12.2), (12.3)),and the apparent height of a feature from the observing platform, with latitude of 43.7271 deg and longitude 7.3364 deg, computed with (13.1).

Table 13.1: *List of the landscape features (peaks, depressions) visible in Corsica from a place near the Col d'Eze around Nice, at an altitude of 550 m. The lines are sorted in increasing azimuth, starting from the east with the northernmost visible peak in the Cap Corse. The angular height can be negative, when the feature is below the optical horizon for this observing station.*

Name	**latitude**	**longitude**	**altitude**	**arc**	**azimuth**	**distance**	**height**
	deg	deg	m	deg	deg	km	arcmin
Alticcione	42.8605	9.4019	1140	1.7352	119.25	193.3	8.12
Bocca di Viezza	42.8541	9.3986	1040	1.7364	119.47	193.4	6.30
Croce a Viezza	42.8484	9.3941	1165	1.7365	119.69	193.4	8.52
Bocca di a Serra	42.8451	9.3919	1005	1.7368	119.81	193.5	5.67
Codoli	42.8356	9.3854	1260	1.7377	120.16	193.6	10.17
Prato	42.8350	9.3851	1280	1.7378	120.18	193.6	10.52
Follice	42.8272	9.3857	1325	1.7423	120.39	194.1	11.17
Canetto	42.8260	9.3806	1256	1.7397	120.49	193.8	10.03
Cibiolla	42.8038	9.4068	1195	1.7678	120.77	196.9	8.06
Bocca Corvo	42.7920	9.4154	1085	1.7794	120.99	198.2	5.79
Stello	42.7883	9.4180	1307	1.7830	121.05	198.6	9.52
Stello2	42.7850	9.4203	1266	1.7862	121.11	199.0	8.71
Bocca Sta Maria	42.7779	9.4157	1095	1.7872	121.36	199.1	5.73
Capra	42.7743	9.4153	1205	1.7889	121.47	199.3	7.57
Bocca di Antigliu	42.7634	9.4056	880	1.7889	121.88	199.3	1.97
Foscu	42.7560	9.3962	1105	1.7872	122.20	199.1	5.90
Prunu	42.7504	9.3876	1190	1.7851	122.46	198.8	7.43
Bocca San Leonardo	42.7358	9.3972	850	1.7991	122.72	200.4	1.16
Mte San Leonardo	42.7345	9.3954	968	1.7987	122.78	200.3	3.20
Mte di Giagoppa	42.7316	9.3912	1038	1.7978	122.91	200.2	4.43

Continued on next page

Name	latitude	longitude	altitude	arc	azimuth	distance	height
	deg	deg	m	deg	deg	km	arcmin
Gratera	42.7288	9.3900	1025	1.7987	123.00	200.3	4.18
Murzaio	42.7087	9.4038	870	1.8184	123.35	202.5	0.96
Pigno	42.6943	9.3996	953	1.8241	123.77	203.2	2.20
mte a Torra	42.6491	9.3783	852	1.8380	125.21	204.7	0.11
Furtine	42.6393	9.3838	845	1.8471	125.38	205.7	-0.26
Zucarello	42.6285	9.3844	955	1.8539	125.63	206.4	1.38
San Giovanni	42.6134	9.3728	805	1.8563	126.17	206.7	-1.18
Pinzali	42.6107	9.3724	770	1.8577	126.24	206.9	-1.80
Tafonni	42.5599	9.3816	1120	1.8944	127.33	210.9	2.91
Evoli	42.5563	9.3749	1152	1.8928	127.51	210.8	3.48
Cutone	42.5457	9.3599	1180	1.8909	127.97	210.5	3.99
Spazzolu	42.5463	9.3491	1235	1.8844	128.11	209.8	5.09
Rocca Spazzolu	42.5445	9.3423	1230	1.8817	128.25	209.5	5.10
Tanoria	42.5408	9.3386	1221	1.8819	128.39	209.5	4.94
Ambrica	42.6181	9.1812	1060	1.7435	128.86	194.1	6.46
Muzzelli	42.6055	9.2020	1300	1.7633	128.86	196.3	10.06
Alturaia	42.5833	9.2211	1370	1.7884	129.11	199.1	10.45
San Angelo	42.4645	9.4072	1218	1.9698	129.15	219.3	2.19
A Taula	42.5799	9.2155	1470	1.7874	129.28	199.0	12.21
Asto	42.5819	9.2098	1530	1.7829	129.32	198.5	13.40
Grimaseta	42.5729	9.2154	1510	1.7919	129.45	199.5	12.75
San Anghiuli	42.5260	9.2497	1390	1.8418	130.04	205.0	9.03
Reghi Pozzo	42.5395	9.2270	1470	1.8203	130.07	202.7	11.09
Tasso	42.5154	9.2481	1380	1.8479	130.31	205.7	8.66
di Chienta	42.5092	9.2497	1340	1.8529	130.43	206.3	7.83
Quercitello	42.5041	9.2476	1245	1.8552	130.58	206.5	6.18
Pruno	42.5094	9.2188	1150	1.8359	130.90	204.4	5.19
Tevisi	42.5037	9.2183	1145	1.8394	131.04	204.8	5.00

Continued on next page

Name	latitude	longitude	altitude	arc	azimuth	distance	height
	deg	deg	m	deg	deg	km	arcmin
St Petrone	42.3972	9.3260	1767	1.9701	131.77	219.3	10.79
Luda	42.5304	9.0919	905	1.7531	132.44	195.1	3.44
Teghielle	42.5583	9.0418	1030	1.7071	132.62	190.0	7.03
Caldone	42.3317	9.3456	1725	2.0258	132.84	225.5	8.22
Lecca	42.5514	9.0340	1220	1.7077	132.92	190.1	10.45
Cugnolu	42.5307	9.0618	1100	1.7369	132.94	193.3	7.38
Modico	42.4943	9.0936	1230	1.7791	133.26	198.0	8.34
Tornabue	42.5492	9.0147	1285	1.6991	133.31	189.1	11.91
Puzolla	42.3514	9.2475	1545	1.9604	133.91	218.2	7.64
Muntacchione	42.4833	9.0658	1270	1.7723	133.98	197.3	9.25
Piano Maggiore	42.3435	9.2533	1580	1.9690	133.98	219.2	7.90
Cavallare	42.4371	9.1071	1650	1.8265	134.32	203.3	13.94
mte Tolo	42.5391	8.9711	1330	1.6835	134.32	187.4	13.25
Giuelli	42.4305	9.0978	1863	1.8265	134.62	203.3	17.54
St Parteo	42.5204	8.9629	1680	1.6927	134.91	188.4	19.33
Asco	42.4298	9.0770	2020	1.8163	134.98	202.1	20.59
Cima a i Mori	42.4221	9.0799	2160	1.8234	135.10	202.9	22.69
Cima Gazelle	42.5164	8.9394	1610	1.6836	135.43	187.4	18.39
Selollo	42.4723	8.9889	2273	1.7407	135.56	193.7	28.08
Padru	42.4686	8.9880	2390	1.7430	135.65	194.0	30.05
Mte Grosso	42.5013	8.9214	1940	1.6855	136.11	187.6	24.37
Statoghia	42.4556	8.9606	2300	1.7387	136.43	193.5	28.64
Biancu	42.4039	8.9877	2550	1.7905	137.08	199.2	30.75
Corona	42.4604	8.9180	2140	1.7141	137.10	190.7	26.83
Perdato	42.3909	8.9784	2586	1.7957	137.52	199.8	31.15
Ciuntrone	42.3847	8.9493	2656	1.7862	138.17	198.8	32.78
Cinto	42.3793	8.9449	2710	1.7882	138.36	199.0	33.62
Capo Larghia	42.3751	8.9276	2480	1.7831	138.76	198.4	29.87

Continued on next page

Name	latitude	longitude	altitude	arc	azimuth	distance	height
	deg	deg	m	deg	deg	km	arcmin
Falu	42.3697	8.9300	2550	1.7884	138.83	199.0	30.85
Minuta	42.3771	8.9139	2550	1.7751	138.97	197.5	31.45
Tighiettu	42.3619	8.8966	2270	1.7786	139.60	197.9	26.43
Alcellu	42.3564	8.8912	2280	1.7804	139.81	198.1	26.53
Paglia Orba	42.3454	8.8790	2525	1.7833	140.26	198.4	30.65
Tafunatu	42.3443	8.8694	2270	1.7797	140.46	198.0	26.39
Ghiarghiole	42.3323	8.8559	2090	1.7830	140.95	198.4	23.13
Cricche	42.3029	8.8571	2057	1.8067	141.50	201.0	21.62
Cuccula	42.2992	8.8486	2049	1.8059	141.73	200.9	21.51
Capo Penna	42.3223	8.8051	1580	1.7681	142.11	196.7	14.82
Scatella	42.2610	8.8555	1495	1.8395	142.32	204.6	10.89
Capo a Media	42.3489	8.7650	1480	1.7290	142.36	192.3	14.43
Frasselo	42.2945	8.8146	1530	1.7945	142.46	199.6	13.03
Chiavalle	42.3287	8.7729	1585	1.7487	142.60	194.5	15.60
Ghiallichiecia	42.3412	8.7569	1620	1.7316	142.67	192.6	16.83
U Celu	42.3272	8.7682	1585	1.7479	142.73	194.4	15.63
Manganellu	42.3546	8.7148	1025	1.7025	143.25	189.4	7.10
Capo Acitoriu	42.2923	8.7638	1150	1.7742	143.48	197.4	7.12
Vacaghia	42.2886	8.7586	1150	1.7750	143.65	197.4	7.09
Salisei	42.3514	8.6917	930	1.6952	143.78	188.6	5.59
Capo Vetta	42.2845	8.7553	1275	1.7769	143.79	197.7	9.21
Capo di Larrata	42.2799	8.7485	1270	1.7778	144.01	197.7	9.09
Capo di Ota	42.2651	8.7378	890	1.7854	144.49	198.6	2.27
Capo San Petru	42.2802	8.7207	920	1.7658	144.55	196.4	3.35
Polmonaccia	42.2360	8.7533	1185	1.8159	144.71	202.0	6.42
Terraghiu	42.2327	8.7501	1180	1.8173	144.83	202.1	6.29
Pulellu	42.2290	8.7447	1180	1.8181	145.00	202.2	6.27
Macendole	42.2224	8.7347	1205	1.8195	145.31	202.4	6.65

Continued on next page

Name	latitude	longitude	altitude	arc	azimuth	distance	height
	deg	deg	m	deg	deg	km	arcmin
Capo d'Orto	42.2503	8.7070	1295	1.7849	145.36	198.5	9.30
Capo Pirellu	42.2273	8.7195	1203	1.8092	145.52	201.2	6.94
Capo a Curnacchia	42.2263	8.7056	1123	1.8043	145.81	200.7	5.72
Capo Vitullo	42.2310	8.6914	1330	1.7946	146.01	199.6	9.59
capo Palazzu	42.1888	8.7005	1130	1.8338	146.55	203.9	4.94
Capo Riccio	42.1879	8.6940	1050	1.8319	146.69	203.7	3.65
Monte Ravu	42.2150	8.6101	727	1.7762	147.92	197.5	-0.30

Table completed

13.5 Marked-up panoramas

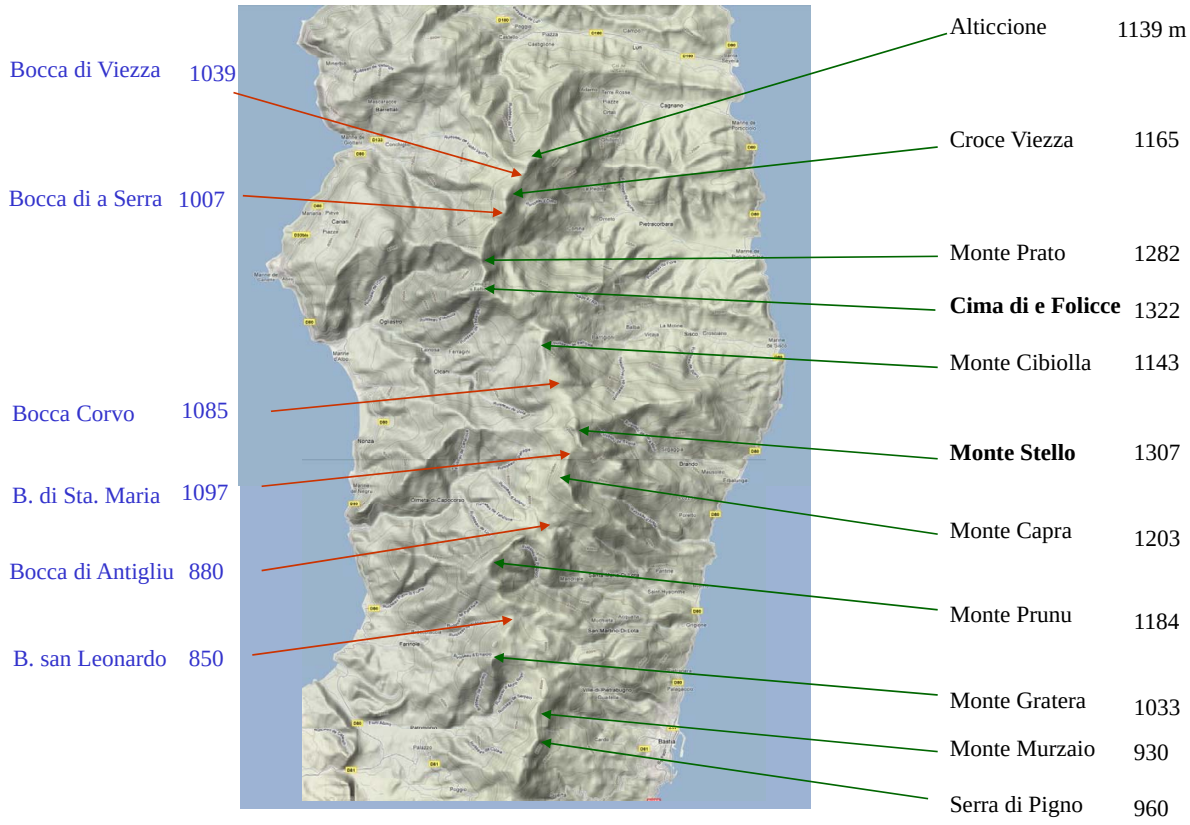


FIGURE 13.2: Map of the southern section of the Cap Corse with the names of the peaks and passes visible from the surroundings of Nice. The altitude of the hills in Cap Corse decreases quickly in the north of the Alticione, and that northern section is not visible from Nice area, except from the top of the Mont Agel or from the inland mountains. The true annotated picture is shown in Fig. 13.3.

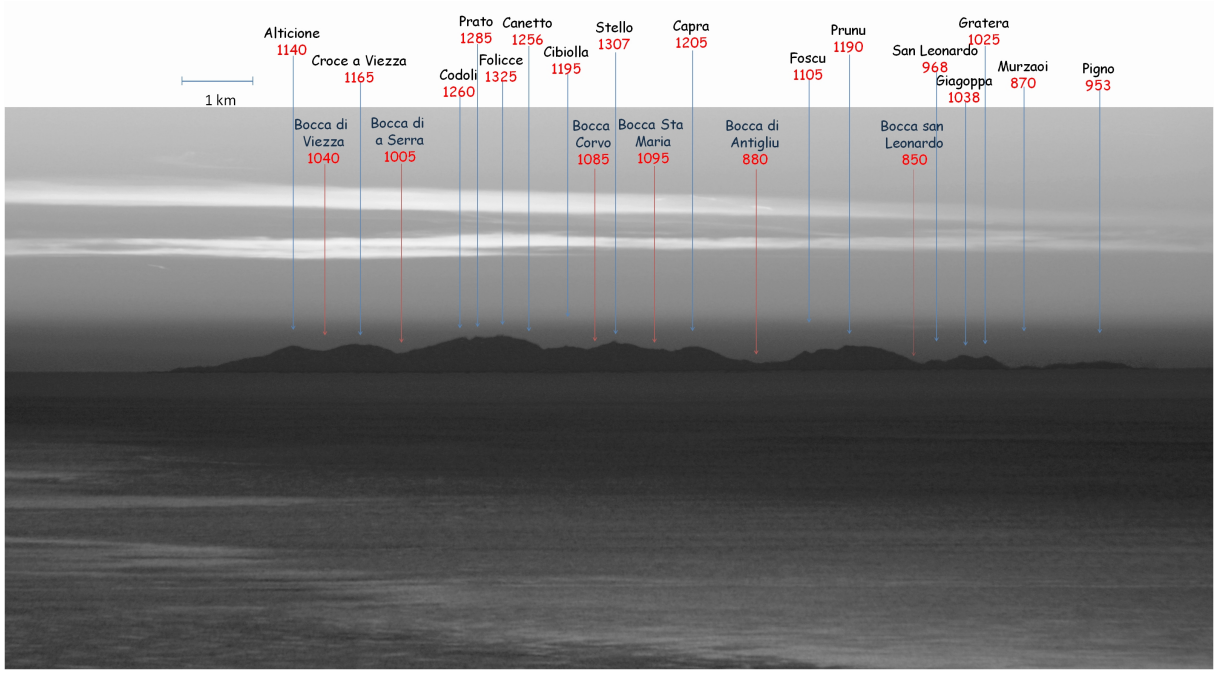


FIGURE 13.3: Panorama and full identification of peaks and passes visible in the Cap Corse area. The picture has been taken at an altitude of 550 m near the Col d'Eze. Altitudes are in m.



FIGURE 13.4: Colour panorama of the Cap Corse visible from the Col d'Eze at an altitude of 550 m. The picture has been taken few minutes before the sunrise on a 13 December.

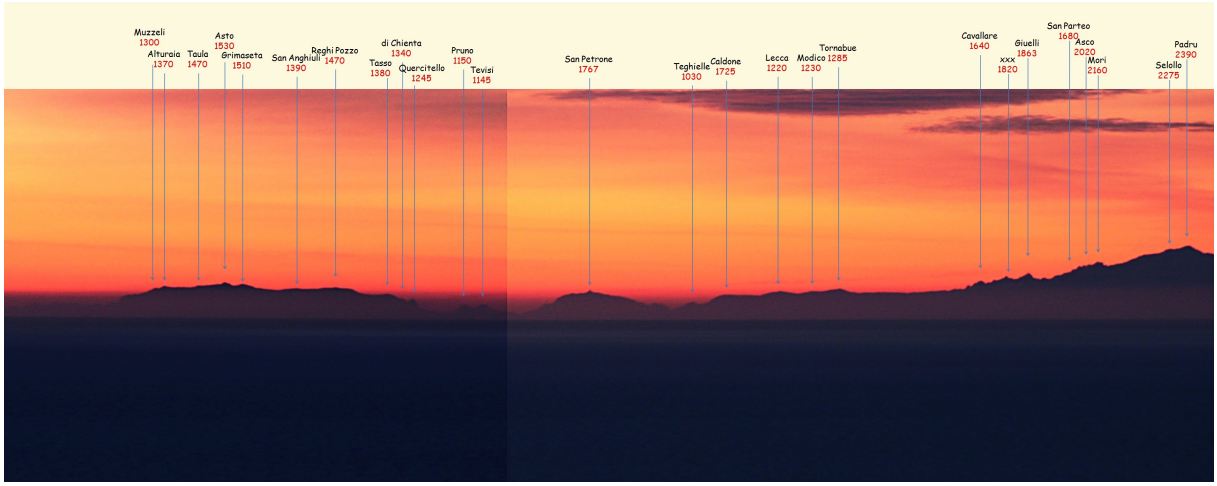


FIGURE 13.5: Panorama and identification of the Corsica landscape comprised between the Cap Corse and the west side of the central section. The San Petrone is the most distant feature visible from the hills around Nice. This is an isolated peak at a distance of 220 km with an altitude of 1770 m. The picture has enough resolution to be seen with a large zooming factor, enabling to read the names comfortably.



FIGURE 13.6: Panorama and identification of Corsica landscape for the Cinto area. This is the central part of Corsica visible from Nice and the most commonly seen. The picture has enough resolution to be seen with a large zooming factor, enabling to read the names comfortably.

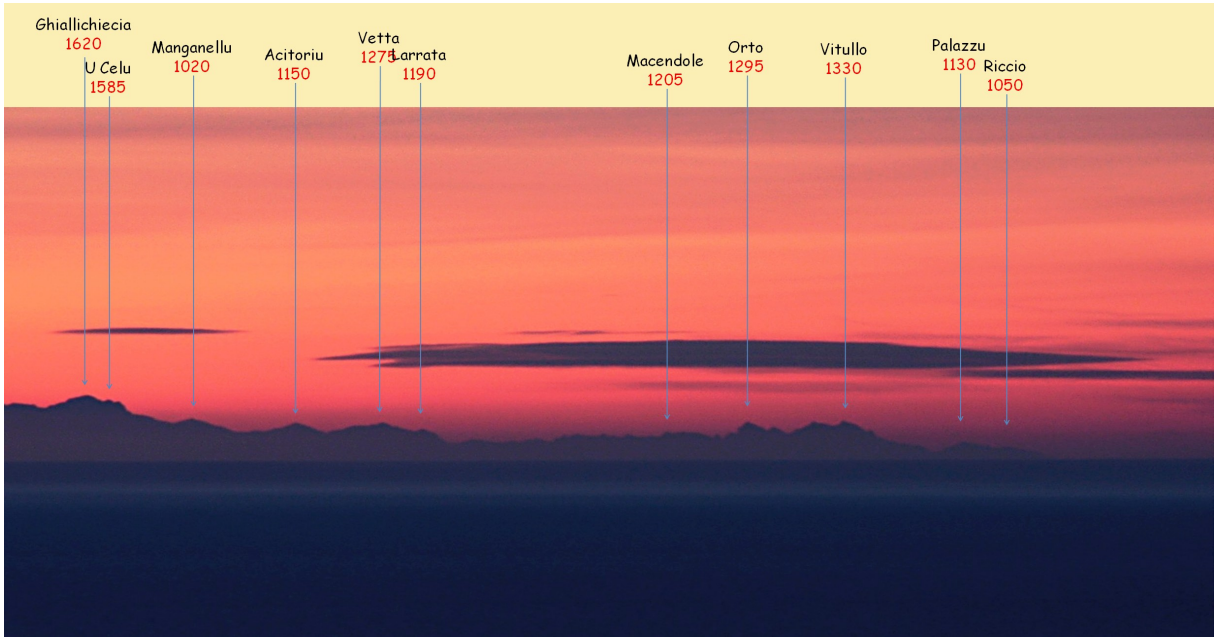


FIGURE 13.7: Panorama and identification of the Corsica landscape extending on the west to the Bay of Porto, with peaks of relatively low altitude. The picture of relatively poor quality should be looked at with a moderate zooming factor, enabling to read the names comfortably, without too much degradation.

14 Final gallery

This final section is an assorted set of additional plots, pictures or pictures arrangements providing examples of the visibility of Corsica in normal or extreme conditions, including mirages.

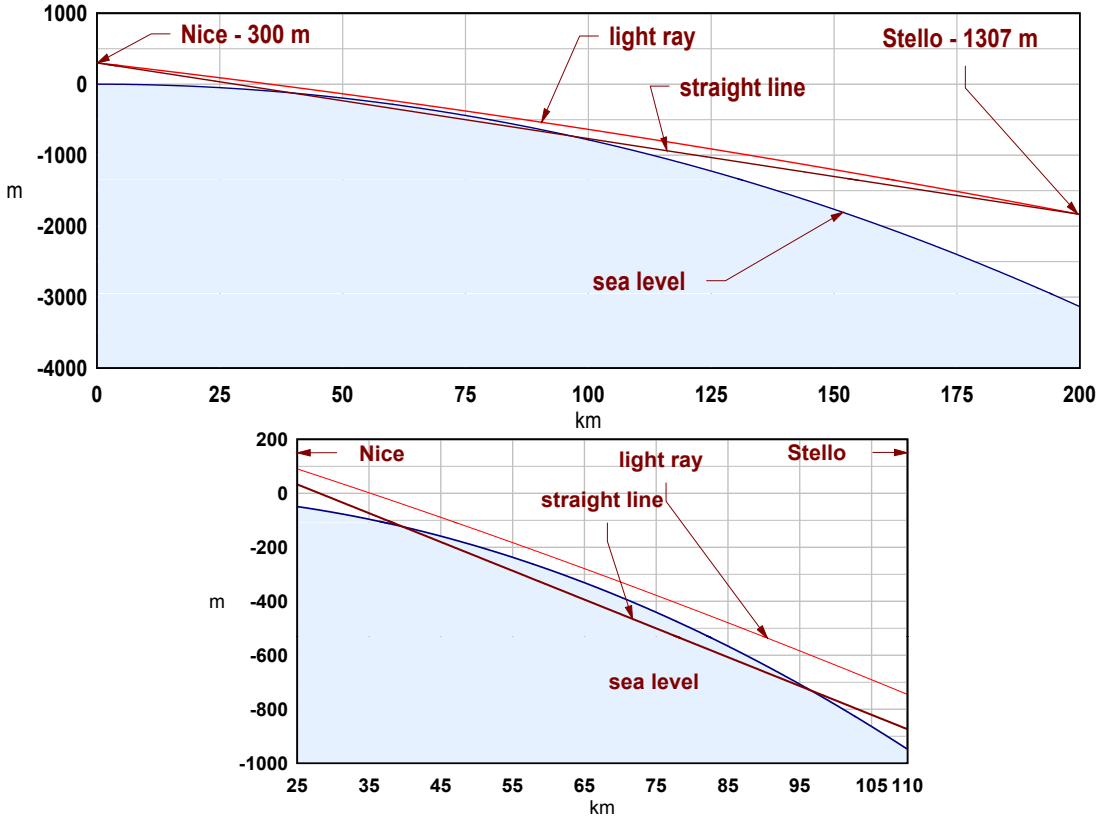


FIGURE 14.1: Limiting visibility of the Monte Stello in the Cap Corse from an altitude of 300 m in the east of Nice. The plot compares the light ray propagation with refraction (upper curve) with the geometric straight line joining the two end-points. In this configuration, the Stello is only visible thanks to refraction bending. The bottom plot is an enlargement of the central section. See Fig. 14.5 for an actual observation.

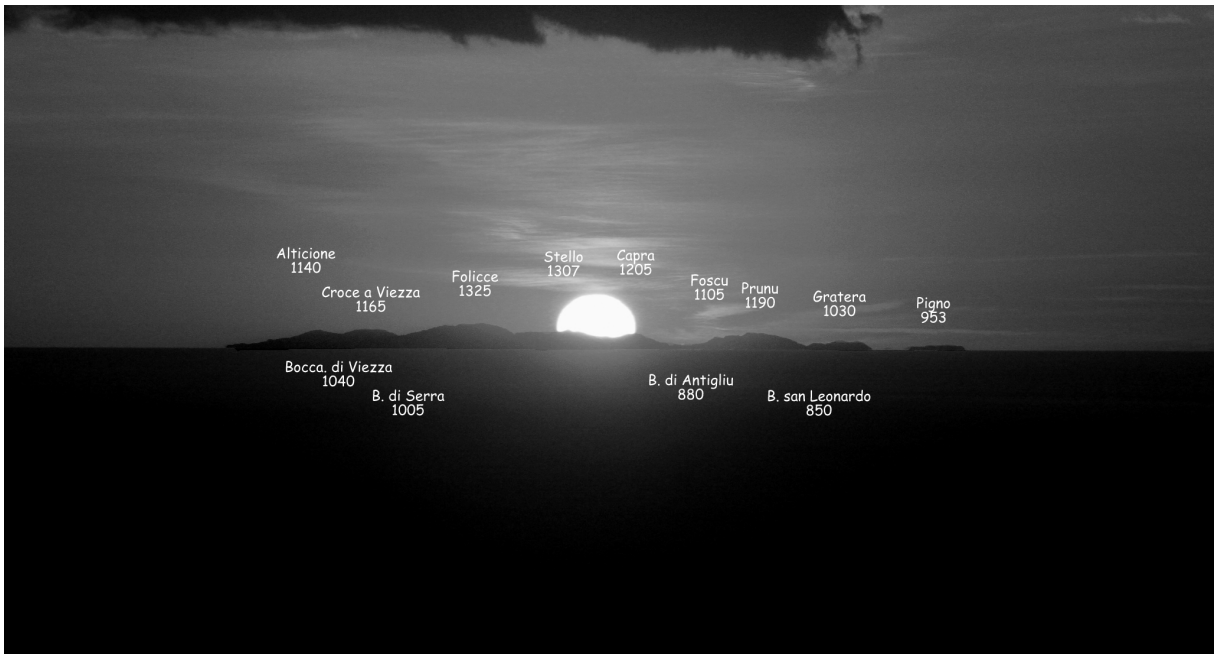


FIGURE 14.2: Sunrise behind the Cap Corse on January 3 rd from the Col d'Eze, with the names of the main features. The sun gives the scale of the landscape on the picture. It rises here above the Bocca Santa Maria, between the Stello and the Capra. A displacement of the observer one km east or west, changes the intersection of the line of sight with the Cap Corse of the same amount. The effect can be appreciated with the scale given in Fig. 13.3.



FIGURE 14.3: Cap Corse seen from an altitude 370 m, with only the top part of the peaks visible. The inferior mirages are conspicuous with the peaks looking like islands floating beyond the optical horizon. The dotted line corresponds to the vanishing line discussed in the text. The landscape is mirrored with distortion below this line and the remaining sky-coloured strip between the vanishing line and the optical horizon, is the reflected sky situated above the peaks.



FIGURE 14.4: Views of Central Corsica from various altitudes around Nice. The altitude scale in the bottom picture is purely indicative, since the peaks are not all a the same distance, and there is no simple mapping between a position on the picture and a given altitude. The Ghiallichiccia on the right is shown close to 1800 m instead of 1600 m, because it is located in the foreground at only 192.5 km instead of 198-200 km for the other main peaks.

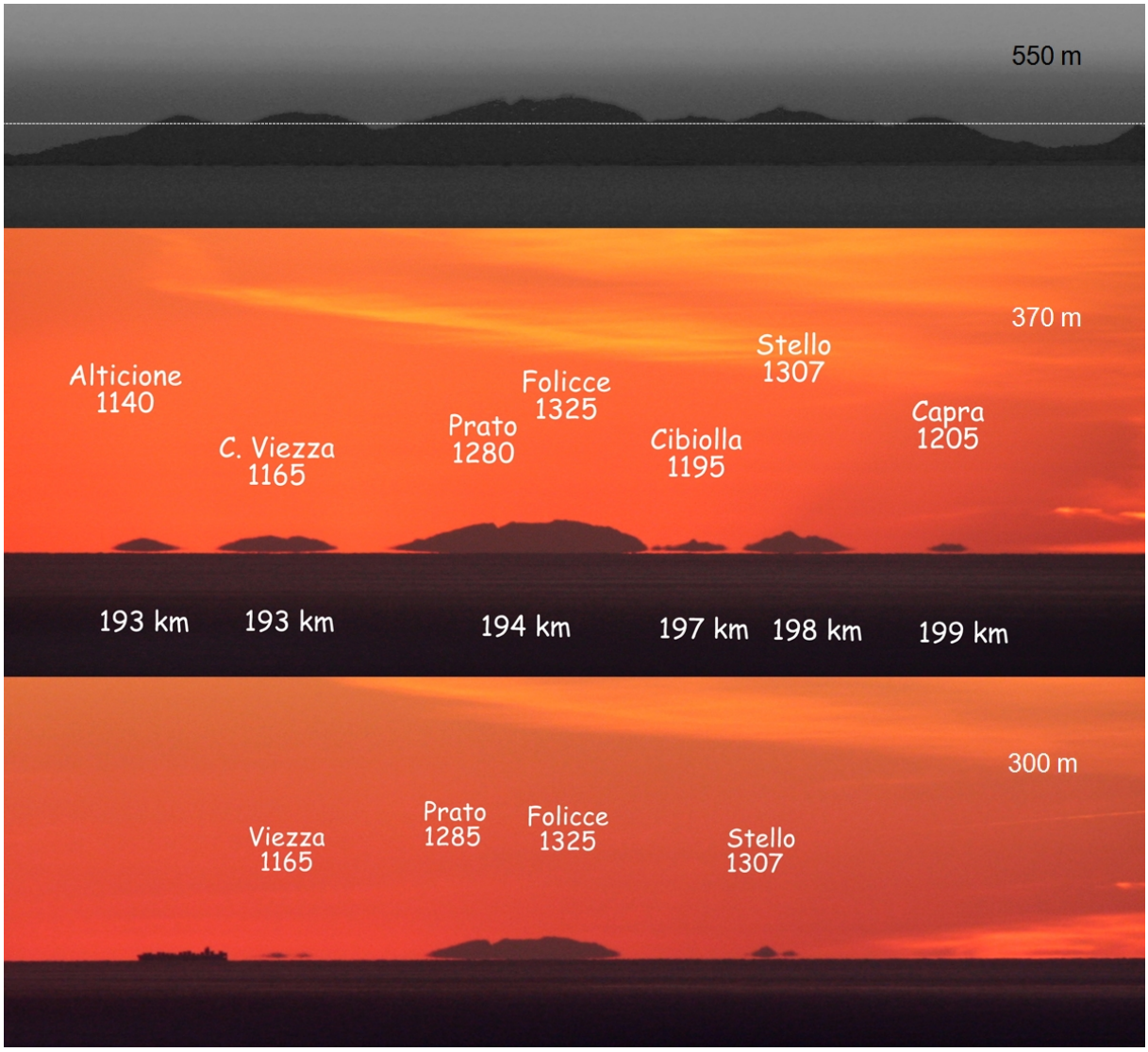


FIGURE 14.5: Views of the Cap Corse from three different altitudes in the east of Nice. The lowest picture taken at $\sim$ 300 m shows only the top of the highest peaks, topping at or above 1150 m for the nearest to the observer. This agrees very well with the figures listed in table 4.1 for the minimum altitude visible at a distance of 195 or 200 km. The middle panel is a view from an altitude of $\sim$ 370, with more details showing up. The effect of a small change in the distance is striking when comparing the Alticione (1140 m, 193 km) on the left and the Capra (1205 m, 199 km) on the right. The top panel from 550 m has all the peaks visible and the dotted line allows to identify exactly the features seen in the lower panels.



FIGURE 14.6: View of central Corsica from the sea level along the Promenade des Anglais in Nice. This is possible only with the curved rays as shown by comparison of tables 3.1 and 4.1. The shot was taken in winter and there are conspicuous inferior mirages with the symmetric and compressed image of the Monte Cinto and the sky above, visible near the optical horizon. The identification with an image taken at 50 m leaves no doubt about what is seen. The Punta Minuta lies at a distance of 197.5 km while the other are at 199 km. In these extreme conditions, this is sufficient to make a significant difference in visibility.

15 References

15.1 Books

TRICKER R. A. R., *Introduction to Meteorological Optics* American Elsevier, New York, **1970**. An excellent book to start with, covering the usual issues of atmospheric optics, like rainbows, ice haloes, glories, visibility with elementary maths, primarily geometry and trigonometry.

MINNAERT, M. G. J., *Light and Color in the Outdoors,* Springer, **1993**. A very successful and truly enjoyable book (with a Dover edition available) first published in 1937 with updated and enlarged editions until 1968. The Springer issue is the English translation of the last Dutch edition. It covers in a lively style, supplemented by numerous pictures and diagrams, every aspect of light phenomena in the open air in a purely descriptive way reflecting the author fascination for practical observations.

GREENLER, R., *Rainbows, Halos and Glories* Cambridge U.P. **1980**. The author is a physicist who got himself involved in ice-crystal optics and put in this book the main results of his investigations on ice halos. It contains many results of numerical simulations, done in the mid 70s with limited computer resources and graphical displays. The presentation of the inferior and superior mirages has been very helpful for my own understanding. He is also an excellent photographer and his pictures, many in the plate section of the book, have become a classic source in this field.

CHAUVENET, W. *Spherical Astronomy* Lippincott Company, **1889**. If you want to see the full mathematical treatment of the astronomical refraction in classical astronomy, before the computer era, you will find the subject dissected in 80 pages in this successful treatise of spherical and practical astronomy

.

15.2 Websites

ANDREW T. YOUNG, *Topic: atmospheric optics* `http://mintaka.sdsu.edu/GF/bibliog/overview.html` A really great and comprehensive Website on the atmospheric refraction with plenty of material on the terrestrial and astronomical refraction, all kind of mirages, extinction, the green flash and a gem: a giant annotated bibliography of books and papers on the subject, equivalent to 700 printed pages. Nice plots and

numerical experiments, nothing flashy but rigourous information masterly expounded. Sometimes hard to navigate through all the links. A site map would be helpful.

A. ORIGNÉ, *Topic: Canigou from Marseille* `http://canigou.allauch.free.fr/index.html` A Website (in French) entirely devoted to the visibility and observations of the Canigou from Marseille area, complemented by his archive of exceptional images of the phenomenon. The site is well organised, fact-packed, and presents the associated subjects, like refraction, atmospheric parameters, flattening of the sun with many informative, original and nicely crafted diagrams. If you think that *a picture is worth a thousand words* to describe complex ideas, this is the place to go.

L. COWLEY, *Topic: atmospheric optics* `http://www.atoptics.co.uk/` The reference on the Web on atmospheric optics covering rays propagation on water drops, dust or ice crystals and their associated visual spectacles like rainbows, halos, coronas, glories, explored in details, with numerical simulations and dedicated diagrams. To my taste, sometimes a few formulas, even elementary, would easily replace textual description.

J. LE ROUX, *Topic: Corsica from Nice* `http://users.polytech.unice.fr/~leroux/VoirlaCorsedepuislesAlpesMaritimes3.htm` The only page (in French) I found with a genuine computation of the light ray path between Nice and Corsica by numerical integration. Unfortunately the page is poorly designed, hardly readable, and contains no broader result beyond the particular case under consideration. But at least there is a realistic plot of a curved light-ray between Nice and Corsica.

G. EHRENTRAN, *Topic: Picture of Corsica from Nice* `http://www.nice-image.com/corse/corse-vue-du-continent.php` The author is a professional photographer and proposes a collection of pictures of Corsica seen from Nice area, including a panorama with identifications and a view from the Mercantour where the visibility extends down the Corsica coastline, together with the Island of Elba in the east. In addition his comments on the conditions of visibility and the (minor) role of refraction, are very relevant.

E. VAROQUAUX, *Topic: Picture of Corsica from Nice surroundings* `http://emmanuel.varoquaux.free.fr/corse.php` The author is computer scientist, a seasoned mountaineer coupled with a skilled photographer. Nice views of Corsica from the continent with good explanation of the underlying physics. This is the only place where I found images taken during daylight from the inland peaks at altitudes higher than 2500 m, with

the visibility extending to Elba or the Alpi Apuane in Tuscany.